

**U.S. Department of Energy
Office of FreedomCAR and Vehicle Technologies
1000 Independence Avenue S.W.
Washington, DC 20585-0121**

FY 2002

**Progress Report for Automotive Propulsion
Materials Program**

Energy Efficiency and Renewable Energy
Office of FreedomCAR and Vehicle Technologies

Steven Chalk Program Manager

December 2002

CONTENTS

INTRODUCTION	1
2. POWER ELECTRONICS	9
A. Low-Cost, High-Energy-Product Permanent Magnets.....	9
B. Development of Improved Powder for Bonded Permanent Magnets.....	15
C. Carbon Foam for Electronics Cooling.....	21
D. dc Bus Capacitors for Hybrid Vehicle Power Electronics.....	27
E. Mechanical Reliability of Electronic Ceramics and Electronic Ceramic Devices	33
3. FUEL CELLS.....	39
A. Carbon Composite Bipolar Plates.....	39
B. Cost-Effective Surface Modification for Metallic Bipolar Plates	43
C. Low-Friction Coatings and Materials for Fuel Cell Air Compressors	49
D. Microstructural Characterization of PEM Fuel Cells	55
E. Nano-Particulate Porous Oxide Electrolyte Membranes as Proton Exchange Membranes	61
F. Bacterial Cellulose Membranes.....	67
G. Carbon Foam for Radiators for Fuel Cells	71
4. ADVANCED COMBUSTION	79
A. Materials Improvements and Durability Testing of a Third-Generation Microwave- Regenerated Diesel Particulate Filter	79
B. Rapid Surface Modifications of Aluminum Automotive Components for Weight Reduction	85
C. Material Support for Nonthermal Plasma Diesel Engine Exhaust Emission Control	91
D. Fabrication of Small Fuel-Injector Orifices.....	95
E. Technology for Producing Small Holes in Advanced Materials	99
F. Electrochemical NO _x Sensor for Monitoring Diesel Emissions.....	103
APPENDIX A: ACRONYMS AND ABBREVIATIONS.....	107

1. INTRODUCTION

Automotive Propulsion Materials R&D: Enabling Technologies to Meet Technology Program Goals



Nancy L. Garland
Technology Development
Manager



Rogelio Sullivan
Technology Development
Manager

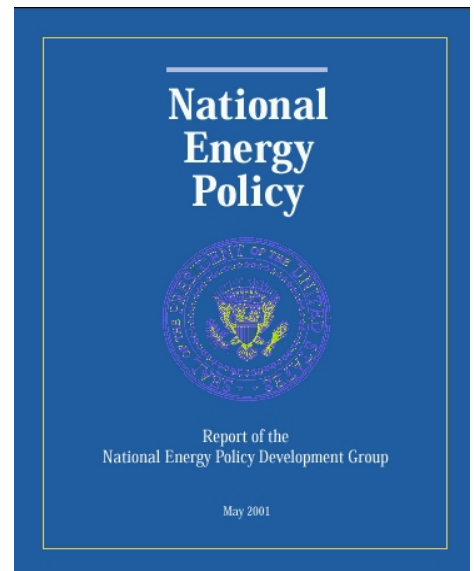
On behalf of the Department of Energy's (DOE's) Office of FreedomCAR and Vehicle Technologies (FCVT), I am pleased to introduce the FY 2002 Annual Progress Report for the Automotive Propulsion Materials Research and Development Program. I am also pleased to introduce you to Rogelio Sullivan, who is taking over management of this important program starting in FY 2003. For the last ten years, Rogelio has worked at DOE on a variety of automotive engineering projects, including the development of electronics/electric drive systems and lightweight materials. Rogelio is currently the Team Leader for the Automotive Lightweight

Materials group in the FCVT Office. It is noteworthy that the materials projects that support the goals of the Fuel Cell Program will be moving with me in FY 2003 to the Hydrogen, Fuel Cells, and Infrastructure Technologies Program. Together with DOE national laboratories and in partnership with private industry and universities across the United States, the program will continue to engage in high-risk research and development (R&D) that provides enabling materials technology for fuel-efficient and environmentally friendly light-duty vehicles.

This introduction summarizes the objectives and progress of the program in FY 2002 and highlights the technical barriers remaining and the future direction of the program. The FY 2002 annual progress reports on *Combustion and Emission Control for Advanced CIDI Engines* and *Hydrogen, Fuel Cells, and Infrastructure Technologies* provide additional information on FCVT's R&D activities that support the development of propulsion materials technology.

In May of 2001, the President's National Energy Policy Development Group published the National Energy Policy (NEP). This comprehensive energy policy specifically addresses the development of energy-efficient vehicle technologies, including hybrid systems, advanced emission control technologies, fuel cells, and hydrogen-based systems. The NEP is a strong indicator of the continuing federal support for advanced automotive technologies and the materials work that supports them.

The Automotive Propulsion Materials R&D Program has supported the FreedomCAR Program since its inception. FreedomCAR is not an automobile or prototype but rather a new approach to powering the vehicles of the future. In research areas where industry views the risks as too high and uncertain, the FreedomCAR Program conducts long-term research, development, and demonstration activities for cars, light trucks, and heavy vehicles to reduce oil consumption and emissions.



**Report of the National Energy
Policy Development Group**

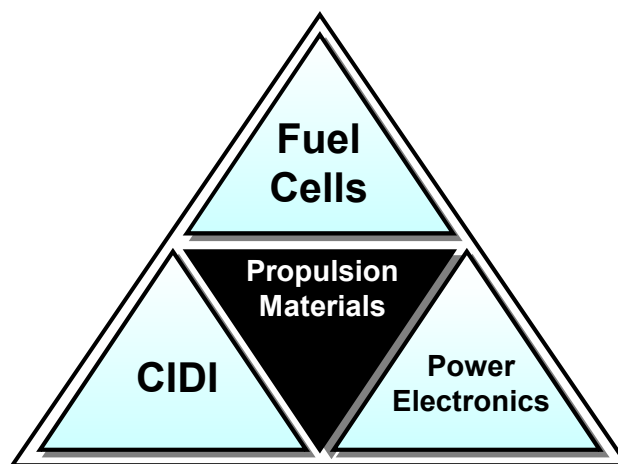
The Automotive Propulsion Materials Program is a partner with the programs for Vehicle Power Electronics and Electric Machines, Combustion and Emissions Control for Advanced CIDI Engines, and Fuel Cells for Transportation. Projects within the Automotive Propulsion Materials Program address materials concerns that directly impact the critical technical barriers in each of these programs—barriers such as thermal management, emissions reduction, and reduced manufacturing costs. The program engages only the barriers that involve basic, high-risk materials issues.

Enabling Technologies

The Automotive Propulsion Materials Program focuses on enabling materials technologies that are critical in removing barriers to the power electronics, fuel cell, and compression-ignition, direct-injection (CIDI) engine combustion and emissions control research programs.

Thermal management is a cross-cutting materials issue that affects both the power electronics and fuel cell programs. The components necessary for high-fuel-economy, low-emission hybrid vehicles require that power electronics be smaller and lighter and operate at higher temperatures. These requirements are being addressed by developing electronic materials (i.e., low-cost dc bus capacitors) that operate at higher temperatures and by improving the capability to dissipate heat generated in electronic devices.

Fuel cell systems also require improved heat dissipation because the lower operating temperature of the fuel cell system (80°C) provides a smaller temperature differential between the fuel cell system and ambient conditions. The Propulsion Materials Program has been addressing both heat dissipation issues through the development of advanced carbon foam technology.



The Propulsion Materials Program focuses on three applications.

The Program has supported the development of two innovative membrane materials for polymer electrolyte membrane (PEM) fuel cells: high-surface-area microporous inorganic oxide (TiO₂ and Al₂O₃) and metallized bacterial cellulose. Both types of membranes promise to be capable of operating at temperatures above 100°C, to improve waste heat dissipation, to involve minimal water management problems and less CO poisoning, and to reduce the cost of the fuel cell system by minimizing the quantity of expensive platinum required.

CIDI engine and aftertreatment system development will greatly benefit from the Program's efforts to develop improved particulate filters for diesel engines. Current CIDI engine technology must strike a difficult balance between engine efficiency and tailpipe emissions. The Propulsion Materials Program initiated two projects in FY 2002 to develop technology to produce very small (~50 microns) orifices for fuel injectors used in high-pressure common rail systems. The smaller orifices would enable better control of fuel vaporization and would increase efficiency and reduce emissions. The Program is working to reduce emissions through the development of advanced particulate filters and is collaborating with Pacific Northwest National Laboratory in the development of a nonthermal plasma aftertreatment device to reduce NO_x emissions from diesel engines.

Collaboration and Cooperation

As with other programs under FreedomCAR, collaboration and cooperation across organizations is a critical part of the Automotive Propulsion Materials Program. Across the materials projects, scientists at the national

laboratories are collaborating with manufacturers to identify and refine the characteristics necessary for meeting performance requirements. Researchers at Lawrence Livermore National Laboratory are working with Ford to develop low-cost, rapid-response NO_x sensors that can be utilized in feedback control loops to minimize NO_x emissions from diesel engines. Component manufacturers and scientists from the national laboratories and from contractors are also working together to identify the technological barriers to manufacturing optimal materials to meet component requirements.

There is also cooperation among national laboratories to take advantage of the expertise of each

facility. Oak Ridge and Argonne National Laboratories (ORNL and ANL), for example, are collaborating in the development of higher-strength NdFeB permanent magnets that will enable significant reductions in the size, weight, and cost of electric motors used in hybrid vehicles. In another project, Sandia National Laboratories (SNL) is fabricating smaller, higher-temperature dc bus capacitors; and ORNL is developing techniques to characterize the ~5-micron-thick polymer films developed by SNL and correlate their mechanical properties with their dielectric behavior.

In addition to national laboratory and large industry participation, the FY 2002 Automotive Propulsion Materials Program included important R&D conducted by a small business. Industrial Ceramic Solutions, LLC (ICS), located in Oak Ridge, Tennessee, is developing a ceramic filter to reduce particulate emissions from diesel engines. As in the collaborative efforts of national laboratories with industry, researchers at ICS are working closely with representatives from DaimlerChrysler, Ford, General Motors, and ORNL to develop a filter that will meet the emissions targets of the program.

Accomplishments

FY 2002 featured notable accomplishments in all three materials program areas. The remainder of the report provides summaries of all of the Automotive Propulsion Materials projects; this section highlights some major accomplishments during FY 2002. Materials R&D in support of power electronics, for example, resulted in the development of improved heat sinks capable of dissipating the heat generated by high-power devices. Fuel-cell-related materials projects demonstrated metallic bipolar plates that are low in cost, weigh about half as much as graphite materials, and have significantly better electrical properties. Finally, materials research supporting combustion engine and aftertreatment technologies led to the demonstration of microwave-regenerated exhaust particulate filters in diesel-powered vehicles.

Power Electronics

High-power electronic components like power modules and inverters being developed for hybrid electric vehicles generate significantly more heat than conventional devices. Heat generated by these devices must be effectively dissipated to prevent overheating and failure of the devices. In the past, air-cooled aluminum or

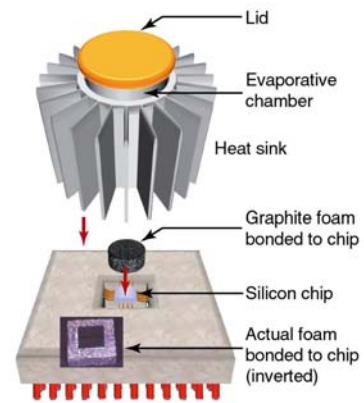
Laboratory/Contractor-Industry Collaboration

Laboratory		Industrial Partner	
Argonne National Laboratory	✓	Ability Engineering Technology, Inc.	✓ Daimler-Chrysler Corporation
	✓	Atlas Cylinders, Inc.	✓ Ford Motor Company
	✓	Bronson and Bratton, Inc.	✓ Lucas-Varity
	✓	Cryomagnetics, Inc.	✓ Purdue University
	✓	CRUMAX	✓ UGIMAG, Inc.
Oak Ridge National Laboratory	✓	AVX	✓ Industrial Ceramic Solutions
	✓	Bronson and Bratton, Inc.	✓ Motorola
	✓	Caterpillar	✓ Murata
	✓	Conoco Corporation	✓ Peterbilt
	✓	Cryomagnetics, Inc.	✓ Poco Graphite
	✓	CRUMAX	✓ Plug Power, LLC
	✓	Daimler-Chrysler Corporation	✓ UGIMAG, Inc.
	✓	Dow Chemical Company	✓ SatCon
	✓	Ford Motor Company	✓ University of Tennessee
	✓	General Motors	✓ University of Wisconsin
	Sandia National Laboratory	✓	AVX
✓		Daimler-Chrysler Corporation	✓ Pennsylvania State University
✓		Ford Motor Company	✓ TAM
✓		General Motors	✓ Tokay
✓		Degussa	✓ TPC Ligne Puissance
✓		Ferro	✓ TPL, Inc.
✓		Kemet	✓ TRS Ceramics
✓		Materials Research Associates	

copper heat sinks could easily handle the heat load ($<25 \text{ W/cm}^2$). The higher power requirements of today's devices generate significantly more heat and will require more sophisticated heat sinks.

Current computer chips are packaged printed-side-up in a ceramic package with over-the-top wire bonds. Unfortunately, this design is not suited for significant heat dissipation through the top of the package to a standard heat sink because there is an insulating air gap between the silicon chip and the ceramic package. A new concept being developed is the flip-chip design in which the silicon chip is inverted, with the back of the printed chip oriented toward the top of the package. In this design, a heat spreader can be joined directly to the chip with no air gap to impede the heat flow. The National Security Agency (NSA) has been working for a number of years to develop an evaporatively-cooled heat sink that immerses the heat spreader in a cooling fluid such as fluorocarbon. In this process, the latent heat of vaporization removes significantly more heat than is transferred to the fins of a conventional heat sink. The limitations of this design are the surface area and thermal conductivity of the heat spreader attached to the back of the chip. The heat spreader developed by the NSA is polycrystalline diamond wafers with a thermal conductivity of $\sim 1600 \text{ W/m}\cdot\text{K}$. The maximum power density achieved without overheating the system was 28 W/cm^2 .

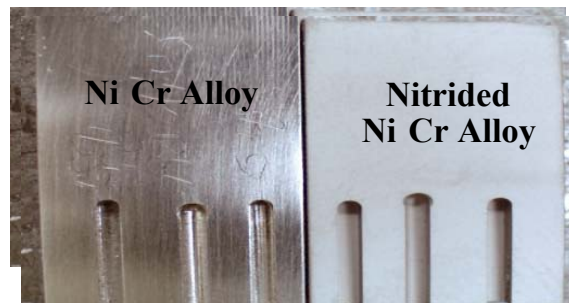
A collaborative effort between the NSA and ORNL has effectively used high-conductivity carbon foam to dramatically increase the cooling capacity of the system. The lightweight carbon foam has a ligament thermal conductivity comparable to that of diamond wafers but has a surface area that is more than 2 orders of magnitude greater. When the diamond spreader was replaced by graphite foam, a power density of greater than 110 W/cm^2 was attained without overheating the system (see schematic). The same technology has been used to develop a low-cost passive heat sink for power modules and inverters.



Fuel Cells R&D

PEM fuel cells are of great current interest for automotive applications because they are highly efficient and environmentally friendly, producing near-zero emissions. Cost remains a key barrier to their widespread use. One of the most expensive components in PEM fuel cells is the bipolar plate that serves to electrically connect individual cells in a stack and to separate and distribute reactant and product streams. Thin metallic bipolar plates offer the potential for significantly lower cost than benchmark machined graphite bipolar plates, and better power density performance than developmental polymer/carbon fiber and graphite composite bipolar plates currently under consideration. However, inadequate corrosion resistance can lead to high electrical resistance caused by the formation of resistive surface oxides and/or can contaminate the PEM with metal ions, both of which degrade performance.

To solve this problem, ORNL is developing a new family of Ni-Cr base alloys specifically designed to form a protective and electrically conductive Cr-nitride surface layer upon thermal nitridation. Thermal nitridation is an inexpensive, well-established industrial technique and is viable for covering complex geometries such as bipolar plate flow field features (see the figure). Further, the alloy can be formed into final shape by inexpensive metal forming techniques, such as stamping, prior to the nitridation treatment.



Nitrate coverage of flow field grooves.

The nitrided Ni-Cr base alloys exhibited minimal corrosion (current densities of less than $1 \times 10^{-6} \text{ A/cm}^2$) in an 80°C , pH 3 sulfuric acid environment designed to simulate PEM fuel cell operating conditions. Over

1800 h of exposure have also been accumulated in the Los Alamos National Laboratory Bipolar Plate Corrosion Test Cell Facility with electrical resistance increases of only 0.5 mV/1000 h at the anode and 2mV/1000 h at the cathode (for comparison, 316 stainless steel exhibits resistance increases of 16 and 21 mV/1000 h, respectively). A provisional patent disclosure on this family of alloys has been filed and coupons have been delivered to several fuel cell manufacturers for evaluation. Delivery of 50-cm² active-area plates to Los Alamos National Laboratory for in-cell testing is planned for Fall 2002.

Advanced Combustion Engine and Emissions R&D

A major FreedomCAR goal is to develop a vehicle with outstanding fuel economy that meets stringent emissions standards. Balancing high fuel economy with low emissions is a challenge being addressed through materials activities in support of the R&D program for Combustion and Emission Control for Advanced CIDI Engines. Specifically, work conducted at ICS has led to the development and demonstration of an advanced exhaust filter system capable of capturing more than 95% of the carbon particulates from diesel engine exhaust. ICS has developed a new, patented technology known as the “microwave-cleaned particulate filter system” that can remove and destroy fine particulate pollution from diesel exhaust streams. The system features a ceramic-fiber filter that can be automatically cleaned through the use of microwave power.

During FY 2002, ICS developed a pleated filter that exhibits only 1/20 the backpressure of the wall-flow filters that were used in the past. ICS developed a technology that uses a ceramic binder, rather than a thermosetting resin, to pleat the fibrous filter paper. Evaluated on a 1.7-L Mercedes diesel engine at ORNL, the filter demonstrated a 96 to 98% particulate removal efficiency with a low backpressure. The microwave filter was installed on a Ford F-250 7.3-L diesel pickup, with full exhaust backpressure and temperature data acquisition. Road testing proved that the filter could survive the full loading of 1000 ft³ per minute of exhaust flow without mechanical failure. A fully automated microwave filter system with the flat, pleated filters is being installed on the Ford truck for a 7000-mile controlled test track evaluation, with periodic Federal Test Protocol cycle emission testing. Data from these on-road tests will be used to improve the performance of the microwave-regenerated particulate filter, verify system durability, and precisely quantify the fuel penalty resulting from filter operation.

Positive results from these tests should lead to product development partnerships with exhaust system suppliers, engine builders, or vehicle manufacturers. These strategic partnerships can move this technology to integration into a total commercial diesel exhaust emissions control system for pick-up trucks, sport utility vehicles, and large trucks.

Scale-Up/Commercialization

Durability-enhancing coatings for automotive applications—such as engine block cylinder liners, compressor housings, and fuel pumps—have been developed at ORNL using innovative rapid, high-density infrared (IR) surface modification processes. A collaborative effort with researchers at Ford has developed an improved joining and resin curing process that uses this process. The Lincoln LS has a welded seam in the middle of the C-pillar (behind the rear door). The finishing process for the seam included labor-intensive welding, thermal spraying, and multi-step sanding and painting processes. The process is operator-dependent and susceptible to quality concerns and throughput issues.



On-road controlled test-track vehicle.



Flat, pleated microwave regenerated particulate filter.

A one-component epoxy material was chosen to replace the thermal-sprayed silicon bronze that Ford had been using. The epoxy is conductive to the electrostatic coat, is fully paintable and sandable, and has low porosity. The IR line heater developed at ORNL was found to be an efficient, robust in-line heating source to cure the epoxy coating. The heater can go from cold to full power in less than a second, converts electrical power into radiant energy at 90% efficiency, and targets the energy to only the area that needs curing. Full commercial-scale process trials proved that the IR heater cured the epoxy in only 20 seconds, from a distance of 6 inches and in a 10-inch-wide sweep, to achieve a 92% cure that was suitable for grinding and finishing. The process was so successful that Ford adopted the IR lamp technology in one of its plants. The benefits of using the epoxy filler and IR curing include (1) a cost savings of \$28 per vehicle, (2) a 2-minute reduction in cycle time, (3) less porosity in the coating, (4) reduced energy consumption, and (5) safer, more environmentally friendly processing.



Epoxy being cured with IR heating on the Lincoln LS prototype



Lincoln LS joint before (top) and after IR cure and finishing.

High-Performance Bipolar Plate

Through licensing of a key material and manufacturing method invented at ORNL, Porvair Fuel Cell Technology (PFCT) is scaling up a process to manufacture large quantities of composite bipolar plates. The 3-year program will result in a process capable of manufacturing 300 plates per hour. The ORNL technology uses a low-cost, water-based carbon fiber slurry-molding process to produce a porous carbon-fiber preform. The molded carbon-fiber component has impressed flow-field channels for diffusing fuel or air to the electrolyte surface. The bipolar plate is made hermetic through chemical vapor infiltration with carbon. The carbon deposit provides exceptional strength and enhanced conductivity to the bipolar plate material. The high strength of the material enables it to be formed into bipolar plates that are thinner than those made through competitive technologies, and the high conductivity increases fuel cell performance.



Prototype thermal processing equipment for bipolar plates

The benefits of the manufacturing technology include

- Suitability for mass production
- Low cost
- High material strength
- High bulk conductivity
- Non-corrosiveness of carbon
- Potential for very thin plates
- Excellent sealing performance

PFCT is actively supplying test plates to major fuel cell manufacturers. Fuel cell testing has confirmed that the product achieves excellent performance in a stack, and aggressive production activities are under way to supply prototype materials for commercial and transportation applications. Price

estimates have been provided to one customer for interim-production quantities in CY 2003 to support introductory product requirements for bipolar plates in the short term. Plans are to accelerate the development of the proposed high-volume production line to mid-year 2003 to stay ahead of anticipated product demand.

Future Direction

The Automotive Propulsion Materials Program will continue to work closely with FreedomCAR partners and industry to understand propulsion materials-related requirements. Building upon the recent advances in materials technologies, many of this year's projects will be moved out of the laboratory and over to industry for testing. Strategic partnerships will be established in 2003 with exhaust system, engine, or vehicle manufacturers to move the microwave particulate filter system from vehicle testing toward commercialization. The scale-up and commercialization of carbon foam at POCO Graphite for thermal management applications will continue, with the focus on cost reduction. Other projects will continue to refine manufacturing requirements and necessary characteristics to meet the challenges of the FreedomCAR program.

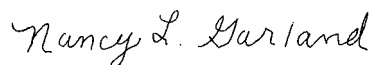
A promising new activity in the Automotive Propulsion Materials Program for FY 2002 was the collaboration between Ford Motor Company and ORNL to develop a resin curing process that was commercialized on the Lincoln LS vehicle. This cost-effective process will be extended in FY 2003 to other applications at Ford as well as at other companies.

As advanced automotive technology developments uncover new challenges, the Automotive Propulsion Materials Program will continue to provide breakthrough technology solutions through collaboration with industry, FreedomCAR partners, national laboratories, and small businesses.

Project Abstracts

The remainder of this report communicates the progress achieved during FY 2002 under the Automotive Propulsion Materials Program. It consists of 18 abstracts of national laboratory projects—five that address power electronics, six that address combustion and emission technologies, and seven that address fuel cells. The abstracts provide an overview of the critical work being conducted to improve these systems, reduce overall cost, and maintain component performance. In addition, these abstracts provide insight into the challenges and opportunities associated with advanced materials for high-efficiency automobiles.

Nancy L. Garland



Technology Development Manager
Office of FreedomCAR and Vehicle Technologies
Energy Efficiency and Renewable Energy

2. POWER ELECTRONICS

A. Low-Cost, High-Energy-Product Permanent Magnets

Y. S. Cha and John R. Hull

Energy Technology Division, Bldg. 335

Argonne National Laboratory, Argonne, IL 60439

(630) 252-5899; fax: (630) 252-5568; e-mail: yscha@anl.gov

Andrew E. Payzant

Oak Ridge National Laboratory

P.O. Box 2008, MS 6064

Oak Ridge, TN 37831-6069

(865) 574-6538; fax: (865) 574-3940; e-mail: payzanta@ornl.gov

DOE Technology Development Manager: Nancy Garland

(202) 586-5673; fax: (202) 586-9811; e-mail: nancy.garland@ee.doe.gov

ORNL Technical Advisor: David Stinton

(865) 574-4556; fax: (865) 241-0411; e-mail: stintondp@ornl.gov

Contractor: Argonne National Laboratory, Argonne, Illinois

Prime Contract No.: W-31-109-Eng-38

Objectives

- Develop a low-cost process to fabricate an anisotropic NdFeB permanent magnet (PM) with an increase in energy product of up to 25%, which is a measure of the torque that a motor can produce for a given magnet mass. The higher-performance magnets will replace ones made by traditional powder metallurgy processing and enable significant size and weight reductions in traction motors for hybrid vehicles.
- Use high fields of superconducting solenoids to improve magnetic grain alignment while pressing compacts for sintering, thus producing higher-performance magnets.

Approach

- Develop a batch-mode press that enables alignment of the magnetic domains of NdFeB powders in the higher-strength magnetic fields created by a superconducting solenoid.
- Characterize, compare, and correlate engineering and microscopic magnetic properties of magnets processed under varying conditions, including some in current production.
- Use a reciprocating feed to automate the insertion of loose and compacted magnet powder into, and its removal from, the steady magnetic field of a superconducting solenoid.

Accomplishments

- Achieved energy products that were within 10% of the theoretical maximum by optimizing batch-mode alignment/pressing of cylindrical axial-die-pressed PMs in a 9-Tesla (T) superconducting solenoid. The magnetic properties are comparable to those of the more expensive magnets made by the transverse-die pressing technique.
- Achieved energy product improvements of 15% for thin near-final-shape magnets, production of which is the current cost-saving thrust in the PM industry. Additional PMs made with relatively small length-to-diameter ratios ($L/D < 0.5$) support the previous findings.
- Proved the crucial step in making automation feasible. For the first time, powder-filled dies were inserted into and pressed compacts were removed from an active (always on) superconducting solenoid. Most important, these magnets were the best made.
- Carried out electromagnetic code study of grain alignment in powder compacts. The results show that the distortion of the alignment field (caused by the self-field of the compact) is proportional to the density of the compact and inversely proportional to the magnitude of the alignment field. There is a maximum distortion of the alignment field at a certain L/D ratio. These results will help us provide scale-up design rules to industry.
- Characterized the microscopic texture (alignment) of PMs made in the Argonne National Laboratory axial-die press facility and correlated the alignment with macroscopic magnetic properties.

Future Direction

- Demonstrate the feasibility of competitive factory operation by fabricating and operating a reciprocating press in continuous-mode operation.
- Continue the electromagnetic code study to better understand the grain alignment process.
- Provide design rules for the fabrication of PMs, including knowledge related to scale-up to larger magnets at commercial rates of production.
- Continue to collaborate with Oak Ridge National Laboratory (ORNL) on microstructure characterization of the finished PM samples and with Ames Laboratory on processing the NdFeB powder for bonded PMs.

Introduction

Industry considers an improvement of 2–3% in the magnetic properties of today's PMs as significant. The properties of current PMs can be brought to within 5–25% of their theoretical maximums. The strength of the magnet greatly depends on the method by which the compact is aligned magnetically and pressed. Large blocks can be made by cold-isostatic pressing that are within 5% of their theoretical maximum, but then the blocks must be sliced, diced, and ground to final shape. Machining operations add significantly to the cost of magnets. Magnets that are axial-die pressed and sintered to near-final shape have magnetic properties farthest from their theoretical maximums, but they are the least expensive to make. The current industry goal is to make better near-final-shape magnets by axial-die pressing. The major objectives of this project are to improve the magnetic

properties (mainly the energy product) of the sintered PMs and to develop low-cost methods of production for high energy-product, near-final-shape PMs.

Approach

Our approach is to align the NdFeB powder in a superconducting magnet, which can generate magnetic fields much higher than those generated by an electromagnet commonly used in industry. The alignment of the powder in higher magnetic fields is expected to improve the properties of the PMs. To develop a low-cost production method for high-energy-product PMs, we plan to design, fabricate, and demonstrate the reciprocating axial-die press system for automation.

Previously, a 9-T superconducting solenoid, which can produce alignment fields that significantly exceed those of the 2-T electromagnets

in common industrial use, was completed in the fourth quarter of 2000. Production-grade magnet powder was obtained from Magnequench UG. The 3- to 5-micron, single-crystal grains of powder were aligned in the same direction and compacted at Argonne. Then anisotropic compacts, with their grains mechanically locked in place, were returned to Magnequench UG for sintering, annealing, machining, and measurement of engineering magnetic properties. Finally, selected PMs were sent to ORNL for measurement of microscopic properties and texture (the alignment of the crystals' easy magnetic axes). The better the alignment, the greater is the energy product.

Results

Previously, we have demonstrated that significant improvement (10–15%) of energy product can be achieved by using higher alignment fields (>2 T). These results were based on a limited number of PM samples.¹ In FY 2002, we continued the previous study with an emphasis on a smaller L/D ratio where improvement in energy product is expected to be greater. The most effective use of the high alignment fields that can be provided by superconducting solenoids is in making near-final-shape magnets. Their finite and usually short length in the direction of magnetization makes alignment of the powder grains especially difficult. When subjected to a uniform alignment field, the powder in the die cavity develops a highly nonuniform self-field. Because grains align along the total field lines, unidirectional alignment can be achieved only by increasing the strength of the applied alignment field until the effects of the self-field become negligible. Because the self-field distortion becomes greater for shorter magnets, there will always exist short magnets that the 2-T electromagnets of industry cannot adequately align.

Clearly, the higher fields produced by a superconducting solenoid can provide the necessary alignment. A total of 69 compacts were fabricated with L/D ratios ranging from 0.27 to 0.52. These powder compacts were processed in alignment fields ranging from 1 to 8 T. The results are shown in Figure 1, where the remnant magnetization B_r

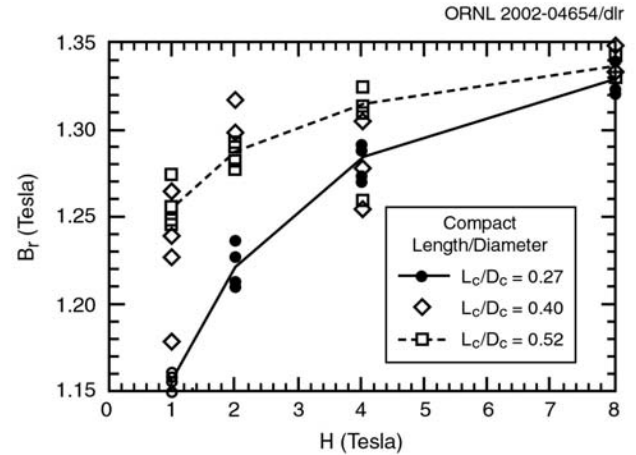


Figure 1. Remnant flux density B_r (T) of different L_c/D_c compacts pressed in increasing alignment fields H (T).

(the energy product is proportional to the square of the remnant magnetization) is plotted against the alignment field H . It can be observed that in general, the remnant magnetization increases with the alignment field. The improvement in B_r is the greatest for the smallest L/D ratio (0.27). These results confirm the trends of improvement in B_r of the previous study.

An attempt was made to fabricate PMs with even smaller L/D ratio (<0.25) where cost savings may be even greater because distortion of the alignment field due to the self-field of the powder is expected to be greater. A 1.125-in. die (the die used in the previous study was 5/8 in.) was designed, fabricated, and used to make PMs with an L/D ratio of less than 0.25. The attempt was not successful because the samples cracked during ejection from the die. Unlike the system used by the industrial manufacturer, the present die and press set is not designed so that it can eject the sample under pressure, which could have prevented it from cracking. We plan to investigate methods for alleviating this problem.

To understand the effect of the self-field of the magnet powder on the distortion of the alignment field, we carried out an electromagnetic study of grain alignment in powder compacts using the computer code Opera developed by Vector Field, Inc. The results of this study will be helpful in scaling up design rules to industry. Figures 2 to 4

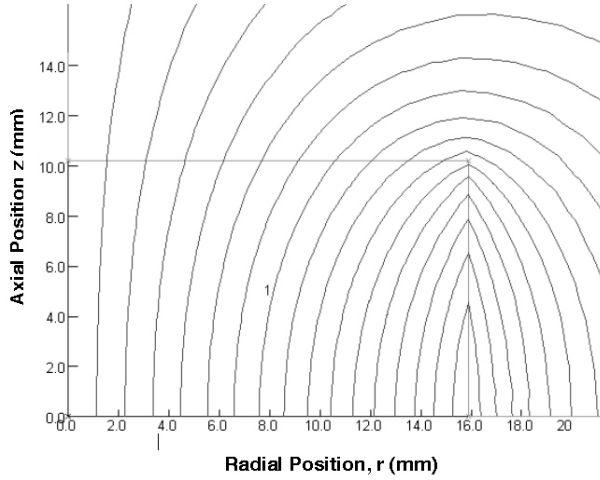


Figure 2. Field lines (one-quarter) for compact partially pressed to mechanical lockup, with no alignment field, $H \sim 0$. Parameters: $\rho_1 = 3.5 \text{ g/m}^3$, $L/D = 0.643$, $B_0 = 0.65 \text{ T}$.

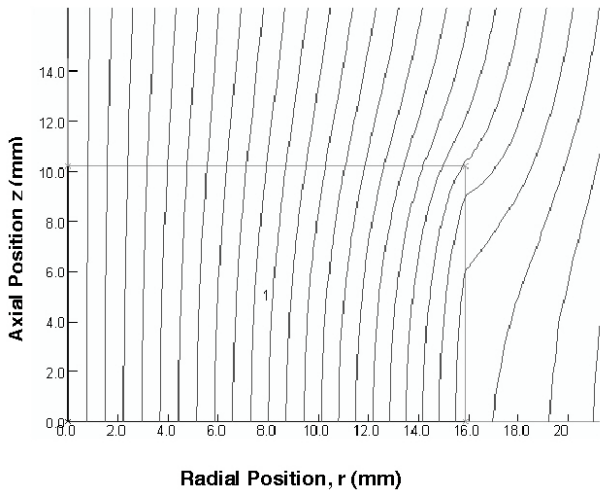


Figure 3. Field lines (one-quarter) for compact partially pressed to mechanical lockup. Alignment field $H = 1 \text{ T}$. Parameters: $\rho_1 = 3.5 \text{ g/m}^3$, $L/D = 0.643$, $B_0 = 0.65 \text{ T}$.

show the calculated field lines of one-quarter of a PM in increasing alignment fields of 0, 1, and 8 T, respectively. These calculations were carried out using the same powder density (3.5 g/m^3) and the same L/D ratio (0.643). The field lines will all be parallel to the z -axis if there is no distortion. It is clear that distortion of the alignment field is the largest when the alignment field is zero (Figure 2). The distortion decreases with increasing alignment field. At an alignment field of 8 T, the distortion becomes very small (Figure 4). The distortion

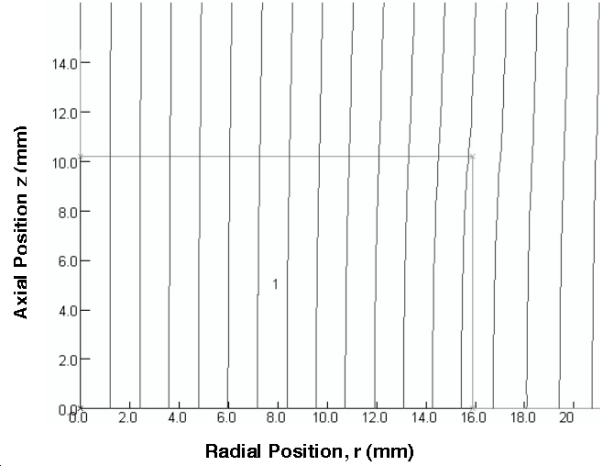


Figure 4. Field lines (one-quarter) for compact partially pressed to mechanical lockup. Alignment field $H = 8 \text{ T}$. Parameters: $\rho_1 = 3.5 \text{ g/m}^3$, $L/D = 0.643$, $B_0 = 0.65 \text{ T}$.

appears to be largest on the faces of the PM, and it increases with the radial position.

Figure 5 shows the inclination of the field line along the magnet upper face ($z = 10.2 \text{ mm}$) as a function of the radial position and the alignment field. It shows that the inclination (distortion) increases with radial position and decreases with alignment field. If B_r and B_z are defined as the radial and the axial components of the magnetic flux density B , respectively, then the volume average of the ratio B_r/B_z is a good measure of the overall distortion of the field lines. We have found that the following equation describes the overall distortion of the field lines very well for all the cases calculated by the computer code Opera.

$$(B_r/B_z)_{\text{vol}} (\%) = 10.5 B_0 / (H + 0.4430) ,$$

where B_0 is the residual field of the powder compact (B_0 is proportional to the density of the powder) and H is the alignment field. This equation clearly shows that the overall distortion of the alignment field is proportional to the density of the powder compact and inversely proportional to the alignment field. Our calculations also show that the overall distortion of the field lines peaks at an L/D between 0.6 and 0.7. However, this conclusion depends on the assumption made in the analysis. The main assumption was that the powder is a perfectly hard material, which resulted in providing a lower bound on the distortion of the field lines. We plan to

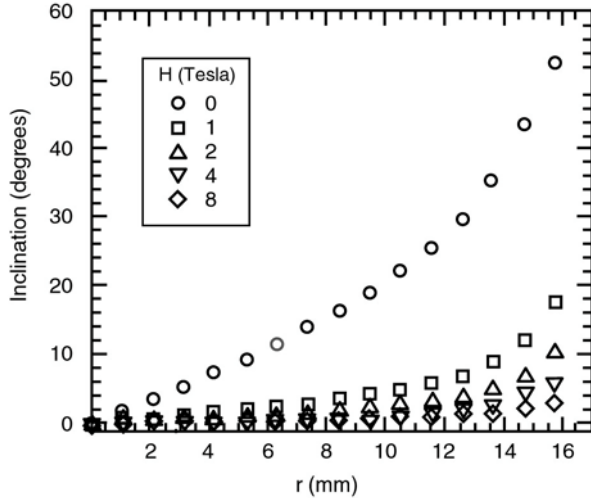


Figure 5. Field-line inclination along face ($z = 10.2$ mm) of compact partially pressed to mechanical lockup and subject to different alignment $0 \leq H(T) \leq 8$ T. Parameters: $\rho_1 = 3.5$ g/m³, $L/D = 0.643$, $B_0 = 0.65$ T.

continue the electromagnetic code analysis by assuming that the powder is a soft magnetic material. All the information obtained from the analysis will help to make better PMs and provide guidance on scaling up to industrial production.

At ORNL, crystallite size, texture (or preferred orientation), and composition of the PM materials pressed at Argonne are being characterized using X-ray diffraction measurements (or neutron diffraction, if required). All these features impact the macroscopic magnetic properties. A goal of this part of the project is to characterize, compare, and correlate engineering and microscopic magnetic properties of magnets aligned in the superconducting solenoid. A select group of the magnets, whose energy products are included in Figure 1, were shipped to ORNL for characterization. The condensed (105) pole figure data for these samples is given in Figure 6. The poorest alignment is observed for sample #200 ($L/D = 0.27$, $H = 1$ T). Consistent with the previous discussion, the best alignments were observed for the highest (8-T) fields, irrespective of the L/D ratio, indicating that these fields overcome the L/D geometric effects; but at lower fields the L/D ratio becomes more significant.

Finally, in FY 2002, we began to collaborate with Ames Laboratory on processing the NdFeB

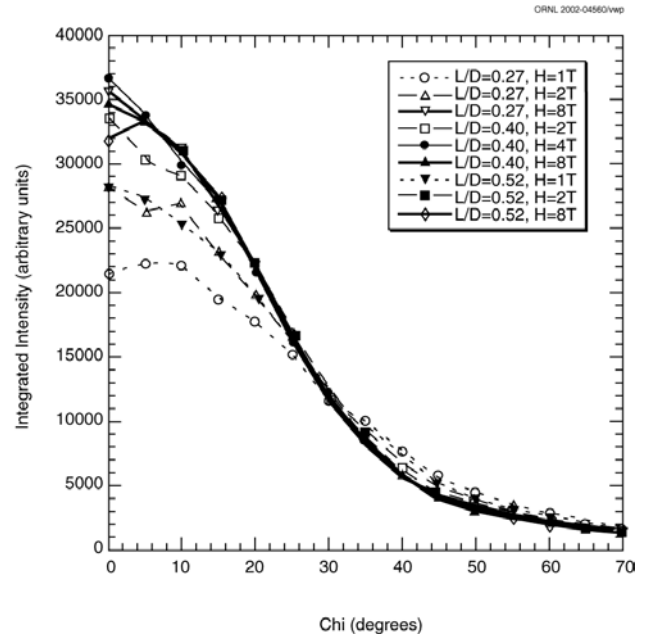


Figure 6. Condensed (105) pole figure data for ANL samples.

powder for bonded PMs in our 9-T superconducting magnet. A number of powder samples were processed and shipped back to Ames Laboratory for further examination and characterization.

Conclusions

A total of 69 PM samples were fabricated for relatively small L/D s (≤ 0.52) under alignment fields between 1 and 8 T. Results from measurements show that the relative improvement in remnant magnetization or energy product is of the same order of magnitude as in the previous study on a limited number of samples.¹ The improvement in energy product is of the order of 10–15%, with greater improvement in shorter samples (smaller L/D). Industry considers an improvement of 4–6% in the energy product of current PMs as significant. The present and previous results demonstrate convincingly that alignment of PM powder in higher magnetic fields, such as the 9-T superconducting solenoid used in these studies, can indeed improve the properties of the PM.

To better understand the alignment process, we carried out an electromagnetic analysis using the computer code Opera. The alignment field is distorted by the self-field of the powder compact, and the distortion varies with several parameters,

such as the L/D ratio, the powder density, and the magnitude of the alignment field. Our results show that overall distortion of the alignment field in the powder compact is proportional to the density of the powder compact and inversely proportional to the magnitude of the alignment field. We also found that there is a maximum in the overall distortion when it is plotted against the L/D ratio. The information obtained from the electromagnetic analysis will help to make better PMs and provide guidance on scaling up to industrial production.

Finally, a selected number of samples were sent to ORNL for microstructure characterization so that engineering and microscopic magnetic properties of the processed PMs can be correlated. We also collaborated with Ames Laboratory (see next report) and processed a number of NdFeB powder samples for bonded magnets in the 9-T superconducting magnet facility at Argonne National Laboratory.

References

1. *2001 Annual Progress Report, Automotive Propulsion Materials*, U. S. Department of Energy, Office of Energy Efficiency and Renewable Energy, Office of Transportation Technologies, Washington, D.C.

FY 2002 Publications/Presentations

T. M. Mulcahy, J. R. Hull, E. Rozendaal, and J. H. Wise, "NdFeB Magnets Aligned in a 9-Tesla Superconducting Solenoid," presented at the 17th International Workshop on Rare Earth Magnets and their Applications, Newark, Delaware, August 18–22, 2002.

T. M. Mulcahy and J. R. Hull, "A Superconducting Solenoid and Press for Permanent Magnet Fabrication," presented at the 2002 Applied Superconductivity Conference, Houston, Texas, August 4–9, 2002.

B. Development of Improved Powder for Bonded Permanent Magnets

Iver E. Anderson, R. William McCallum, and Matthew J. Kramer

Metallurgy and Ceramics Program

Ames Laboratory, Iowa State University

Ames, IA 50011

(515) 294-9791; fax: (515) 294-8727; e-mail: andersoni@ameslab.gov

DOE Technology Development Manager: David Hamilton

(202) 586-2314; fax: (202) 586-1600; e-mail: david.hamilton@ee.doe.gov

Contractor: Ames Laboratory, Iowa State University, Ames, Iowa
Prime Contract No.: W-7405-Eng-82

Objectives

- Increase the maximum operating temperature of electric drive motors from 150 to 200°C while maintaining sufficient operating characteristics.
- Reduce the cost of permanent magnet (PM) material in electric drive motors through the use of bonded magnets and injection molding technologies for high-volume net-shape manufacturing.

Approach

- Develop innovative PM alloy design and processing technology for production of improved PM alloy powders for bonded magnets with a tolerance for high temperatures.
- Investigate alloy design improvements through melt-spinning methods, with the specific goal of developing an improved spherical magnet alloy powder through gas atomization processing.
- Develop an enhanced gas atomization process, along with a gas-phase powder surface reaction capability, for production and environmental protection of powder for bonded magnets.
- Explore the effect of a novel crystallization/alignment procedure at high magnetic field in collaboration with Argonne National Laboratory (ANL).
- Conduct experimental magnet molding trials on as-atomized and annealed magnet powders to characterize bonded magnet properties in collaboration with Oak Ridge National Laboratory (ORNL).

Accomplishments

- Demonstrated and quantified quench compatibility between melt spinning and gas atomization in ribbon and powder samples of experimental PM alloys for bonded magnets.
- Demonstrated improved high-temperature magnetic stability in preliminary work on a design approach that uses an alternative magnet alloy.
- Produced an increased yield of amorphous magnet alloy powders, suitable for controlled annealing to enhance bonded magnet properties, using modified high-pressure helium atomization processing.
- Demonstrated a fluidized bed fluorination process concept for magnet alloy powders, resulting in improved resistance to air oxidation of coated powder in initial testing.

Future Direction

- Proceed with the development path for a new family of PM alloys to boost coercivity at elevated temperatures, adjusting alloy constituents to balance gains in ambient-temperature magnetic strength and high-temperature magnetic stability. Perform test of required quenchability for gas atomization.
- Continue parallel alloy development path with highly quenchable alloys (Nd₂Fe₁₄B-based) that exhibit high magnetic strength at ambient temperature and that may gain high-temperature magnetic stability from extrinsic effects.
- Develop a gas-phase reaction coating process for atomized PM alloy powder beyond the initial concept to protect PM powders during the injection molding process and bonded magnet use.
- Characterize the magnetic properties of bonded magnets as a function of process variables, especially modifications of crystallization conditions and temperature (up to 200EC), in collaboration with ORNL and an industrial partner.

Introduction

To meet the cost and performance objectives of advanced electric drive motors for automotive applications, it is essential to improve the alloy design and processing of PM powders. To enable the widespread introduction of electric drive automobiles, two primary objectives to be pursued for PM materials are (1) to increase the useful operating temperature for magnets to 200EC and (2) to reduce the active magnet material cost to about 25% of its current level. Currently, magnet material can operate in temperatures ranging from 120 to 150EC, and the finished cost of sintered magnetic material is approximately \$90/kg. As an alternative PM material form, polymer-bonded particulate magnets offer the benefit of greatly simplified manufacturing, but at a more moderate level of stored magnetic energy that is still compatible with innovative PM motor designs. However, to exploit the potential of bonded PM materials for such motors, it is necessary to develop a particulate magnet material with high-temperature properties that can be loaded to a high volume fraction in an advanced polymer binder. Improving materials and processing to allow for increased operating temperature and mass production of net-shape bonded magnets by gas atomization and injection molding will be a significant advance toward high-volume production of advanced electric drive motors at reduced cost.

Approach

Innovative PM alloy design and processing technology will be developed for production of

improved PM alloy powders for bonded PM magnets with a tolerance for high temperatures. Melt-spinning will be used to select alloy modifications that boost coercivity at elevated temperatures (up to 200EC) and improve alloy quenchability for optimum yield from a gas atomization process. This effort builds on an alloy concept that was patented by Ames Laboratory. A modified high-pressure gas atomization process will be developed for the improved PM alloys to enhance the yield of spherical, rapidly solidified powder. This work furthers another Ames Laboratory patented technology. A gas-phase reaction coating process will be developed to enable enhanced environmental protection of fine atomized powder without degrading magnetic properties or molding rheology, building on recent studies of fluidized bed fluorination of similar rare earth alloy powders. A model polymer will be selected and used to test injection molding properties for high-temperature bonded magnets. The effects of a conceptual crystallization/alignment procedure conducted at a high magnetic field [8 Tesla (T)] will be investigated in collaboration with ANL. The magnetic properties of bonded powder samples will be determined as a function of loading fraction, powder size, annealing schedule, coating treatment, and temperature, up to a maximum of 200EC. Some of the bonded magnets also will be provided to ORNL for additional characterization. To improve the potential for successful technology transfer, industrial interactions have been emphasized at Ames Laboratory. These include work with Magnequench International (Raleigh-Durham, North Carolina) on alloy design and rapid solidification processing

through a DOE cooperative research and development agreement on advanced sensors and control of the melt-spinning process.

Results

Innovative PM alloy design and processing technology is being developed for production of improved PM alloy powders for bonded PM magnets with tolerance for high temperatures. Melt-spinning methods generated ribbon samples that can be crushed into particulate (see Figure 1) and that permit rapid alloy design modifications. Modified high-pressure gas atomization allowed production of enhanced yields of spherical, rapidly solidified powder (see Figure 1) of the improved PM alloys for magnetic characterization, for development of a

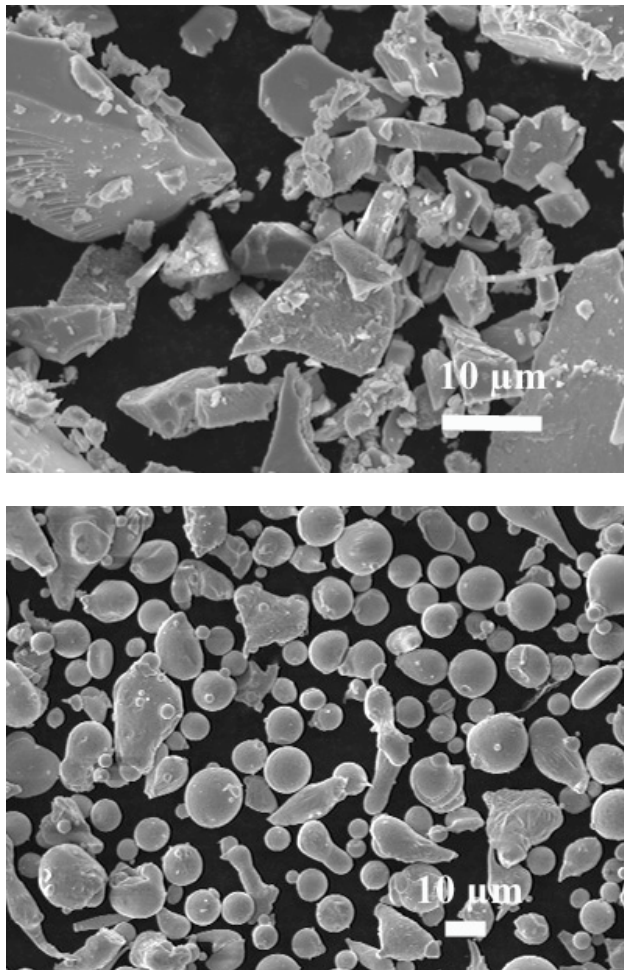


Figure 1. A micrograph from a scanning electron microscope shows fragmented flake powder from melt spun ribbon (*top*), compared with spherical powder from the high-pressure gas atomization process (*bottom*).

protective coating process, and for development of bonded magnet processing methods. Modified high-pressure helium atomization processing produced an increased yield of amorphous magnet alloy powders, suitable for controlled annealing to enhance bonded magnet properties.

Quench compatibility between melt spinning and gas atomization has been demonstrated and quantified in ribbon and powder samples of experimental PM alloys for bonded magnets. Figure 2 shows magnetic hysteresis loops for melt spun ribbon samples and gas atomized powder of the same magnet alloy powder in both the as-solidified and annealed condition. The magnetic characterization results for the ribbon sample with a wheel speed of 16m/s seem compatible with the results for powder of a diameter of <25µm in this example.

A gas-phase reaction coating process, fluidized bed fluorination, is being developed to enable enhanced environmental protection of fine atomized powder without degrading magnetic properties or molding rheology. The effectiveness of this process can be indicated by the Auger electron spectroscopy results shown in Figure 3. The depth of penetration

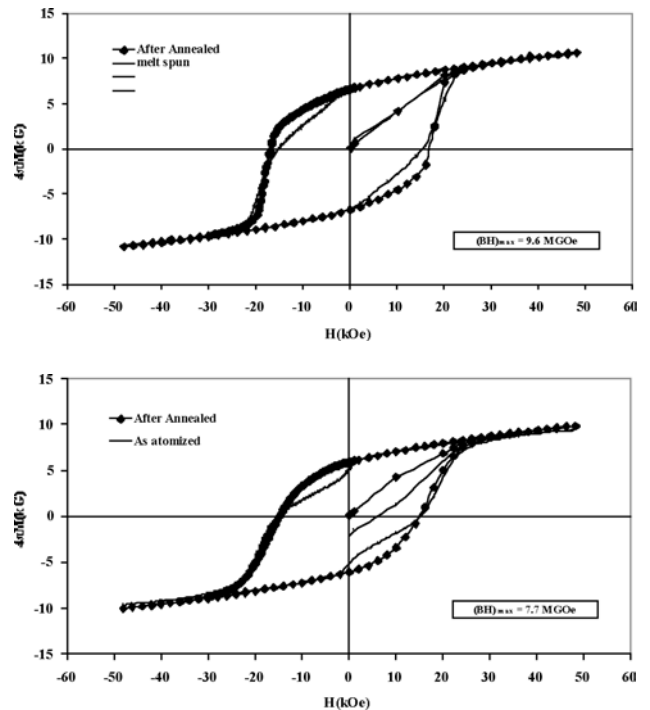


Figure 2. Comparison of magnetic hysteresis measurements for melt spun ribbon (*top*) and for gas atomized powder (*bottom*) of the same magnet alloy.

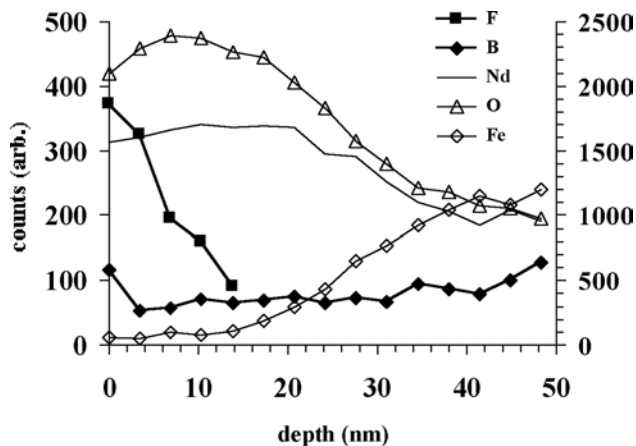


Figure 3. Scanning Auger electron spectroscopy depth profile showing the presence of a 15-nm fluorine-containing layer on the surface of treated powders.

of fluorine appears to be about 15 nm, suggesting the formation of NdF_3 on the surface of this powder particle.

Improved high-temperature magnetic stability has been shown in preliminary work on an alternative magnet alloy design approach with significant patent potential. The alloy design appears to stabilize coercivity and remnance at elevated temperatures (tested at up to 127EC) in the data that are presented in Table 1, compared with the best data for commercial powder products available from Magnequench International.

Some experimental magnet material annealing trials were performed at ANL to investigate the effect of a high-energy alignment procedure. Crystallization annealing experiments under high (8 T) magnetic field were performed at ANL to investigate the potential for alignment of new magnetic grains from an amorphous parent phase in melt spun ribbon samples of a $Nd_2Fe_{14}B$ -Ti-C magnet alloy. Polyphenyl sulfide has been selected as the model polymer for testing injection-molding

properties for high-temperature bonded magnets in collaboration with industrial partners. Industrial interactions have been initiated with both Arnold Engineering and Magnequench International to develop relevant comparisons of bonded magnet samples.

Conclusions

New alloy design work with a melt-spinning approach can use a quench rate based on wheel speeds of about 16 m/s to produce the magnetic properties of as-atomized (Ar) powders with a diameter of $<25 \mu m$ (approximately). A novel alloy design approach for high-temperature magnetic stability has the potential for enhanced ambient-temperature energy product with a further reduction of temperature coefficient, better for traction motor applications than the current commercial powders. Melt-spun ribbons of $Nd_2Fe_{14}B$ -Ti-C magnet alloy in a partially crystallized state appear to have insufficient anisotropy in paramagnetic susceptibility to affect crystal growth alignment during annealing in a dc magnetic field at temperatures of as low as $650^\circ C$. Helium atomization processing may be adopted as a standard practice to maximize the yield of amorphous and microcrystalline magnet alloy powders as precursors of high-performance bonded magnets. Fluidized bed fluorination appears promising for developing improved oxidation and corrosion resistant coatings on magnet alloy powders based on $Nd_2Fe_{14}B$.

Bibliography

R. W. McCallum, K. W. Dennis, B. K. Lograsso, and I. E. Anderson, "Method of Making Bonded or Sintered Permanent Magnets," U.S. Patent 5,240,513, August 31, 1993.

Table 1. Magnetic properties and temperature coefficient of "high-performance" magnetic materials

	MQP-S-9-8	MQP-O	MQ1-8-13	X5-132B
B_r (kG)	6.8–7.2	7.9–8.2	6.0–6.4	6.1
$(BH)_{max}$ (MGOe)	8.5–10.0	12.6–14.0	7.7	8.1
Intrinsic coercivity H_{ci} (kOe)	8.0–9.5	11–14	11	15
Coercive force H_c (kOe)	4.8–5.3	6.2–7.0	5.2	5.5
Temperature coefficient for B_r	$-0.11 \%/C^\circ$		$-0.13 \%/C^\circ$	$-0.07 \%/C^\circ$
	(to $100^\circ C$)		(to $100^\circ C$)	(to $130^\circ C$)
Temperature coefficient of H_{ci}	$-0.4 \%/C^\circ$		$-0.37 \%/C^\circ$	$-0.33 \%/C^\circ$
	(to $100^\circ C$)		(to $100^\circ C$)	(to $130^\circ C$)

I. E. Anderson, B. K. Lograsso, and R. L. Terpstra, "Environmentally Stable Reactive Alloy Powders and Method of Making Same," U.S. Patent 5,372,629, December 13, 1994.

R. W. McCallum, K. W. Dennis, B. K. Lograsso, and I. E. Anderson, "Method of Making Bonded or Sintered Permanent Magnets (continuation)," U.S. Patent 5,470,401, November 28, 1995.

I. E. Anderson and R. L. Terpstra, "Apparatus for Making Environmentally Stable Reactive Alloy Powders," U.S. Patent 5,589,199, December 31, 1996.

I. E. Anderson, B. K. Lograsso, and R. L. Terpstra, "Environmentally Stable Reactive Alloy Powders and Method of Making Same," U.S. Patent 5,811,187, September 22, 1998.

R. W. McCallum and D. J. Branagan, "Carbide/Nitride Grain Refined Rare Earth-Iron-Boron Permanent Magnet and Method of Making," U.S. Patent 5,803,992, September 8, 1998.

R. W. McCallum and D. J. Branagan, "Carbide/Nitride Grain Refined Rare Earth-Iron-Boron Permanent Magnet and Method of Making," U.S. Patent 5,486,240, January 23, 1996.

D. J. Branagan and R. W. McCallum, "The Effects of Ti, C, and TiC on the Crystallization of Amorphous $\text{Nd}_2\text{Fe}_{14}\text{B}$," *J. Alloys and Compds.*, **245** (1996).

D. J. Branagan, T. A. Hyde, C. H. Sellers, and R. W. McCallum, "Developing Rare Earth Permanent Magnet Alloys for Gas Atomization," *J. Phys. D: Appl. Phys.*, **29**, p. 2376 (1996).

M. J. Kramer, C. P. Li, K. W. Dennis, R. W. McCallum, C. H. Sellers, D. J. Branagan, L. H. Lewis, and J. Y. Wang, "Effect of TiC Additions to the Microstructure and Magnetic Properties of $\text{Nd}_{0.5}\text{Fe}_{84.5}\text{B}_6$ Melt-spun Ribbons," *J. Appl. Phys.*, **83**(11), pt. 2, p. 6631 (1998).

D. J. Branagan and R. W. McCallum, "Changes in Glass Formation and Glass Forming Ability of $\text{Nd}_2\text{Fe}_{14}\text{B}$ by the Addition of TiC," *J. Alloys and Compds.*, **244** (1–2), p. 40 (1996).

Publications/Presentations

Iver E. Anderson, Youwen Xu, Kevin Dennis, R. William McCallum, and Matthew J. Kramer, "Permanent Magnet Alloy Development for Gas Atomization Processing," 2002 International Conference on Powder Metallurgy and Particulate Materials, Orlando, Fla., June 16–21, 2002.

C. Carbon Foam for Electronics Cooling

J. W. Klett, April McMillan, and Nidia Gallego

Carbon and Insulation Materials Technology Group

Oak Ridge National Laboratory

P.O. Box 2008, MS 6087, Bldg. 4508

Oak Ridge, TN 37831-6087

(865) 574-5220; fax: (865) 576-8424; e-mail: klettjw@ornl.gov

DOE Technology Development Manager: Nancy Garland

(202) 586-5673; fax: (202) 586-9811; e-mail: nancy.garland@ee.doe.gov

ORNL Technical Advisor: David Stinton

(865) 574-4556; fax: (865) 574-6918; e-mail: stintondp@ornl.gov

Contractor: Oak Ridge National Laboratory, Oak Ridge, Tennessee
Prime Contract No.: DE-AC05-00OR22725

Objective

- Coordinate with automotive partners to develop a carbon foam heat exchanger and heat sink designs to dissipate 30 W/cm² using current cooling fluids, achieving a targeted heat flux/weight ratio of >30% over current standards.

Approach

- Study fundamental mechanisms of heat transfer utilizing the carbon foam and engineering solutions to reduce pressure drop.
- Compare results with existing data on heat sinks and current heat exchanger designs.
- Collaborate with original equipment manufacturers (OEMs) on designs and explore options together.

Accomplishments

- Demonstrated heat transfer capabilities of 22 W/cm² with a reduction in pressure drop of more than an order of magnitude compared with previous tests, yielding a heat sink with pressure drops equivalent to those of metal foams but with higher heat transfer.
- Began environmental testing according to SAE J1211, "Recommended Environment Practices for Electronic Equipment."

Future Direction

- Continue collaboration with industrial suppliers and OEMs for enhanced design studies.
 - Conduct processing studies to increase understanding of the effects of processing conditions on foam microstructure and thermal and mechanical properties (strength, durability, and toughness).
 - Develop relationships with industrial partners to get several more licensees for the fabrication of the foam, thereby improving competition and reducing costs.
 - Continue development of the foam extrusion process.
-

Introduction

Approximately two-thirds of the world's energy consumption is wasted as heat (e.g., incandescent light bulbs, internal combustion engines, air conditioning, power plants). This situation is likely to get worse as the power levels of computer processors and other electronic devices increase. Computer chips with power levels of up to 1000 W may be commonplace in less than 5 years; unfortunately, the means to cool these chips are not available at an affordable price. High-efficiency heat exchangers are being incorporated into computers and electronics to recover some of the heat lost and increase efficiencies. The primary function of the heat exchanger in these applications is to reduce the temperature of the electronics, improving both life and reliability. The second task of the heat exchanger is to recover the energy for use in other applications, thereby reducing the total energy consumed. Unfortunately, most heat exchangers dissipate captured heat from the electronics as low-quality heat (a very low temperature compared with the ambient). Subsequently, this recovered heat is simply dumped to the ambient environment and wasted.

A unique graphite foam developed at the Oak Ridge National Laboratory (ORNL) and licensed to Poco Graphite, Inc., promises to allow for novel, more-efficient heat exchanger designs that can possibly dump high-quality heat, allowing recovery of energy for other applications. This unique graphite foam (Figure 1) has density values of between 0.2 and 0.6 g/cm³ and a bulk thermal conductivity of between 40 and 187 W/m·K. The ligaments of the foam exhibit a thermal conductivity higher than that of artificial diamond. The high conductivity, combined with a very accessible surface area (>4 m²/g), results in overall heat transfer coefficients for foam-based heat exchangers that are up to two orders of magnitude greater than those of conventional heat exchangers. As a result, foam-based heat exchangers could be dramatically smaller and lighter than conventional designs.

Power Electronics Cooling

In previous research, it was shown that graphite foam performed substantially better in transferring heat in a smaller package than the existing heat transfer mediums (Figure 2). However, the biggest

concern is the overall large pressure drop through the

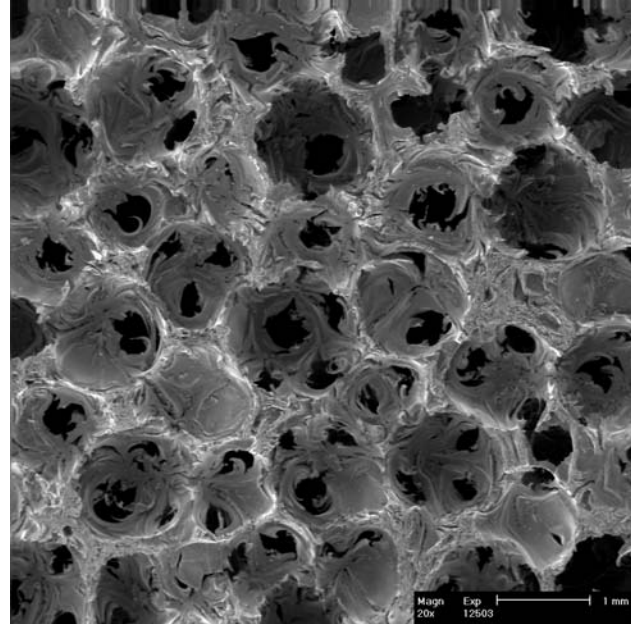


Figure 1. Graphite foam material developed at ORNL.

foam. A large pressure drop requires large amounts of pumping power and thus increases the parasitic losses. Therefore, research was focused on engineering a design using the foam in which the heat transfer remains high, but the pressure drop is reduced. Several designs were considered, i.e., horizontal blind holes, vertical blind holes, and corrugation.

To characterize the behavior of a simulated heat sink, a test chamber was built that allowed measurements of the power dissipation capacity. As shown in Figure 3, the foam was mounted to an aluminum plate (usually by brazing) and placed in a cavity where the cooling fluid flows. The system was designed with no gap around the foam, forcing the fluid to pass through the pores of the foam. The system was sealed with O-rings, and pressure taps were inserted into the chamber to measure the pressure drop of the foam heat sink. A simulated power inverter, capable of generating up to 800 W (32 W/cm²), was mounted to the aluminum plate. As the cooling fluid passed through the system, the temperatures of the heater and inlet and outlet fluid were measured. The overall heat transfer coefficient (U_o) was calculated from Eq. (1) where ΔT_{LM} is the log mean temperature difference between the heater and the cooling fluid, A is the area (foot print) of

foam attached to the aluminum plate, and q is the

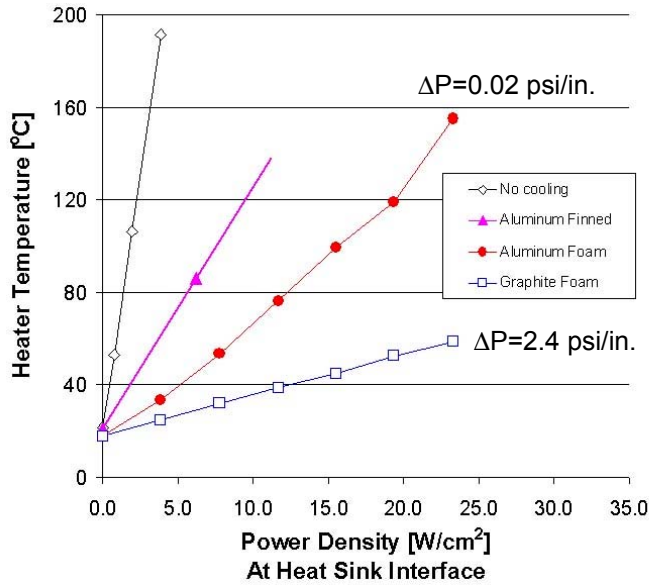


Figure 2. Simulated power electronic temperature vs power density for various heat sinks.

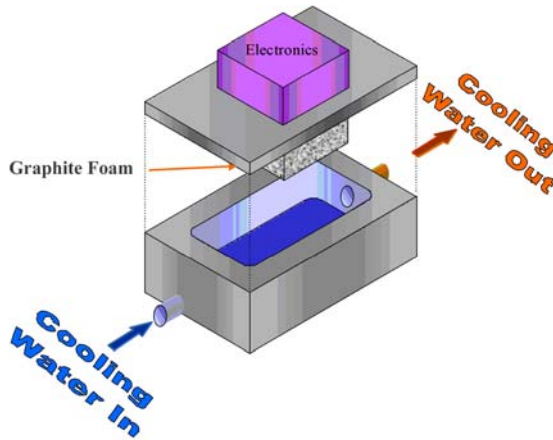


Figure 3. Schematic of test rig to evaluate heat sink geometries.

used to measure heat transfer coefficients with different base plates, foam geometries, and other heat sink devices, such as aluminum foam.

$$U_o = q / (A \cdot \Delta T_{LM}) \tag{1}$$

Figure 4 illustrates the design concept of corrugation to reduce pressure drop. In the solid block, the fluid has to pass through a given length of foam with tiny pores. However, in the corrugated foam, the overall length of the heat sink is the same, but the flow length is reduced dramatically. Since the pressure drop is linearly related to the flow

heat dissipated to the cooling fluid. This test rig was

Water flow: 0.75 gpm

Aluminum Foam:

ERG DUOCEL™ 40 ppi
Density = 0.33 g/cm³
Thermal conductivity = 12 W/m·K

Graphite Foam

PocoFoam™
Density = 0.54 g/cm³
Thermal conductivity = 150 W/m·K

length, the overall pressure drop can be reduced by more

than an order of magnitude if the flow length is reduced by a similar amount. Figure 5 illustrates the effects of corrugating a solid graphite foam heat sink. As can be seen, the heat transfer was still dramatically greater than that of the aluminum foam, but the pressure drop was reduced to 7% of that of the original solid graphite foam heat sink. Obviously, this design needs to be optimized, but it was demonstrated that the pumping power required for the foam can be dramatically reduced.

Environmental Testing

Another focus of this year’s effort has been the testing of the foams in different environmental conditions. As was recommended by the Electrical and Electronic Tech Team, testing is being conducted using SAE J1211, “Recommended Environment Practices for Electronic Equipment.” A test plan was developed and testing has begun. Testing includes thermal cycling, humidity, salt spray, immersion and splash, dust bombardment, and vibration. The test plan requires the use of five different forms of the graphite foam in each test (control, nickel plated, chromium plated, brazed to copper and brazed to aluminum). Each sample will be evaluated both physically and thermally prior to testing and post-testing. Then compression testing

will be conducted to determine effects on mechanical properties of the foams.

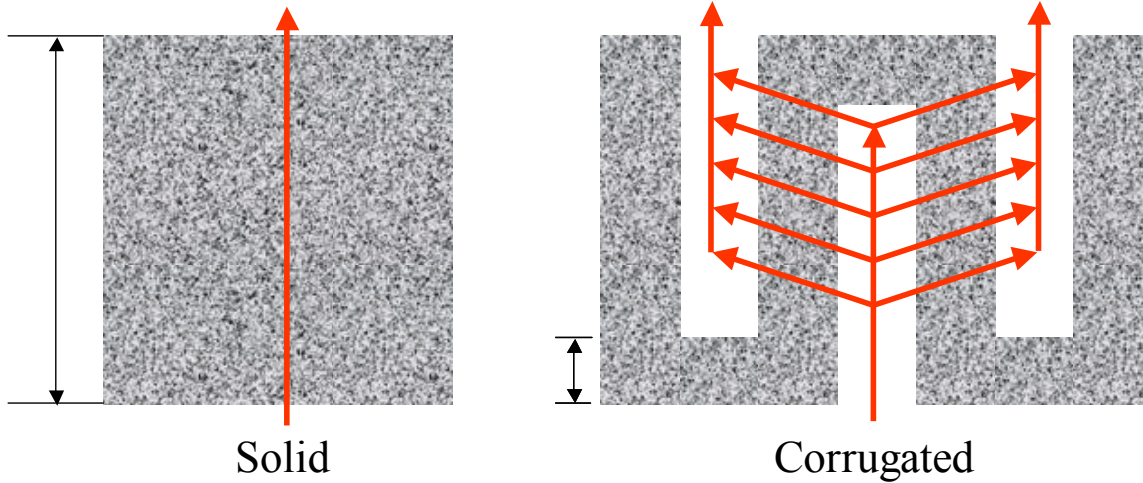
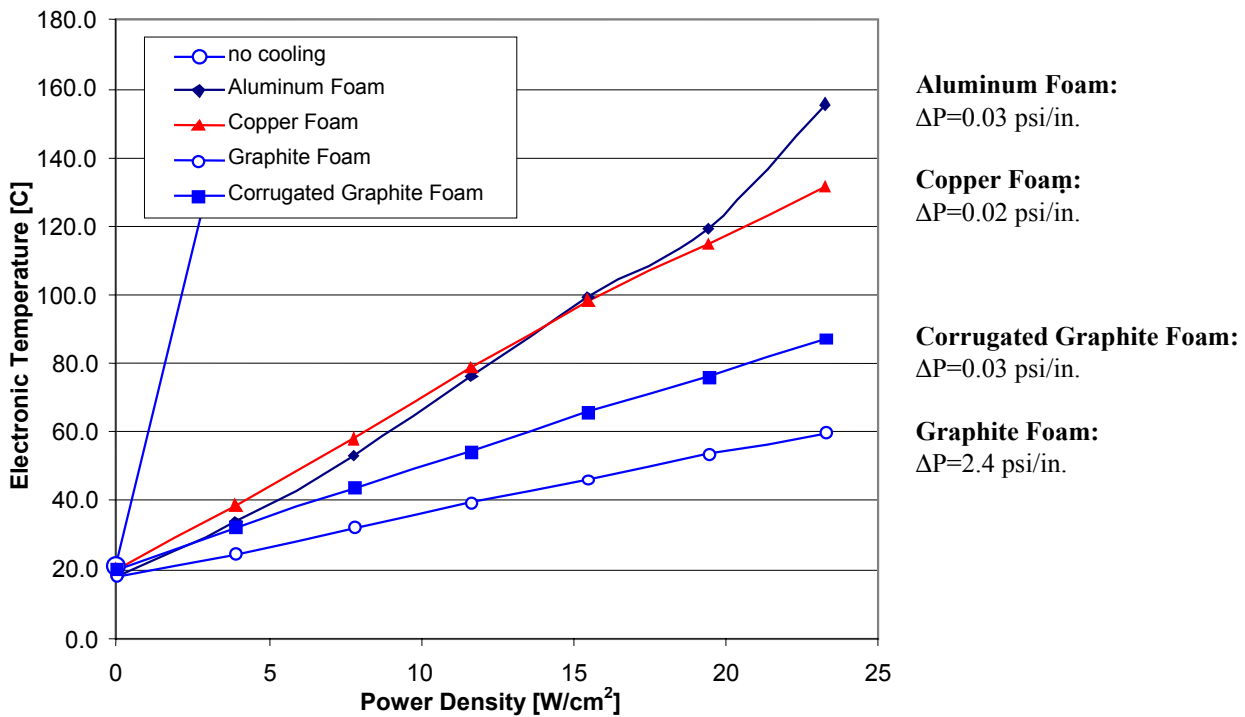


Figure 4. Schematic illustrating the effects of corrugation on the resulting pressure drop.



Aluminum Foam:
 $\Delta P=0.03$ psi/in.

Copper Foam:
 $\Delta P=0.02$ psi/in.

Corrugated Graphite Foam:
 $\Delta P=0.03$ psi/in.

Graphite Foam:
 $\Delta P=2.4$ psi/in.

Figure 5. Heat transfer properties of corrugated graphite foam with other foam heat sinks.

Conclusions

It has been shown that the graphite foam heat sinks can be engineered to reduce the overall pumping power needed while maintaining high heat transfer coefficients. Through modification of the slot thickness, web thickness, and flow length,

corrugated graphite foams can be almost as effective as a solid block of graphite foam in removing heat,

but maintain a low pressure drop. In fact, it was shown that the corrugation yielded a pressure drop with water to a level similar to that exhibited by copper and aluminum foams. This research further

demonstrates the tailorability of the graphite foam into an excellent heat sink for power electronics.

Environmental durability testing has begun according to SAE J1211, and results are expected sequentially over the next year.

References

“Recommended Environment Practices for Electronic Equipment,” SAE J1211, Society of Automotive Engineers, 1978.

FY 2002 Publications

J. Klett, A. D. McMillan, and Dave Stinton, “Modeling Geometric Effects on Heat Transfer with Graphite Foam,” 26th Annual Conference on Ceramic, Metal, and Carbon Composites, Materials, and Structures, Cocoa Beach, Florida, January 2002.

J. Klett, A. D. McMillan, Lynn B. Klett, “The Effect of Thermal Cycling on Prototype Graphite Foam Heat Exchangers,” 26th Annual Conference on Ceramic, Metal, and Carbon Composites, Materials, and Structures,” Cocoa Beach, Florida, January 2002.

Patents Issued

J. W. Klett, “Process for Making Carbon Foam,” U.S. Patent Number 6,033,506, March 7, 2000.

J. W. Klett and T. D. Burchell, “Pitch-Based Carbon Foam Heat Sink with Phase Change Material,” U.S. Patent Number 6,037,032, March 14, 2000.

J. W. Klett, “Pitch-Based Carbon Foam and Composites,” U.S. Patent Number 6,261,485, July 17, 2001.

J. W. Klett, “Pitch-Based Foam with Particulate,” U.S. Patent Number 6,287,375, September 11, 2001.

J. W. Klett, “Method for Extruding Pitch-based Carbon Foam,” U.S. Patent Number 6,344,159, February 5, 2002.

J. W. Klett, “Pitch Based Carbon Foam and Composites,” U.S. Patent Number 6,387,343, May 14, 2002.

J. W. Klett, “Method of Casting Pitch-Based Carbon Foam,” U.S. Patent Number 6,398,994, June 4, 2002.

J. W. Klett and T. D. Burchell, “Pitch-based Carbon Foam Heat Sink with Phase Change Material,” U.S. Patent Number 6,399,149, June 4, 2002.

D. dc Bus Capacitors for Hybrid Vehicle Power Electronics

B. A. Tuttle, G. Jamison, D. Wheeler, J. S. Wheeler, and D. Dimos

Sandia National Laboratories

P.O. Box 5800, MS 1411

Albuquerque, NM 87185-1405

(505) 845-8026; fax: (505) 844-2974; e-mail: batuttle@sandia.gov

DOE Technology Development Managers: David Hamilton

(202) 586-2314; fax: (202) 586-1600; e-mail: david.hamilton@ee.doe.gov

Rogelio Sullivan

(202) 586-8042; fax: (202) 586-1600; e-mail: rogelio.sullivan@ee.doe.gov

Contractor: Sandia National Laboratory, Albuquerque, New Mexico

Prime Contract No.: 04-94AL85000

Objectives

- Develop a replacement technology for the currently used aluminum electrolytic dc bus capacitors for hybrid electric vehicles.
- Develop a high-temperature polymer dielectric film technology that has dielectric properties technically superior to those of aluminum electrolytic dc bus capacitors and is of comparable or smaller size.
- Scale up cost-competitive polymer film dielectric technology: (1) develop a continuous process for dielectric sheet fabrication and (2) fabricate prototype capacitors.

Approach

- Work with automobile design and component engineers, dielectric powder and polymer film suppliers, and capacitor manufacturers to determine state-of-the-art capabilities and to define market-enabling technical goals.
- Develop a project plan with automobile manufacturers and large and small capacitor companies to fabricate polymer dielectric sheets suitable for the manufacture of capacitors for hybrid electric vehicles.
- Synthesize unique conjugated polyaromatic chemical solution precursors that result in dielectric films with low dissipation factors (DFs) and excellent high-temperature dielectric properties.
- Develop polymer film processes and technologies that will lower costs to permit competitive high-volume capacitor manufacturing.
- Interact with Oak Ridge National Laboratory (ORNL) with regard to mechanical characterization of films.

Accomplishments

- Invented chemical synthesis procedures that resulted in polymer films with four times the energy density of commercial polyphenylene sulfide at 110EC. Scaled-up hydroxylated polystyrene or polyvinyl phenol (PVP) films exhibited dielectric constants of 4.7 and DFs of 0.009 at up to 110EC, meeting technical requirements for commercialization.
- Collaborated with TPL, Inc., to develop a continuous process for Sandia National Laboratories' (SNL's) dielectric film fabrication and fabricated 25-cm-wide and 20-m-long rolls of dielectric film that had breakdown strengths of greater than 4 MV/cm from -40E to 110EC.
- Collaborated with Brady Corporation, a high-volume capacitor manufacturer, to co-develop fabrication procedures for 25-cm-wide, 90-m lengths of SNL dielectric film on a pilot production prototype coater.

- Collaborated with Steiner Corporation to develop a high-volume electrode process for our dielectric films. Developments are still needed to provide adequate release from the underlying carrier.
- Collaborated with ORNL to characterize mechanical properties of PVP films.

Future Direction

- Perform extensive electric field and temperature characterization to determine that the SNL polyfilm dielectrics fabricated using high-volume processes will meet FreedomCAR requirements for breakdown field and DF for temperatures from -40E to 110EC.
- Perform extensive electric field and temperature characterization on 1- μ F to 10- μ F wound capacitors to determine if they will meet General Motors (GM) requirements. Supply capacitors to GM for testing in inverter-type environments.
- Interface with Brady Corporation and TPL to fabricate large rolls of slit dielectric polymer sheet (10-kg lots) on a production caster that are suitable for fabrication of multilayer capacitors (20 to 200 μ F).
- Along with GM, evaluate large-value (20- μ F to 200- μ F) capacitors fabricated by vendor(s) in simulated electric hybrid vehicle environments.

Results

Strategy and Interactions

SNL has actively interacted with a number of representatives from the automobile industry to obtain their perspective on what is needed for hybrid electric vehicles. In FY 2002, SNL has continued its emphasis on the development of polymer film dielectrics for two reasons. First, GM has been adamant about soft-breakdown dielectric film technology—a phenomenon that bulk ceramic capacitors do not exhibit. Second, emphasis on polymer dielectrics provides greater balance of the DOE effort between polyfilm and ceramic technologies, as requested by the Electrical and Electronics (E/E) Tech Team. SNL has developed a close working relationship with development personnel in the Advanced Technology Vehicles Division of GM. SNL has modified project plans for the development of polymer film dielectrics for hybrid vehicle applications according to E/E Tech Team recommendations.

These interactions led us to the conclusion that the most viable replacement technology for electrolytic dc bus capacitors by 2004 was multilayer polymer film capacitors. Reducing the size of the polymer capacitors was most often cited by automobile design engineers and capacitor manufacturers as a needed technology-enabling breakthrough. In addition, it is necessary to improve high-temperature (110EC) performance while keeping the technology cost-competitive. For

polymer film dielectrics, a commercialization goal of a dielectric constant of 6 and a DF of less than 0.01 was initially agreed to by AVX/TPC and GM. However, based on the GM 2004 criterion for capacitance density of 2.0 μ F/cm³, the team agreed that if a polyfilm of $K = 4.5$ could be developed that could meet the temperature requirements, it would be suitable for scale-up activities.

The initial scale-up strategy consisted of the following steps: (1) develop a polymer film technology that meets requirements, (2) synthesize 10-kg to 20-kg batches, (3) develop a continuous process for 3- μ m-thick polymer films, and (4) fabricate them into prototype capacitors. This approach had to be modified because the synthesis and the development of a continuous process had to be broken down into multiple steps to be accomplished. While an initial polymer film technology, hydroxylated polyphenylene (PP+OH), was developed that met all criteria and was exceedingly low-loss, its cost was prohibitive. Although SNL was successful in developing three new processes that reduced the cost of the PP+OH technology by a factor of ten, costs were still not satisfactory for FreedomCAR applications. Thus a second polymer film technology, PVP, was developed that exhibited more loss than PP+OH but is 10 to 100 times more cost-efficient. This new technology has four times the energy-density-handling capability at 110EC of the commercial standard of polyphenylene sulfide.

Inverter designs and operating conditions for dc bus capacitors vary from manufacturer to manufacturer. GM has presented 2- to 5-year and 10-year goals for dc bus capacitors that other auto manufacturers feel are satisfactory milestones for the program. Specific goals for 2004 commercialization include (1) -40E to 110EC operation, (2) greater than 2 $\mu\text{F}/\text{cm}^3$ capacitance density, and (3) 575-V dc with 600-V peak for 50-ms operation. In addition, GM has requested fail-safe operation; Ford and DaimlerChrysler have not voiced as strong an opinion regarding the fail-safe criterion. The fail-safe criterion is analogous to soft breakdown of the dielectric, rather than catastrophic electrical discharge and mechanical failure that can be observed in bulk ceramic dielectrics. Soft breakdown occurs as a result of the vaporization of the thinner electrode layers of the polymer dielectric near electrical breakdown sites.

Based on these criteria, an individual dielectric layer thickness of approximately 3 μm for polyfilm capacitors is projected. These thickness values are based on operating field strengths of 2 MV/cm for the newly developed polyfilm capacitors. Based on these assumptions and on measurement of presently available commercial capacitors, size comparisons and capacitance densities of 500- μF dc bus capacitors for different technologies were obtained (Figure 1). Soft-breakdown behavior and lower cost are assets for polymer film capacitors. The projected polymer film capacitor volume is calculated assuming that 40% of the capacitor space is non-active and 200-nm-thick electrodes are used. Note that the volumetric capacitance efficiency for a $K = 4.5$ polyfilm capacitor of 2.4 $\mu\text{F}/\text{cm}^3$ exceeds the 2004 commercialization goal of 2 $\mu\text{F}/\text{cm}^3$.

Polymer Film Dielectric Development

SNL polymer film dielectric development has been based on the request from manufacturers that the new polyfilm dielectrics have voltage and temperature stability that is equivalent to that of present polyphenylene sulfide (PPS) technology. Thus a structural family of polymer dielectrics has been designed and synthesized to meet two of the most stringent requirements: (1) low dielectric loss and (2) extremely good temperature stability. Figure 2 shows a schematic diagram of Sandia's conjugated, polyaromatic-based structure and indicates the large number of molecular modifications to this structure that are possible. Our present effort emphasizes molecular engineering of higher-polarizability structures that will enhance dielectric constants yet retain acceptable dielectric loss characteristics. A patent disclosure has been initiated covering the design and synthesis techniques for this polymeric family.¹ Three initial molecular modifications to the base structure were made: (1) propyl bridge substitution, (2) sulfur bridge substitution, and (3) replacement of R-side groups with high-electronegativity fluorine ions to enhance polarizability.

For FY 2002, we have concentrated our efforts on the PVP film structural family. Synthesis routes for PVP films were designed and implemented because the cost of this technology was 1 to 2 orders of magnitude less than that of the PP+OH technology previously developed by SNL. Because of the chemical structure of the PVPs, it was postulated that these films would not have loss characteristics as good as those of the hydroxylated polyphenylene films. Although the PVP loss met specifications (DF <0.01) at 25EC, unacceptable loss

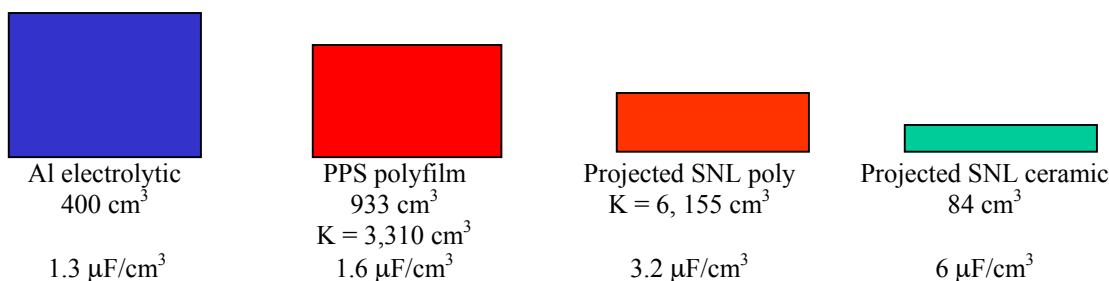


Figure 1. Size diagram of 500- μF dc bus capacitors of different technologies.

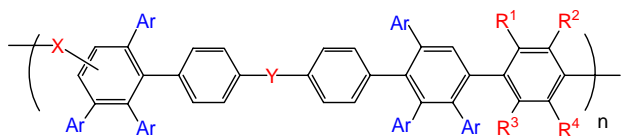


Figure 2. Schematic diagram of SNL conjugated polyaromatic film base structure.

(DF = 0.065) was measured at 110EC. A study was initiated to incorporate crosslinker chemistry into our PVP polymers to reduce the flexibility of the polymer chains and thus decrease dielectric loss. Development and incorporation of a VEctomer crosslinker chemistry reduced the loss to 0.01 at 110EC as shown in Figure 3. As expected, the dielectric constant also decreased. However, the dielectric constant of 4.7 is acceptable for hybrid vehicle applications and scale-up activities.

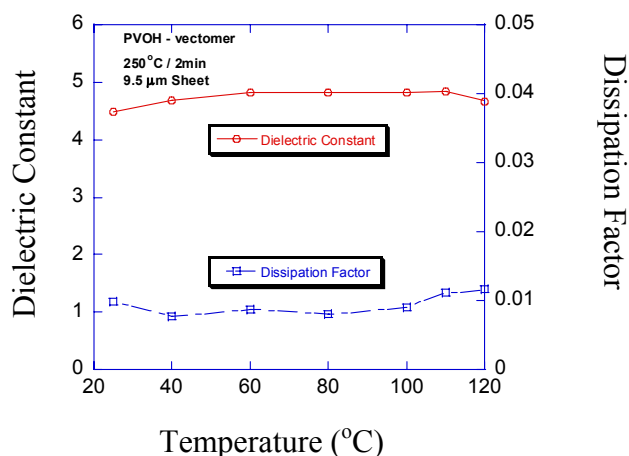


Figure 3. Dielectric constant and dissipation factor of SNL hydroxylated polystyrene film with VEctomer cross-linker.

Figure 4 is a pictorial chronology of our PVP film scale-up activities in FY 2002. Our technology evolved from 5 × 5-in. single-cast dielectric sheets [Figure 4(a)] to continuous slot-die-cast rolls of dielectric sheets of approximate 5 to 20 meter length in December 2001 [Figure 4(b)]. We worked with TPL of Albuquerque to fabricate these rolls. Development of technology that was more amenable to high-volume production required interaction with Brady Corporation of Milwaukee. We were able to cast 150-m lengths of 25-cm-wide polymer film using the Brady prototype caster in March of 2002 on 5-cm-diam. mandrills. A high-volume electrode

deposition process is another process that is essential to manufacturing large-value capacitors. Steiner Corporation deposited aluminum electrodes on SNL films using a proprietary high-volume manufacturing process. The slit and Steiner electrode roll are shown in Figure 4(c). A wound polymer capacitor with the metallized film roll is shown in Figure 4(d). Our dielectric film thickness is presently 4 to 5 μm.

A prototype PVP capacitor was fabricated using metallized paper electrodes. The metallized paper electrodes permitted electrical characterization of the dielectric without having to develop a sophisticated high-volume metallization technology. The dielectric for this capacitor was fabricated using a Brady Corporation prototype coater. The prototype coater at Brady Corporation is shown in Figure 5 during the coating of SNL PVP film on a Mitsubishi smooth Mylar carrier using a reverse Gravure roller configuration. Casting rates were ~1 m/min, and roughly 31 wt % SNL polymer was used in the coating solution. The dielectric film and metallized paper rolls were wound into 0.8 μF capacitors at SNL using a custom dielectric film winder. Termination electrode procedures were performed at TPL. Both capacitance and DF as a function of temperature are shown in Figure 6. The capacitance varies by ± 7% from -40°C to 55°C. DFs were below 0.01 for a temperature range that exceeded 100EC. The DF of 0.007 at 110EC was particularly encouraging. These film properties were considered to be acceptable for continuation of scale-up activities with this technology.

Summary

Critical economic and technical issues for improvements of dc bus capacitors for hybrid electric vehicles were determined through discussion and visitation with automobile design engineers, chemical synthesis companies, and capacitor manufacturers. PVP film dielectric development has been emphasized in FY 2002, and we have developed a multi-step project plan for large-scale commercialization of polymer film dc bus capacitors. In FY 2002, we developed, in conjunction with TPL, a continuous process for fabricating 5- and 20-m-long rolls of SNL PVP sheets. For high-volume production, Brady Corporation in Milwaukee was contacted. Near high-volume continuous casting techniques were

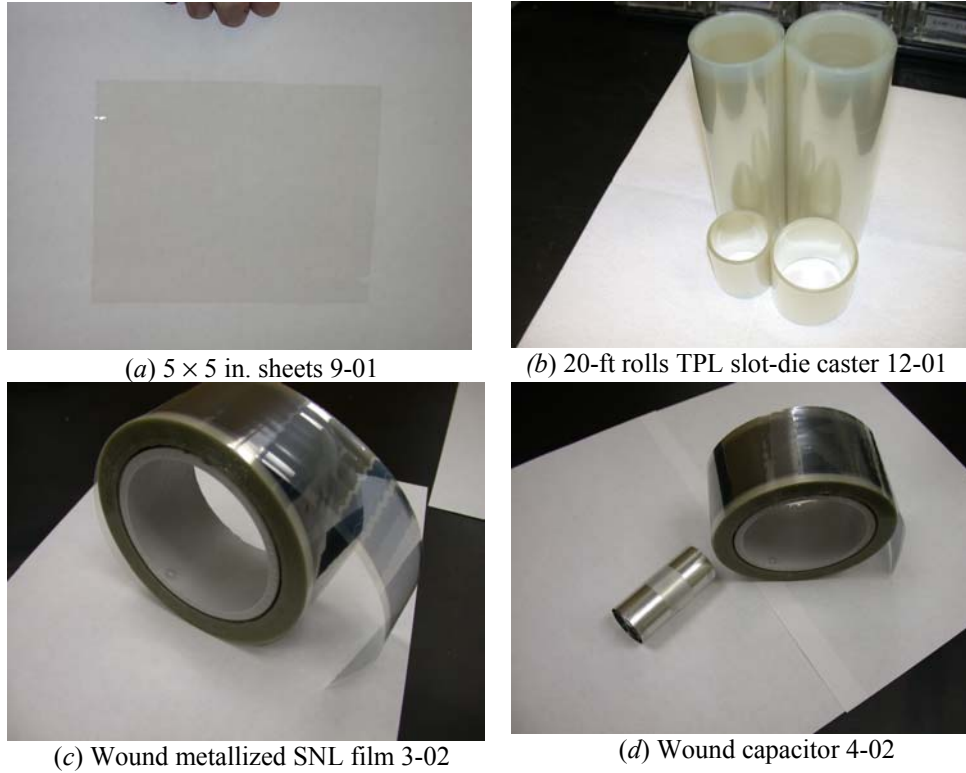


Figure 4. Pictorial chronology of FY 2002 SNL polymer film scale-up activities.



Figure 5. Brady pilot production coater with SNL film.

developed for SNL films on three separate trips to Brady Corporation using Brady’s prototype caster. We also interfaced with Steiner Corporation for high-volume aluminum electrode deposition. After the initial metallization, the film did not release satisfactorily from the underlying smooth Mylar carrier. This problem was attributed to additional curing that occurred during the metallization process. Solving this issue appears to be the final

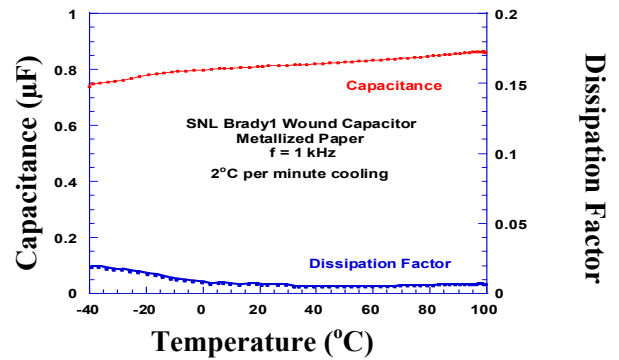


Figure 6. Capacitance and dissipation factor of SNL dielectric—metallized paper capacitor vs temperature.

hurdle before SNL films can be fabricated on the high-volume Brady production caster. Initial SNL polymer film wound capacitors of 1 µF capacitance were fabricated using metallized paper electrodes. These capacitors met the extended temperature requirements for hybrid electric and fuel cell vehicles. Future work includes further interfacing with Steiner Corporation to obtain high-quality SNL

polymer film dielectric using high-volume aluminum deposition procedures. Capacitors in the range of 1 to 4 μF range will be fabricated for high-temperature characterization by SNL. Further, GM will determine their suitability in inverter environments. In addition, we are supplying—on a continuous basis—dielectric films to Matt Ferber of ORNL from our scale-up activities. An understanding of mechanical property–process relationships is critical to developing film technology that exhibits adequate release from the underlying carrier and can thus be used for high-volume manufacturing. When these technical issues are solved, we will use the production scale coater at Brady Corporation to fabricate roughly 3500-m by 3.1-m rolls of polymer film. These film rolls will be used to fabricate a series of 200- μF capacitors for evaluation by SNL, ORNL, GM, Ford, and DaimlerChrysler.

Technical Disclosures

1. D. Wheeler and G. Jamison, “Novel Polymer Film Synthesis Routes of Voltage and Temperature Stable Dielectrics,” October 5, 1999.

Presentations

B. A. Tuttle, D. Wheeler, G. Jamison, and D. Dimos, “dc Bus Capacitors for PNGV Power Electronics,” pp. 27–32 in Automotive Propulsion Materials 2001 Annual Progress Report, October 2001.

B. A. Tuttle, P. G. Clem, D. Wheeler, G. Jamison, P. Yang, W. R. Olson, and J. S. Wheeler, “dc Bus Capacitors for Hybrid Electric Vehicle Power Electronics,” 26th Annual International Conference on Advanced Ceramics and Composites, Cocoa Beach, Florida, January 14, 2002 (invited presentation).

E. Mechanical Reliability of Electronic Ceramics and Electronic Ceramic Devices

M. K. Ferber, L. Riestler, C-H Hsueh, and M. Lance

Mechanical Characterization and Analysis Group

Oak Ridge National Laboratory

P.O. Box 2008, MS 6068, Bldg. 4515

Oak Ridge, TN 37830-6069

(865) 576-0818; fax: (865) 574-6098; e-mail: ferbermk@ornl.gov

DOE Technology Development Manager: Nancy Garland

(202) 586-5673; fax: (202) 586-9811; e-mail: nancy.garland@ee.doe.gov

ORNL Technical Advisor: David Stinton

(865) 574-4556; fax: (865) 241-0411; e-mail: stintondp@ornl.gov

*Contractor: Oak Ridge National Laboratory, Oak Ridge, Tennessee
Prime Contract No.: DE-AC05-00OR22725*

Objectives

- Predict and assess the mechanical reliability of electronic devices with emphasis on those used for automotive power electronics (e.g., capacitors).
- Correlate the mechanical characterization of polymer film capacitors developed by Sandia National Laboratories (SNL) to the dielectric behavior.

Approach

- Develop techniques to characterize polymer films developed by SNL and correlate mechanical behavior with dielectric behavior.
- Correlate mechanical performance of films as a function of processing.

Accomplishments

- Characterized three series of SNL polymer film samples using a mechanical properties microprobe.
- Developed low-cost grips for evaluating the room-temperature tensile stress-strain behavior of polymer films.

Future Direction

- Develop hardware and test procedures for characterizing polymer films as a function of temperature.
- Use the mechanical properties microprobe to track changes in polymer structure resulting from processing variations, as well as in-service use.

Introduction

A major focus of the power electronics effort in the Automotive Propulsion Materials Program is to develop a capacitor technology that will replace current electrolytic dc bus capacitors for power electronics modules in hybrid electric vehicles. The

ultimate objective is to make the power modules more compact while maintaining the tight voltage and temperature requirements. Because of the interest in polymer film capacitors, a collaboration with SNL was initiated to evaluate SNL's materials. Synthetic chemists at SNL are currently fabricating a

number of different temperature-stable polymers for the power electronics program. The 2004 goal is to have a polymer film dielectric that can operate continuously at 110EC. Although these films are expected to be similar to polyphenylene sulfide in terms of properties, they are truly unique films that have not been used before by the capacitor industry. Therefore, the goal of this project is to mechanically characterize these films to (1) generate baseline data for comparison with other commercial films, (2) identify any changes in performance arising from process variations, and (3) evaluate the mechanical behavior of films once they are incorporated into multilayer capacitors. The importance of mechanical characterization of these dielectric films is illustrated in Figure 1, which shows the strong correlation between loss factor and the elastic modulus.

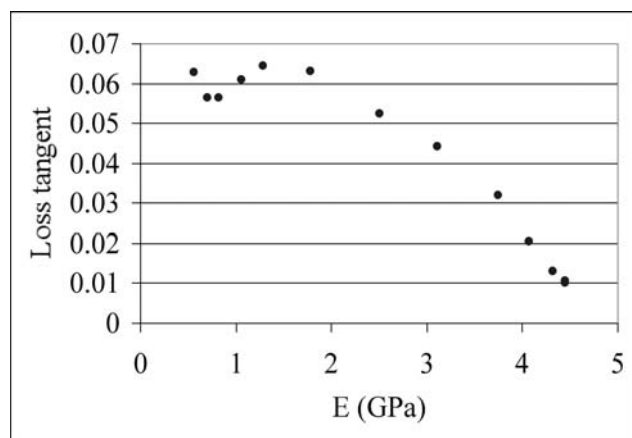


Figure 1. Correlation of mechanical and dielectric performance for a commercial polymer film.

Results

Given the limited thickness of these films (<10 μm), specialized techniques are required to assess the mechanical behavior. One approach is to use a mechanical properties microprobe (MPM) to interrogate the material on the nanometer scale (Figure 2). The MPM is an automated instrument that consists of four primary components: an indenter (Berkovich indenter) whose vertical displacement (nanometer resolution) and applied load (microgram resolution) are controllable; an optical microscope (OM) with several objective lenses; a precision X and Y stage that translates the metallographically prepared specimen between the OM and the indenter; and a computer that controls

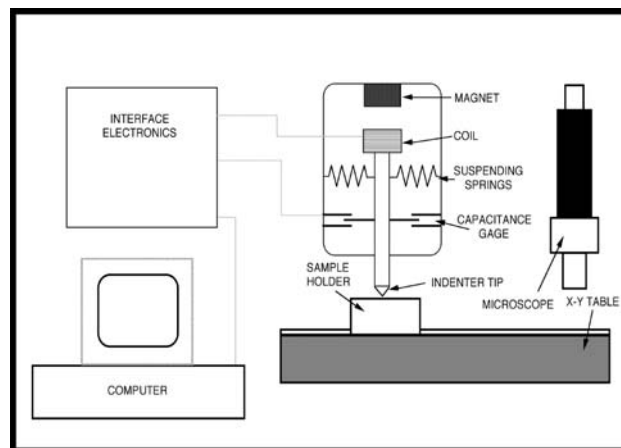


Figure 2. Schematic representation of the mechanical properties microprobe.

the OM’s lens turret (50–1500× magnification), stage movement, and indenter load and displacement. The computer also collects data on the indenter’s displacement and load and is interfaced with a TV monitor and camera that show the microscope’s field of view and allow inspection of each indent. The MPM (not including the computer) is housed inside an insulated cabinet that minimizes its susceptibility to laboratory room temperature fluctuations and vibrations (which are problematic when controlling displacement at the nanometer level). The computer is outside the insulated cabinet to further minimize the introduction of thermal instabilities and remotely operates the MPM.

The load/displacement history generated during indentation can be interpreted with the aid of an appropriate model to calculate elastic modulus (*E*) and hardness (*H*) of the material (Figure 3). Specifically, the hardness is calculated by dividing the peak load by the residual indent area, while the elastic modulus is determined from the slope of the unloading curve.

In the present study, the MPM was initially used to examine a number of films (Table 1) provided by SNL. Six of the initial films were deposited on 100-nm aluminum/400-nm SiO₂/Si wafers. The SiO₂, which is applied by chemical vapor deposition and then thermally annealed, was put on by a commercial manufacturer to passivate the silicon. The second series of films evaluated with the MPM were deposited on a Mylar sheet using the continuous deposition procedures developed under the SNL project. These films were removed from the Mylar before testing.

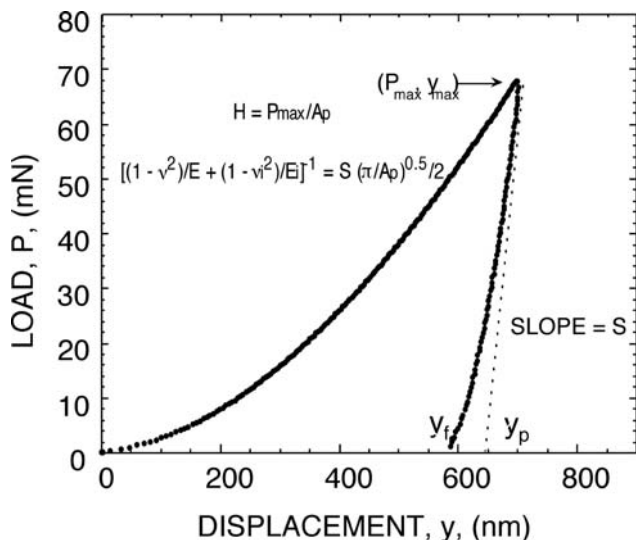


Figure 3. Typical load-displacement curve generated during loading and unloading with the mechanical properties microprobe.

Values of H and E were first measured as a function of residual depth of penetration (y_p), as shown for the first set of films in Figure 4. Note that at some critical value of y_p , H and E increase with increasing y_p . This effect occurs because of the influence of the substrate, which in the case of silicon is both harder and stiffer than the film. The critical value of y_p depends upon the film thickness. Because of this effect, the film properties must be determined from indents that are below the critical depth. A good rule of thumb is that the depth must be less than 1/10th of the film thickness.

In the present study, the indentation data generated at 20 nm and below were used to calculate

the substrate-independent values of H and E . Figure 5 illustrates the effect of film thickness upon E and H for the first set of films. There is a tendency for the H and E to increase slightly as the film thickness decreases.

One limitation of the MPM is that data are typically generated at room temperature only. To evaluate temperature effects in the present study, free-standing films were also mechanically evaluated using a tensile stress-strain test. Initially, commercial grips were used to mechanically load polymer films to ultimate failure. The films were in the shape of rectangular strips 25.4 mm long and 0.0095 mm thick. The stress-strain data are shown in Figure 6. Results for a commercially available film are provided for comparison. The polyvinyl phenol films provided by SNL exhibited limited ductility, as reflected by the low values of failure strain. Subsequent differential scanning calorimetry measurements suggested that the glass transition temperature (temperature below which the amorphous component of the polymer becomes brittle) was in the range 40–45EC. This would explain the limited strain-to-failure values measured in the room-temperature stress-strain testing.

A number of low-cost approaches for gripping the films for stress-strain testing were also investigated. The first approach, similar to that used to test small fibers, involved first gluing the film into a special cardboard holder. This holder was then mounted in the test frame using conventional pin grips. The most successful method required the use of precision stages to mechanically load the film (Figure 7).

Table 1. Summary of polymer films evaluated with the mechanical properties microprobe

No.	Base designation	Substrate	Thickness (μm)	Comments
1	PVP5	Si	0.394	
2	PVP5-2X	Si	2.849	
3	PVP5-2X	Si	2.006	
4	PVP5	Si	0.499	
5	PVP5	Si	0.583	
6	PVP5	Si	0.498	
7	PVP	Mylar	12.000	Smooth roller
8	PVP	Mylar	2.500	Gravure Roller 900 RPM boost motor
9	PVP	Mylar	5.000	Gravure Roller 250 RPM
10	PVP	Mylar	7.500	Gravure Roller 0 RPM, boost off

PVP = polyvinyl phenol, or hydroxylated polystyrene.

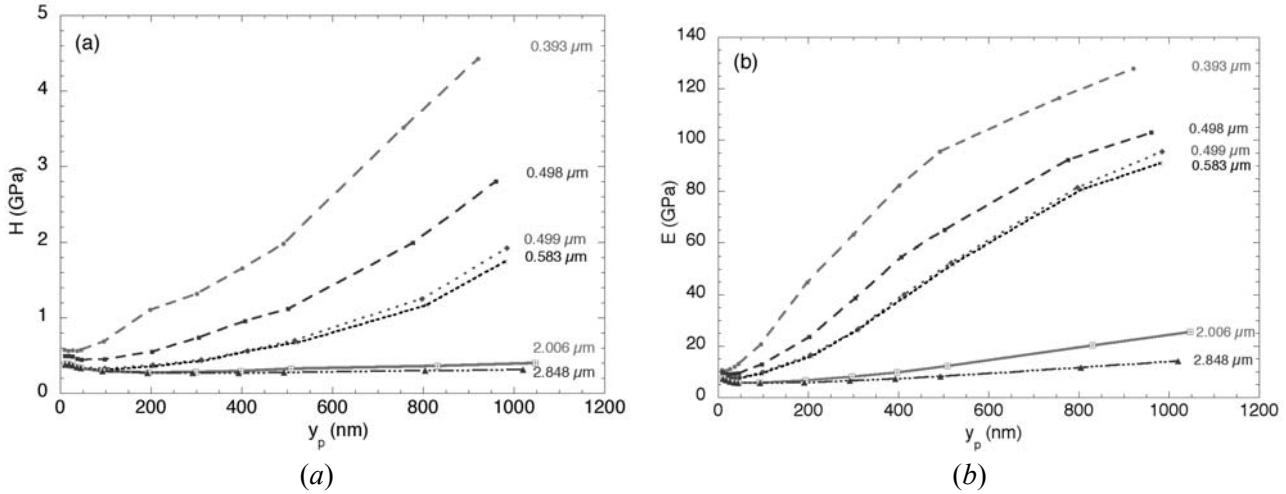


Figure 4. Effect of penetration depth upon hardness (a) and elastic modulus (b).

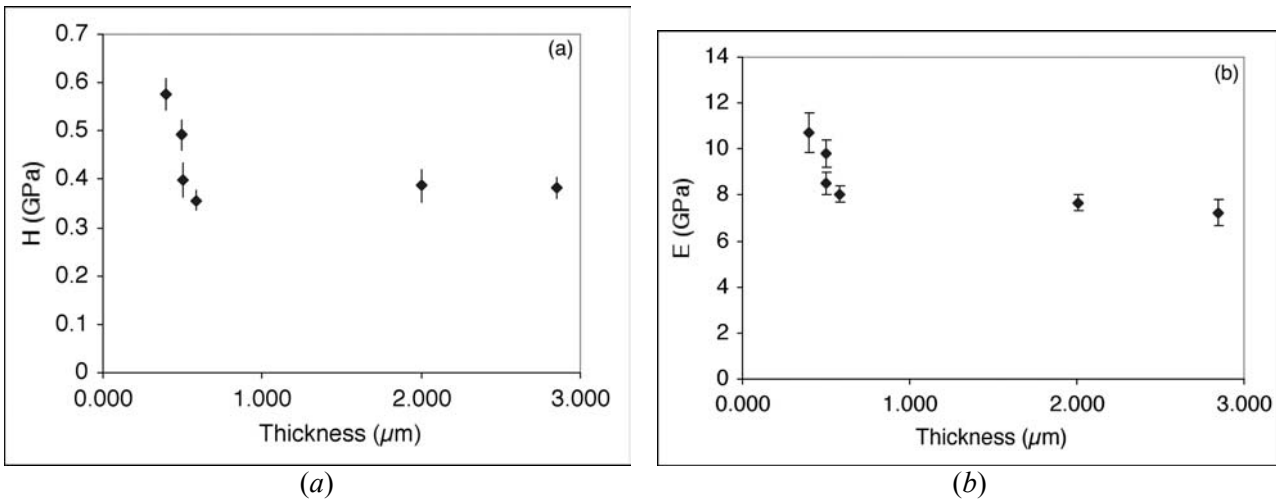


Figure 5. Effect of film thickness upon hardness (a) and elastic modulus (b).

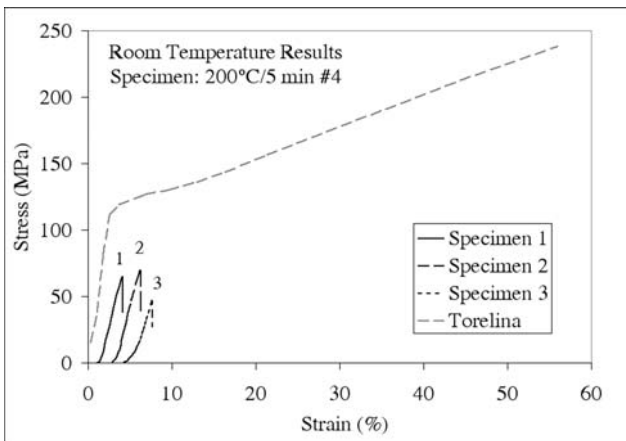


Figure 6. Preliminary tensile stress-strain data obtained using commercially available grips.

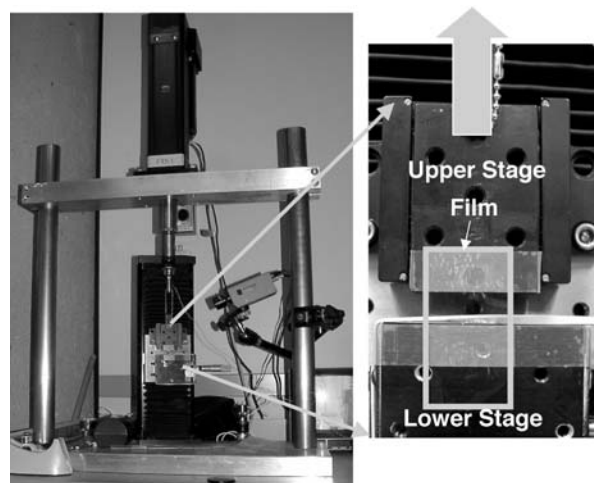


Figure 7. Arrangement of precision stages used to grip films.

Conclusions

The MPM was used to evaluate the hardness and elastic modulus of the polymer films. In the initial testing of the films deposited on the silicon substrates, these properties were found to depend slightly upon film thickness. The subsequent evaluation of the films prepared using the continuous deposition procedures showed that the film properties were relatively independent of the roller characteristics. The first room-temperature tensile stress-strain measurements of a polymer film

were conducted. The addition of a temperature chamber will allow us to conduct measurements throughout the temperature range of interest. The resulting structural information will be correlated with dielectric properties measured at SNL.

Publications

C-H Hsueh and M. K. Ferber, "Effective Coefficient of Thermal Expansion and Residual Stress in Multilayer Capacitors," accepted for publication in *Journal of Composites, Part A*.

3. FUEL CELLS

A. Carbon Composite Bipolar Plates

T. M. Besmann, J. W. Klett, and J. J. Henry, Jr.

Surface Processing and Mechanics Group and Carbon and Insulating Materials Group

Oak Ridge National Laboratory

P.O. Box 2008, MS 6063, Bldg. 4515

Oak Ridge, TN 37831-6063

(865) 574-6852; fax: (865) 574-6198; e-mail: besmannm@ornl.gov

DOE Technology Development Manager: JoAnn Milliken

(202) 586-2480; fax: (202) 586-9811; e-mail: joann.milliken@ee.doe.gov

ORNL Technical Advisor: David Stinton

(865) 574-4556; fax: (865) 241-0411; e-mail: stintondp@ornl.gov

Contractor: Oak Ridge National Laboratory, Oak Ridge, Tennessee

Prime Contract No.: DE-AC05-00OR22725

Objectives

- Develop a slurry-molded carbon fiber material with a carbon chemical-vapor-infiltrated sealed surface as a bipolar plate.
- Collaborate with potential manufacturers with regard to testing and manufacturing of such components.

Approach

- Fabricate fibrous component preforms for the bipolar plate by slurry-molding techniques using carbon fibers of appropriate lengths.
- Fabricate hermetic plates using a final seal with chemical-vapor-infiltrated carbon.
- Develop commercial-scale components for evaluation.

Accomplishments

- Developed a carbon composite material with graphite particulate filler to control pore size and speed surface sealing.
- Further characterized and measured the mechanical properties of the carbon composite plate material.
- Significantly improved wetting of the bipolar plate surface.
- Determined the surface roughness of finished bipolar plate components.
- Supported scale-up efforts at licensee Porvair Fuel Cell Technology.

Future Direction

- Develop bipolar plate material/configuration to meet various users' unique requirements.
- Improve wetting properties of carbon surfaces.

- Decrease component thickness.
 - Transfer technology and aid Porvair with scale-up.
-

Introduction

In FY 2002, the carbon composite bipolar plate effort at Oak Ridge National Laboratory has achieved several programmatic goals in measuring plate properties and improving wetting. It is necessary to have accurate mechanical properties information for the bipolar plates to ensure they will survive handling, assembly, and service. These measurements need to go beyond simple tensile or flexure strength, since the relatively thin plates will be subjected to tension-torsion in assembly and potential high-rate stresses during handling and service. Thus, it is particularly important to understand torsion behavior and fracture toughness. Measurements of these properties, along with methodologies to demonstrate material uniformity through thermal imaging, have been developed.

Approach

Fibrous component preforms for the bipolar plate are prepared by slurry molding using 100- μm carbon fibers (e.g., Fortafil) in water containing phenolic resin, followed by curing. Molds are used to impress channels and other features into the preform, and the surface of the preform is sealed using a chemical vapor infiltration (CVI) technique in which sufficient carbon is deposited on the near-surface fibers to make the surface hermetic. In the current work, differing amounts of carbon flake filler were used and the effects on properties determined. Infrared imaging was performed to identify defects and inhomogeneities by heating one side of the samples and imaging the opposite side. Because shear stress is a good measure of torsion behavior, the Iosipescu method was used to measure shear properties. The efforts to improve wetting of the carbon surface consisted of a simple heat treatment of the components to 1000°C in air.

Results

Slurry-molded preforms 2.5 mm in thickness were produced and cut into 10-cm squares. Illustrative results of the thermal imaging are seen in Figure 1. The relative uniformity indicates little

density difference within the plates and between plates. There is some indication of delamination along the edges, although it is likely due to cutting of a larger plate into the 10-cm samples.

The Iosipescu torsion measurements are given in Table 1, and a sample stress-displacement curve is shown in Figure 2. These values are indicative of a relatively torsion-resistant material, particularly given the low density of the carbon composite. The stress-displacement curves indicate little delamination or other failures until ultimate failure. Filler content appears not to affect shear stress.

The dramatic improvement in wetting of the carbon composite surface is seen in Figure 3. Whereas prior to oxidative treatment, water appeared to have a small wetting angle on the surface of the carbon composite, after treatment, water readily spread on the surface with an apparent large wetting angle.

Conclusions

During this period, the mechanical properties of the carbon composite bipolar plate material were assessed, including measurements of uniformity and defect distribution by infrared imaging. The results indicate good material uniformity and substantial resistance to torsional stresses. Significant improvement in the wetting of the material was demonstrated after a simple oxidation treatment.

FY 2002 Publications/Presentations

T. M. Besmann, J. W. Klett, J. J. Henry, Jr., and T. D. Burchell, "Carbon Composite Bipolar Plates for PEMFC," 26th Annual International Conference on Advanced Ceramics and Composites, January 13–18, Cocoa Beach, Fla.

T. M. Besmann, J. W. Klett, J. J. Henry, Jr., and E. Lara-Curzio, "Carbon/Carbon Composite Bipolar Plate for PEM Fuel Cells," National Meeting of the American Institute of Chemical Engineers, March 10–14, New Orleans.

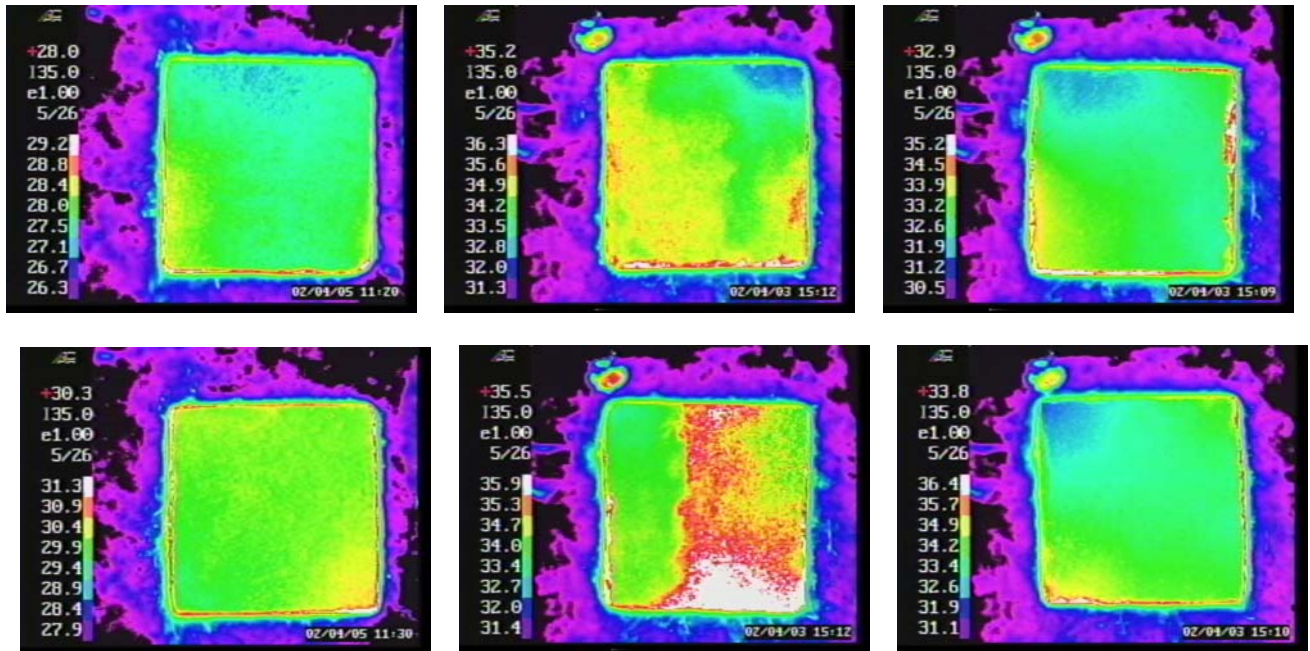


Figure 1. Infrared images of carbon composite bipolar plate material samples.

Table 1. Measurements of shear stress by the Iosipescu method for carbon composite samples with differing amounts of carbon flake filler

Sample (% filler)	Strength measure
PMP10R (0%)	25.9 ± 9.9 MPa
PMP10T (0%)	19.3 MPa (1 test)
PMP09K (15%)	24.4 ± 11.8 MPa
PMP11E (30%)	43.3 ± 2.7 MPa
PMP11G (30%)	17.1 ± 1.1 MPa
PMP11H (30%)	18.7 ± 4.7 MPa

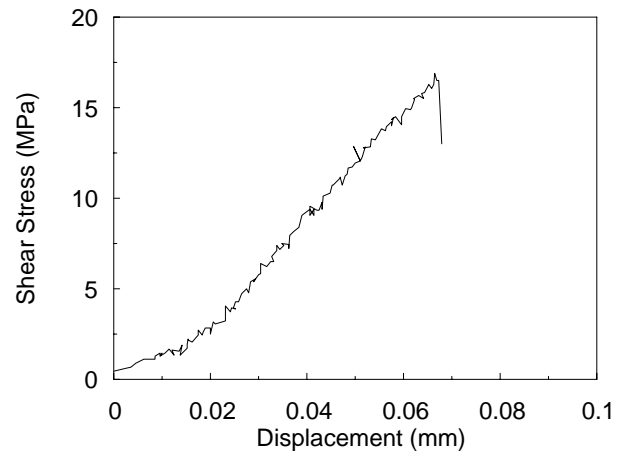


Figure 2. Typical stress-displacement curve for the Iosipescu torsion measurement of the carbon composite bipolar plate material.

Before oxidation



After oxidation



Figure 3. Water illustrates a much larger wetting angle on the carbon composite after oxidative treatment.

B. Cost-Effective Surface Modification for Metallic Bipolar Plates

M. P. Brady

Oak Ridge National Laboratory

P.O. Box 2008, MS 6115

Oak Ridge, TN 37831-6115

(865) 574-5153; fax: (865) 241-0215; e-mail: bradymp@ornl.gov

DOE Technology Development Managers: Nancy Garland

(202) 586-5673; fax: (202) 586-9811; e-mail: nancy.garland@ee.doe.gov

JoAnn Milliken

(202) 586-2480; fax (202) 586-9811; e-mail: joann.milliken@ee.doe.gov

ORNL Technical Advisor: David Stinton

(865) 574-4556; fax: (865) 241-0411; e-mail: stintondp@ornl.gov

Contractor: Oak Ridge National Laboratory, Oak Ridge, Tennessee

Prime Contract No.: DE-AC05-00OR22725

Objective

- Develop a low-cost metallic bipolar plate alloy that will form an electrically conductive and corrosion-resistant nitride surface layer during thermal nitriding to enable its use in a polymer electrolyte membrane (PEM) fuel cell environment.

Approach

- Conduct a study of the nitridation behavior of a series of model Ni-*X* and Fe-*X* base alloys (*X* = nitride-forming elements such as Cr, Nb, Ti, and V) that could meet DOE bipolar plate cost goals.
- Identify the most promising combination of *X* additions, ternary and higher-order alloying addition(s), and nitridation reaction conditions that result in the formation of an adherent, dense nitride surface layer.
- Evaluate corrosion behavior in 80EC sulfuric acid solutions to simulate PEM fuel cell environments (in collaboration with K. Weisbrod and C. Zawodzinski of Los Alamos National Laboratory and I. Paulauskas and R. A. Buchanan of the University of Tennessee).
- Characterize nitride layer microstructure and composition by X-ray diffraction, electron probe microanalysis, scanning electron microscopy, and transmission electron microscopy. Use this information in a feedback loop to modify alloy chemistry and nitridation processing conditions to optimize the protectiveness of the nitride surface layer.
- Measure electrical conductivity of select nitrated alloys by dc four-point probe.
- Down-select a model Ni-Fe-*X* alloy for in-cell performance evaluation and begin modification and optimization of alloy composition/nitridation conditions for commercial scale up, and/or identify nitridation conditions suitable for commercially available alloys (if feasible).

Accomplishments

- Tested a model nitrated Ni-50Cr wt % alloy and found it exhibited no discernible degradation after 1 week of immersion in pH 2 sulfuric acid at 80°C, and a corrosion current density of less than 1×10^{-6} A/cm² up to ~0.9 V vs standard hydrogen electrode (SHE) in pH 3 sulfuric acid at 80EC. This level of corrosion resistance is in the range of the goal for metal bipolar plates and warrants scale-up to in-cell testing and evaluation. Further, the Cr-nitride layers formed on the Ni-50Cr alloy grow in a very robust manner so that features such as

stamped flow fields will always be completely covered. Preliminary measurement of electrical properties of a nitrated coupon indicated an electrical conductivity in the $10^4 \Omega^{-1} \text{ cm}^{-1}$ range, which is two orders of magnitude greater than the DOE target.

- Delivered coupons of nitrated Ni-50Cr to Los Alamos National Laboratory for further corrosion testing and evaluation. Preliminary feedback from ongoing exposure in the corrosion test cell indicates stable electrical resistance (collaboration with K. Weisbrod).
- Submitted a U.S. provisional patent disclosure in April 2002 for nitrated Ni-Cr and related base alloys.

Future Direction

- Pursue in-cell testing of nitrated Ni-50Cr to determine if the promising corrosion resistance translates to in-cell performance.
- Optimize nitridation conditions and reduce the level of chromium to below 40–42 wt % in order to improve the cold formability of the alloy and reduce processing and raw material costs (based on input from commercial alloy producers).
- Investigate the nitriding characteristics of existing commercial high-Cr, Ni- and Fe-based alloys to determine if a similar corrosion-resistant Cr-nitride layer can be formed in order to facilitate scale-up and transfer of this technology.
- Establish partnerships with alloy producers and fuel cell manufacturers.

Introduction

The bipolar plate is one of the most expensive components in PEM fuel cells. Thin metallic bipolar plates offer the potential for significantly lower cost than the machined graphite bipolar plates currently used, as well as reduced weight/volume and better performance than developmental carbon fiber and graphite bipolar plates currently under consideration. However, inadequate corrosion resistance can lead to high electrical resistance and/or contaminate the proton exchange membrane. Metal nitrides (e.g., TiN or Cr₂N) offer electrical conductivities that are up to an order of magnitude greater than that of graphite and are highly corrosion-resistant. Unfortunately, most conventional coating methods (for metal nitrides) are too expensive for PEM fuel cell stack commercialization or tend to leave pinhole defects, which result in accelerated local corrosion and unacceptable performance.

Approach

The goal of this effort is to develop a bipolar plate alloy that will form an electrically conductive and corrosion-resistant nitride surface layer during thermal (gas) nitriding. There are three advantages to this approach. First, with the nitriding performed

at elevated temperatures, pinhole defects are not expected because thermodynamic and kinetic factors favor complete conversion of the metal surface to nitride. Rather, the key issues are nitride layer cracking, adherence, and morphology (discrete internal precipitates vs continuous external scales), which can potentially be controlled through proper selection of alloy composition and nitridation conditions. Second, thermal nitridation is an inexpensive, well-established industrial technique. Third, the alloy can be formed into final shape by inexpensive metal-forming techniques such as stamping prior to thermal nitridation.

Results

A series of model Ni-base alloys with additions of (5–15)Ti, (5–10)Nb, (10–15)V, (5–10)Nb + (5–15)V and (35–50)Cr wt %, to form external Ti-, Nb-, V-, Nb+V-, or Cr-based nitride layers, were studied (Table 1). Ni was selected as the initial alloy base because it is relatively inexpensive (\$2–4/lb) and ductile, does not form a stable nitride during thermal nitridation, and exhibits a relatively low permeability to nitrogen, which favors external nitride layer formation.

Table 1. Summary of nitriding conditions

Alloy base (wt %)	Nitridation conditions (high-purity nitrogen)		Nitrogen uptake (mg/cm ²)
	Temperature	Time (h)	
Ni-(5-15)Ti	1000-1100EC	8-48	0.1-1
Ni-(5-10)Nb	900-1100EC	1-48	0.1-2
Ni-(10-15)V	1100EC	24-48	0.5-1
Ni-(5-10)Nb-(5-15)V	1100EC	24-48	0.5-1
Ni-(35-50)Cr	1100EC	1	1.5-2

Corrosion behavior was screened by a 1-week immersion in pH 2 sulfuric acid at 80EC to optimize alloy composition and nitridation conditions. Anodic polarization testing was then conducted on the most promising nitrided alloys in aerated pH 3 sulfuric acid at 80EC to quantify corrosion resistance. A corrosion current density of less than 1×10^{-6} A/cm² up to a range of approximately 0.9 V vs SHE was considered indicative of sufficiently promising behavior to warrant further development and future in-cell stack testing.

Nitrided Ni-(5-10)Ti base alloys (to form an external TiN base layer) exhibited relatively low corrosion currents (Figure 1). However, regions of

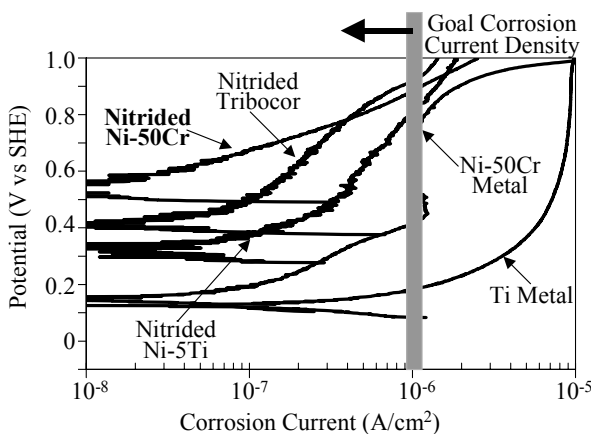


Figure 1. Anodic polarization data in aerated pH 3 sulfuric acid at 80EC (scan rate of 0.1 mV/s) vs standard hydrogen electrode.

through-thickness local attack of the TiN surface layer were evident in most of the coupons. Nitrided Ni-(5-10)Nb + (5-15)V wt % base alloys formed external Ni-Nb-V-N and Nb-V-N scales, which resulted in good corrosion resistance in the 1-week immersion screening in pH 2 sulfuric acid at 80EC (weight loss < -0.05 mg/cm²) but exhibited high corrosion currents in the anodic polarization testing

(10^{-5} to 10^{-4} A/cm² range at 0.9V vs SHE). The Ni-(10-15)V wt % alloys formed external V-N layers after the nitridation treatment, but they exhibited relatively high weight losses in the sulfuric acid immersion screenings (3-5 mg/cm² loss after 1 week). External Nb-N layers could not be formed on Ni-(5-10)Nb wt % alloys under the nitridation conditions used in the present work (Table 1).

Of the nitrided alloys examined, Ni-50Cr wt % exhibited the most corrosion resistance and met the target corrosion current of less than 1×10^{-6} A/cm² up to ~0.9V vs SHE in pH 3 sulfuric acid at 80EC (Figure 2 and Table 1). The post-nitridation microstructure of all the Ni-Cr alloys examined (35Cr, 45Cr, 50Cr wt %), nitrided for 1-2 h at

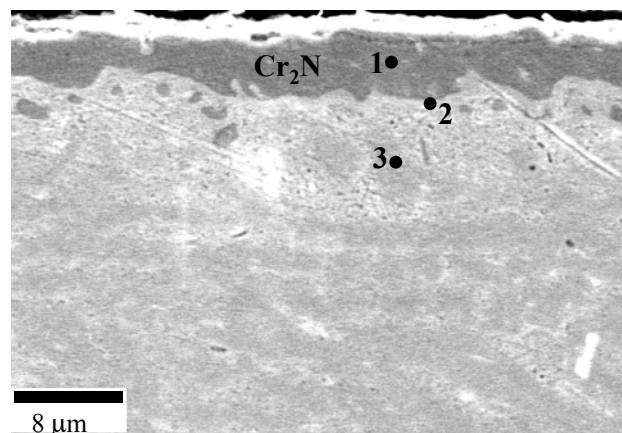


Figure 2. Scanning electron microscopy cross-section of Ni-50Cr wt % nitrided for 2 h at 1100EC in N₂. Point 1: external Cr₂N scale: 69Cr-30N-1Ni atomic percent (at %). Point 2: Cr-depleted Ni(Cr) metal (light): 68Ni-32Cr at % (71Ni-29Cr wt %). Point 3: subscale ternary Ni-Cr-N phase (dark): 52Cr-14N-34Ni at %. Compositions were determined by electron probe microanalysis using pure element standards for Ni-Cr, and a Cr₂N standard for nitrogen.

1100EC in nitrogen, consisted of external Cr₂N overlying a mixed zone of Cr-depleted Ni(Cr) and a ternary Ni-Cr-N subscale nitride (Figure 2).

(Occasional examples of internal Cr_2N were also observed in the lower Cr alloys). The degree of continuity, and hence protectiveness, of the external Cr_2N improved with increasing alloy chromium content, with a dense, nearly continuous/continuous layer formed on Ni-50Cr. Optical analysis after testing revealed no evidence of significant corrosion or breaching of the nitride layer formed on the Ni-50Cr. Uncoated Ni-50Cr metal also exhibited relatively low corrosion currents (Figure 1) but showed evidence of pitting after the test exposure.

The nitridation of the Ni-50Cr alloys was very robust with no evidence of inadequate coverage at sharp corners or edges. Figure 3 shows a coupon of Ni-50Cr that was hand-stamped with the letters "ORNL," nitrided, and then immersed in pH 2 sulfuric acid at 80°C for 1 week; there was no attack evident in the stamped regions. These results suggest that the present approach is amenable to coverage and protection of stamped flow field features in a bipolar plate. Bulk electrical conductivities were in the range of $1\text{--}2 \times 10^4 \Omega^{-1} \text{cm}^{-1}$ after nitriding, which surpasses the DOE electrical conductivity target by two orders of magnitude.

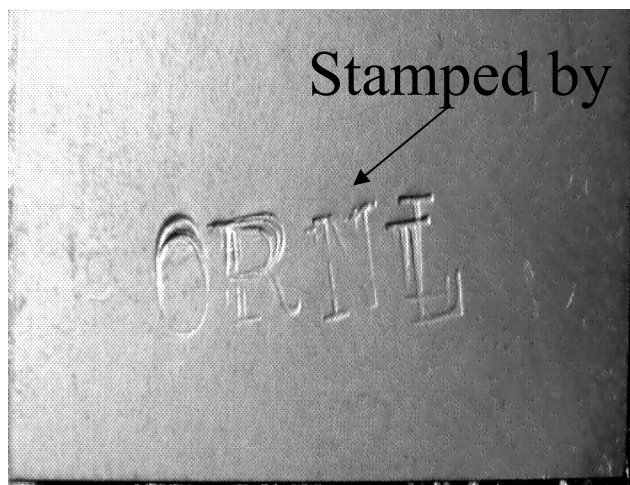


Figure 3. Macrograph of stamped and nitrided Ni-50Cr coupon after 1 week of exposure in pH 2 sulfuric acid at 80°C (coupon dimensions $1 \times \frac{1}{2}$ in.).

Conclusions/Future Work

These results indicate that nitrided Ni-Cr base alloys show potential for use as bipolar plates in PEM fuel cells. Future work will focus on in-cell testing of nitrided Ni-50Cr to determine if the

promising corrosion resistance demonstrated in the anodic polarization testing translates to good in-cell performance. From a cost and alloy processing perspective, lower levels of chromium are needed, $\leq 40\text{--}42$ wt % range (G. Smith and M. Harper, private communication with Special Metals Corp., 2002), particularly in terms of the rate of work hardening during cold rolling to allow the economical production of alloy sheet. The critical level of chromium needed to form an external nitride layer on binary Ni-Cr alloys is in the range of 30–40 wt % chromium,¹ so a reduction to less than 50 wt % chromium appears feasible with proper adjustment of nitridation conditions (e.g., temperature, N_2 vs NH_3 environments, initial surface condition) to form a sufficiently continuous and dense Cr_2N (or possibly CrN) layer. Reduction in chromium level may also be achievable through ternary alloying additions that form nitrides of intermediate thermodynamic stability between those of chromium and nitrogen [i.e., secondary gettering (e.g., ref. 2)]. For example, the level of aluminum needed to form an external alumina layer on Cu-Al alloys can be significantly reduced by additions of zinc (e.g., ref. 2). It may also be possible to form similar corrosion-resistant nitride layers on Fe-Cr or Ni(Fe)-Cr base alloys, which would also further reduce alloy cost. The nitriding characteristics of existing commercial Ni-Fe-Cr alloys will also be investigated. Emphasis in the next year will also be placed on establishing collaborations with commercial alloy producers and fuel cell manufacturers to facilitate technological assessment (particularly in-cell testing) and scale-up of this approach.

References

1. R. P. Rubly and D. L. Douglass, *Oxid. Met.*, **35**, p. 259 (1991).
2. M. P. Brady, B. Gleeson, I. G. Wright, *JOM*, **52**(1), p. 16 (2000).

Publications

“Assessment of Thermal Nitridation to Protect Metal Bipolar Plates in PEM Fuel Cells,” M. P. Brady, K. Weisbrod, C. Zawodzinski, I. Paulauskas, R. A. Buchanan, and L. R. Walker, submitted to *Electrochemical and Solid State Letters*.

Patents

M. P. Brady, J. H. Schneibel, B. A. Pint, and
P. J. Maziasz, "Metallic Bipolar Plate Alloys

Amenable to Inexpensive Surface Modification for
Corrosion Resistance and Electrical Conductivity,"
U.S. Provisional Patent Disclosure, April 2002.

C. Low-Friction Coatings and Materials for Fuel Cell Air Compressors

George R. Fenske, Oyelayo Ajayi, John Woodford, and Ali Erdemir

Argonne National Laboratory

ET-212, 9700 S. Cass Ave.

Argonne, Illinois 60439

(630) 252-5190; fax: 630-252-4798; e-mail: gfenske@anl.gov

DOE Technology Development Manager: Nancy L. Garland

(202) 586-5673; fax: (202) 586-9811; e-mail: nancy.garland@ee.doe.gov

ORNL Technical Advisor: David Stinton

(865) 574-4556; fax: (865) 241-0411; e-mail: stintondp@ornl.gov

Contractor: Argonne National Laboratory, Argonne, Illinois

Prime Contract No.: W-31-109-Eng-38

Objectives

- Develop and evaluate the friction and wear performance of low-friction coatings and materials for fuel cell air compressor/expander systems. Specific goals are
 - 50–75% reduction in friction coefficient
 - An order of magnitude reduction in wear
- Transfer the developed technology to DOE's industrial partners.

Approach

- Identify critical compressor components requiring low friction.
- Apply and evaluate Argonne National Laboratory's (ANL's) near-frictionless carbon (NFC) coatings to the components when appropriate.
- Develop and evaluate polymer composite materials containing boric acid solid lubricant.
- Develop a tribological mechanism-based material selection methodology for various compressor/expander components.

Accomplishments

- Identified the radial air bearings and thrust bearings of Meruit's turbocompressor as components that require both low friction and low wear rate for satisfactory performance.
- Conducted thrust washer wear tests that showed that ANL's NFC coating reduced friction by about four times and wear rate by two orders of magnitude. Both exceeded the project goals.
- Increased the scuffing resistance of a steel surface about 10 times using NFC coatings.
- Began durability testing of NFC-coated air bearing hardware components.
- Completed initial friction and wear testing of nylon-12 polymer with B₂O₃ addition. Significant reduction in wear was observed with the addition of B₂O₃, especially under high relative humidity.
- Achieved a 50% reduction in friction for application in a Vairex-variable displacement compressor/expander using Hitco C/C composite and anodized aluminum contact pairs.

- Designed and constructed a new high-speed friction and wear test rig for evaluation of materials for Mechanology's toroidal intersecting vane machine (TIVM).
- Evaluated the high-speed frictional performance of several candidate materials and coatings for TIVM vanes.

Future Direction

- Evaluate the effect of humidity on the durability of NFC-coated air bearing components.
- Conduct detailed tribological performance evaluation of TIVM select candidate materials based on high-speed frictional behavior.
- Optimize an NFC coating for TIVM vane application.
- Coat TIVM components with optimized NFC for rig testing at Mechanology.
- Continue development of collaborative efforts with DOE fuel cell contractors addressing reliability, durability, and parasitic energy losses in air management systems.

Introduction

A critical need in fuel cell systems for vehicles is an efficient, compact, and cost-effective air management system to pressurize the fuel cell systems to about 3 atmospheres. Pressurization of fuel cells will result in higher power density and lower cost. Several compressor/expander systems are currently being developed for DOE. The efficiency, reliability, and durability of compressors depend on effective lubrication or friction and wear reduction in critical components such as bearings and seals. Conventional oil or grease lubrication of compressor components is not desirable because such lubricants can contaminate and poison the fuel cell stack. The objective of this project is to develop and evaluate low-friction coatings and/or materials for critical components of air compressor/expanders being developed by various contractors for DOE vehicle fuel cell systems. The work this year focused on Meruit's turbocompressor air bearings and Mechanology's TIVM.

Approach

For various air compressor/expanders being developed, we will identify the key critical components that require a low friction coefficient and wear resistance. Over the years, the tribology group at ANL has developed low-friction and low-wear coatings and materials. Most notable is the discovery of an amorphous carbon coating with extremely low friction coefficients (<0.001 in dry

nitrogen) and very low wear. Where appropriate, the NFC coating will be applied to the critical component(s). In other cases, alternative low-friction polymeric materials and other low-friction coatings will be evaluated.

Results

Meruit Air Bearing

As reported in 2001, we started durability testing of NFC-coated, air-bearing hardware components (Figure 1). The durability test consists of start-and-stop cycling of the air bearing. Under full-speed operation, there is no contact in either the journal or the thrust bearings. Contact and sliding between surfaces occur only during start-and-stop periods when damage can occur; hence, they determine the durability of the bearing. Dimples of known dimensions were inserted into contact areas of the coated bearing shaft (Figure 1). A wear measurement is taken after some predetermined number of start/stop cycles by measuring changes in the dimple dimension. In the first test, wear measurements were taken after 250, 1000, 2000, and 4000 cycles. Initial results from this test were presented in the 2001 progress report. Unfortunately, the bearing in this test failed shortly after 4000 cycles because of debris contamination.

After a slight design modification to the air-bearing shaft, a second durability test of an NFC-coated bearing was conducted. Plots of linear wear on both side 1 and side 2 of the air-bearing shaft are

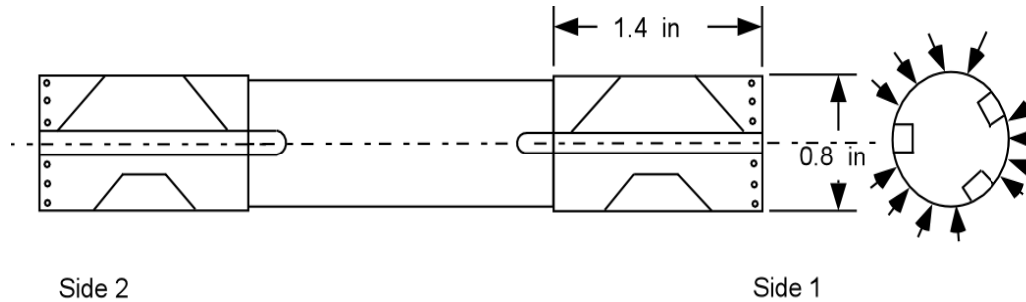


Figure 1. Schematic diagram of dimples on NFC-coated air-bearing shaft for wear measurement after testing.

shown in Figures 2a and 2b. The original coating thickness was about $2.5 \mu\text{m}$. There was considerably more wear on side 2 than on side 1, especially after 8000 start/stop cycles. This difference is due to an apparent imbalance in the air bearing. The bearing finally failed after about 11,000 start/stop cycles, again because of debris contamination. However, at the point of failure, the coating was not worn through in any of the dimples. The coating wear mechanism consists of abrasive polishing, as shown in Figure 3.

Mechanology TIVM

The primary sources of friction in the TIVM are the vane sliding interface, the housing compressor seal, and expander bearings. Design analysis shows that an overall system friction coefficient of <0.3 is required to meet the DOE program target for efficiency. The most critical of these three sources is the vane sliding interface because of its high sliding speed of 60–75 m/s. The selection of an appropriate vane material is critical for successful operation of the TIVM compressor/expander. Frictional behavior as a function of sliding speed was evaluated for several material and coating combinations (including NFC). Some material combinations with adequate friction behavior at high sliding speeds were identified.

When a 440EC stainless steel ball slid against an NFC-coated steel disc, the friction coefficient was about 0.2 at the start of the test, but it increased slightly as the test progressed (Figure 4). There was a frictional spike at the end of the test as a result of

trapping of iron oxide debris generated on the uncoated steel ball surface. When both the steel ball and the disc surfaces were coated with NFC, the friction coefficient was low (0.23) and symmetrical with the sliding speed profile (Figure 5). The friction coefficient showed a very small increase with increasing sliding speed. Furthermore, compared with many other material combinations evaluated, the frictional signal from tests with both surfaces coated was relatively smooth. This result may have an implication for quiet running of the TIVM machine.

Other promising combinations include 440EC steel sliding against PEEK polymeric material (Figure 6). For this combination, the friction coefficient appears to be independent of sliding speed, as the friction coefficient remained nearly constant at about 0.25 for the entire speed range tested. In another combination of 440EC stainless steel and Armoloy- (thin, dense chrome-) coated bronze, the friction coefficient in the high speed range ($> 60\text{m/s}$) was about 0.3. However, for this contact pair, the friction at lower speeds was higher. The frictional behavior is also symmetrical with the speed profile (Figure 7).

Publications

O. O. Ajayi, J. Woodford, A. Erdemir, and G. R. Fenske, "Performance of Amorphous Carbon Coating in Turbocompressor Air Bearing," Society of Automotive Engineers (SAE) Paper 2002-01-1922, SAE Future Car Congress, Arlington, Va., June 3–5, 2002.

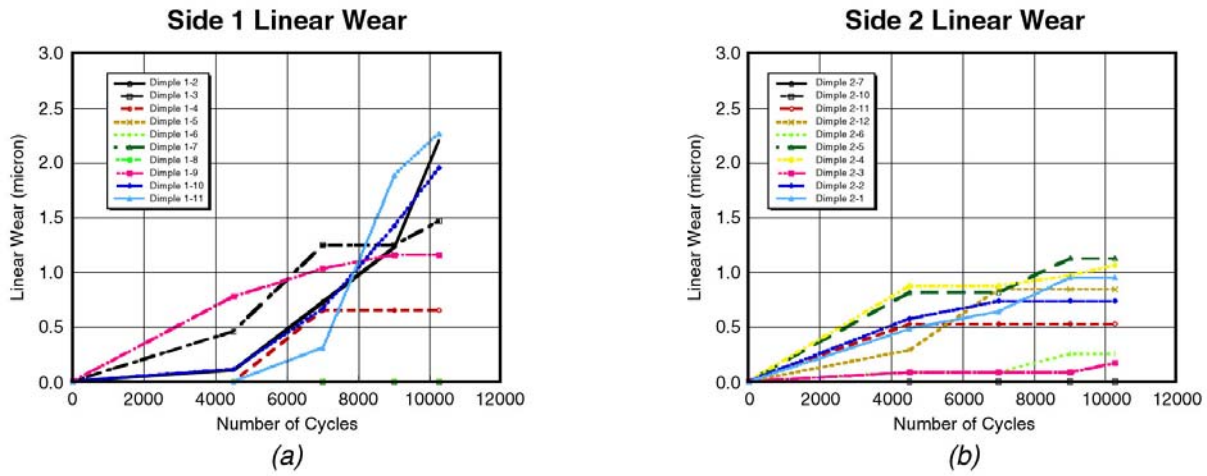


Figure 2. Linear wear (micron) at various dimples on (a) side 1 and (b) side 2 of air-bearing shaft.

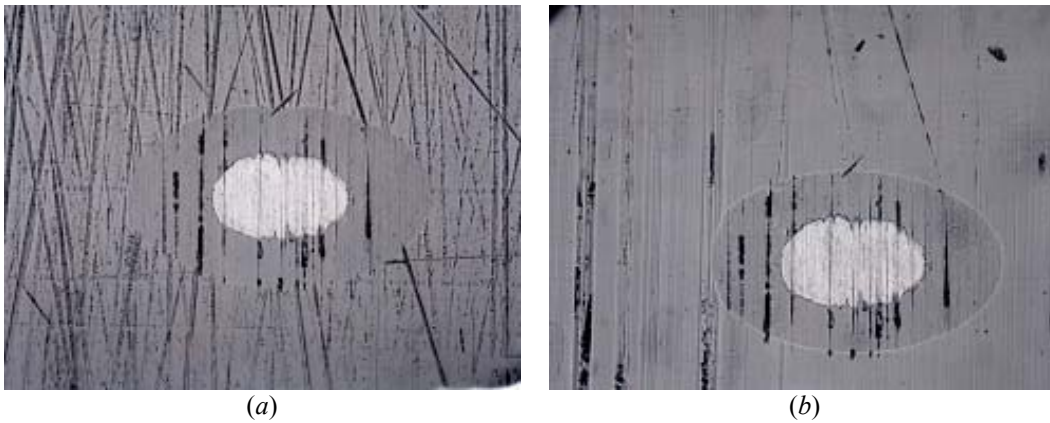


Figure 3. Optical micrograph of dimple 9 on side 1 after (a) 250 cycles and (b) 4000 cycles.

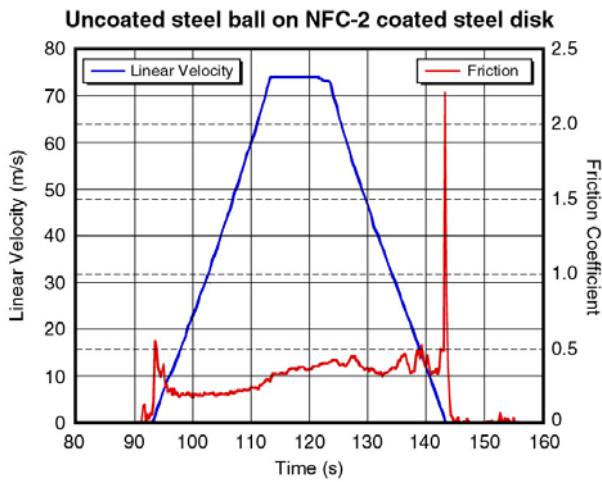


Figure 4. Variation of friction with sliding speed for uncoated steel ball sliding on NFC-coated disc.

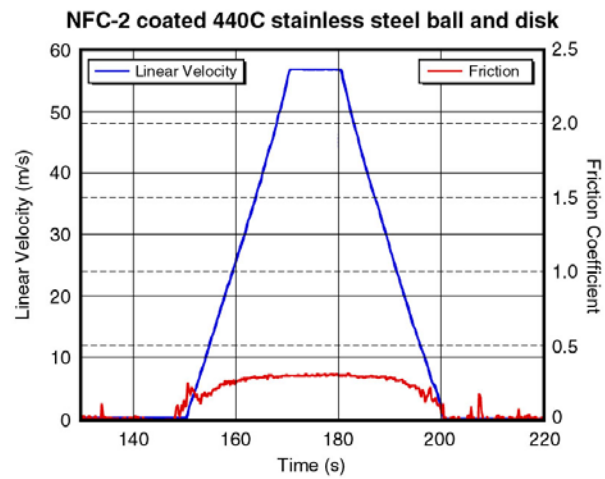


Figure 5. Variation of friction coefficient with sliding velocity for NFC-coated ball sliding on NFC-coated disc.

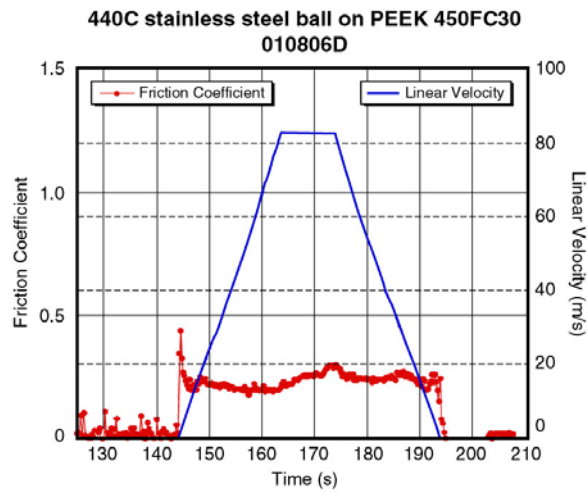


Figure 6. Variation of friction coefficient with sliding velocity for steel-on-PEEK contact pair.

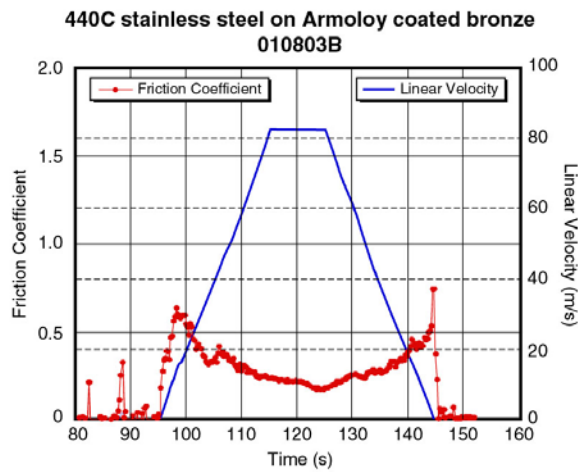


Figure 7. Variation of friction coefficient with sliding speed for steel ball sliding on Armoloy (TDC) coated bronze disc.

D. Microstructural Characterization of PEM Fuel Cells

D. A. Blom and L. F. Allard

Microscopy, Microanalysis, and Microstructures Group

Oak Ridge National Laboratory

P.O. Box 2008, MS 6064, Bldg. 4515

Oak Ridge, TN 37831-6064

(865) 241-3898; fax: (865) 576-5413; e-mail: blomda@ornl.gov

DOE Technology Development Manager: Nancy Garland

(202) 586-5673; fax: (202) 586-9811; e-mail: nancy.garland@ee.doe.gov

ORNL Technical Advisor: David Stinton

(865) 574-4556; fax: (865) 241-0411; e-mail: stintondp@ornl.gov

Contractor: Oak Ridge National Laboratory, Oak Ridge, Tennessee
Prime Contract No.: DE-AC05-00OR22725

Objectives

- Use transmission electron microscopy (TEM) characterization techniques to optimize the distribution of precious metal catalyst for increased efficiency and reduced catalyst loading.
- Characterize/quantify microstructural changes and their relation to performance loss in polymer electrolyte membrane (PEM) membrane electrode assemblies (MEAs) upon use in a fuel cell system to understand issues relating to durability and lifetime

Approach

- Characterize the microstructure and chemical composition of PEM MEAs before and after use to correlate performance to the microstructure at nanometer and greater levels.
- Prepare samples that are thin over large areas for TEM observation to facilitate the ability to understand the entire MEA as a unit.
- Maintain the relationships among the constituents of the MEA in TEM samples in order to achieve insight into the operation of the real system.

Accomplishments

- Established a new state-of-the-art cryo-ultramicrotomy facility at Oak Ridge National Laboratory (ORNL).
- Prepared successful sections of MEA tested to failure.
- Characterized microstructure of failed MEA (aged 1200 h).
- Quantified change in platinum catalyst size distribution upon aging (fresh vs short time vs failed).

Future Direction

- Improve room-temperature sectioning technique to allow for the routine preparation of thin MEA cross-sections.
- Develop cryo-ultramicrotomy technique for preparation of ultrathin (<100-nm) samples to achieve improved analytical results.

- Continue collaborative research with Los Alamos National Laboratory on the microstructural changes that occur during the MEA preparation process.

Introduction

Polymer electrolyte membrane fuel cells hold great promise for use as an environmentally friendly power source for automobiles. One of the key challenges in making PEMs commercially viable is to reduce the cost by reducing the amount of precious metal catalyst necessary to provide high-power-density operation at low temperatures.

For efficient catalysis to occur, gas molecules must be able to easily interact with the surface of the catalyst particles. A pathway for diffusion of protons must exist in close proximity to the active sites on the catalyst, and an electrically conductive pathway from the catalyst to the electrodes is required for electron transport. Finally, water (the by-product of the fuel cell reaction) has to be transported away from the catalyst for continuing reaction to occur. These requirements show the complexity of building an efficient PEM fuel cell and clearly indicate the opportunity for atomic-scale microstructural and chemical characterization to provide feedback on the geometry and distribution of the various components for optimum performance.

Approach

Cross-sections of PEM MEAs were prepared for TEM using an ultramicrotome. Small sections from the MEAs, approximately 3×8 mm, were selected for sample preparation. The samples were placed into silicone embedding molds, and an Araldite epoxy resin was added to the molds to embed the sample. The resin was polymerized at least 16 h at 60°C to produce a solid epoxy piece with the MEA sample embedded. Initial trimming of the epoxy-embedded sample was performed with a Leica EM Trim tungsten carbide trimming tool. A tungsten carbide tip was used to rapidly remove excess epoxy from around the MEA sample and produce a small flat area suitable for ultramicrotomy. The nature of the MEAs dictated a narrow (0.25–0.5 mm), long (1–2 mm) area for ultramicrotomy. The epoxy-embedded MEA was then secured into the cutting arm of a Leica Ultracut UCT Ultramicrotome. The ultramicrotome is designed to allow for the slicing of thin sections of epoxy-embedded samples for

TEM characterization. A 45° diamond knife was used to slice several sections of various thicknesses from each sample. The goal is always to produce the thinnest possible slice for TEM examination. Slice thicknesses were typically 300 nm or less. The thin slices were floated off the diamond knife edge onto distilled water and then collected onto copper mesh grids.

Results

During FY 2002, a new ultramicrotomy facility for room-temperature sectioning of materials was established at ORNL. Figure 1 shows the Leica



Figure 1. Leica UCT ultramicrotome and controller.

ultramicrotome and its control interface. The ultramicrotome is a computer-controlled, motorized device for reproducibly moving the sample past a fixed knife and advancing the sample in a controlled manner to produce thin sections of material. The cutting arm moves up and down to produce the thin sections. The stereomicroscope is used to position the knife appropriately relative to the sample and observe the sectioning action at moderate magnification. Figure 2 is a close-up of a diamond

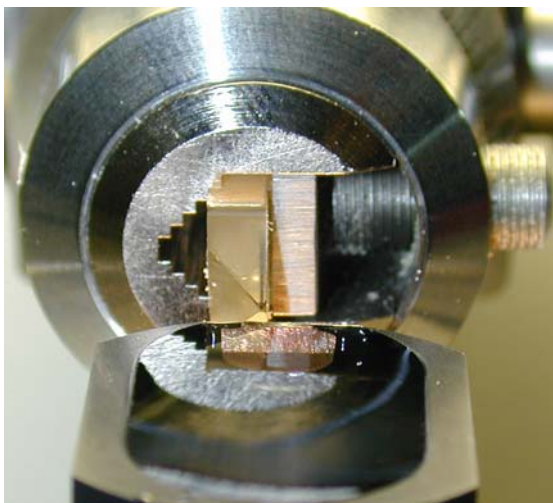


Figure 2. Close-up of cutting arm, sample, and diamond knife.

knife with water trough and the epoxy-embedded sample in the cutting arm.

MEA cross-sections have been successfully prepared for TEM examination using this equipment. The sections are typically 200–300 nm in thickness, which is thicker than desired for best resolution and analytical characterization. Additional work is needed to improve our ability to routinely produce sections that are less than 200 nm thick.

W. L. Gore and Associates aged a third-party MEA for 1200 h at an accelerated rate in order to cause failure of the MEA. Samples from this MEA were prepared for TEM characterization via room-temperature ultramicrotomy. Figure 3 shows the interface between the membrane and the anode for this aged MEA. The image was collected on a Hitachi HF-2000 cold field emission gun 200-kV transmission electron microscope. The small, dark features are the platinum catalyst particles or agglomerates of the catalyst, while the featureless area at the bottom of the figure is the PEM. A high-angle annular dark field, or Z-contrast, image of the same sample is seen in Figure 4. In this case, the platinum particles appear as bright features against the background of the anode.

At least ten images were taken from both the anode and cathode and analyzed to determine the size distribution of the platinum catalysts. Figure 5 is the histogram of platinum catalyst size for an unaged MEA that had previously been analyzed. The most common particle size was less than 1 nm,

with a median size of 1.78 nm. There was no difference in

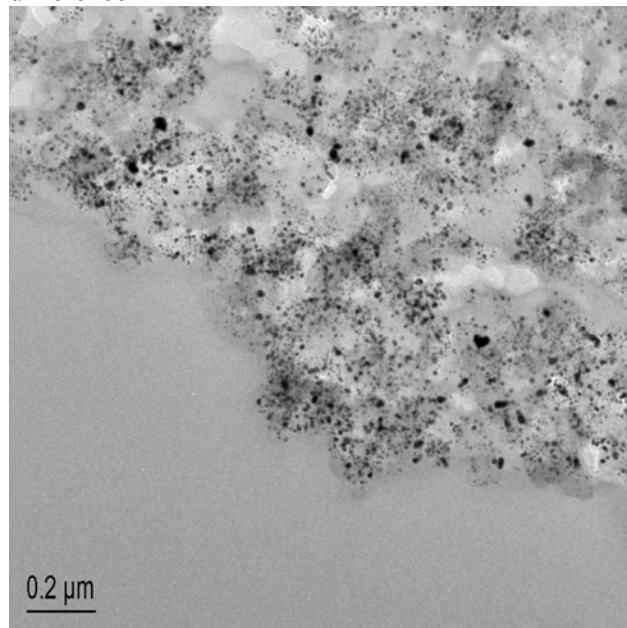


Figure 3. Bright field TEM image of membrane/anode interface in MEA subjected to accelerated aging for 1200 h. Platinum catalyst particles are the small, dark features.

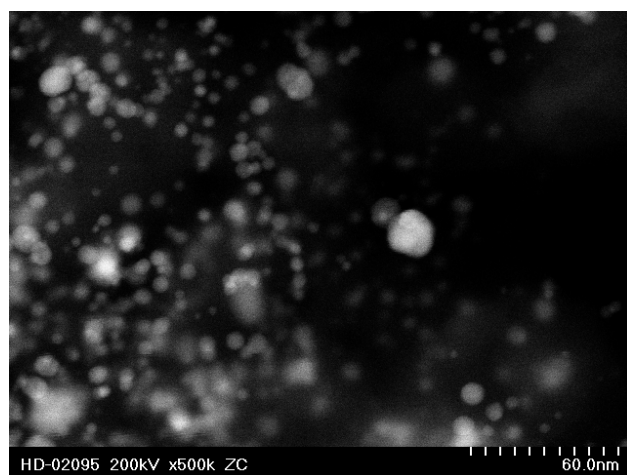


Figure 4. Z-contrast scanning TEM image of aged MEA. The platinum catalyst is bright relative to the electrode.

the distributions between the anode and cathode of the fresh MEA. Figure 6 shows the catalyst size distribution for the anode of the MEA aged for 1200 h (shown in Figures 3 and 4). The most common size was between 2 and 3 nm, and the median size was 4.49 nm. Figure 7 is the size distribution of the catalyst particles in the cathode of

the same MEA. The most common size was between 1 and 2 nm, and the median size was 3.66 nm.

characterization. After the accelerated aging, significant changes in the size distribution of

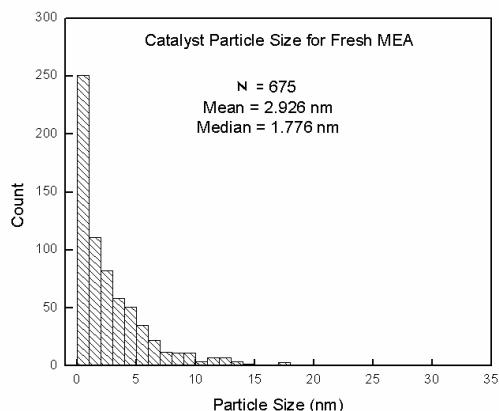


Figure 5. Platinum catalyst size histogram for the fresh MEA. Median particle size is 1.8 nm, and most common size is 0-1 nm.

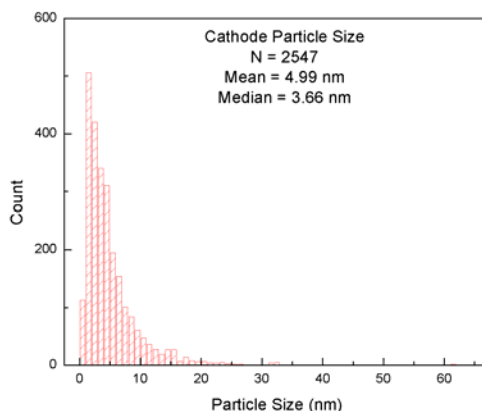


Figure 7. Platinum catalyst size histogram for the cathode of the aged MEA. Median particle size is 3.66 nm, and most common size is 1-2 nm

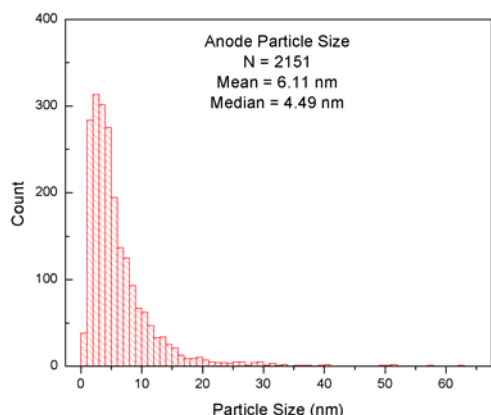


Figure 6. Platinum catalyst size histogram for the anode of the aged MEA. Median particle size is 4.49 nm, and most common size is 2-3 nm

Table 1. Summary of platinum particle size distributions for fresh, 325-h-aged MEA and 1200-h-aged MEA

	Mean (nm)	Median (nm)	No. of particles (N)
Fresh MEA	2.93	1.78	675
After 325 h	4.32	3.16	994
1200 h cathode	4.99	3.66	2547
1200 h anode	6.11	4.49	2151

Table 1 summarizes the particle sizing data, including some data from another MEA that was aged for a shorter period of time and showed no discernible loss of performance.

Conclusions

New ultramicrotomy equipment was established at ORNL. Room-temperature ultrathin sectioning of PEM MEAs was successfully demonstrated. A PEM MEA that had been subjected to an accelerated aging schedule was successfully prepared for TEM

platinum catalyst particles were observed. Even the moderate temperatures of PEM operation (80°C), when coupled with electrochemical driving forces, were sufficient to produce coarsening of the platinum catalyst. The anode catalyst coarsened more than the cathode catalyst. The changes observed are not sufficient to explain the complete failure of the MEA. Degradation of the PEM itself and the development of pinholes across the PEM may account for the complete failure of the MEA. In previous PEM MEAs, a chemically distinct layer was found to form at the interface between the electrodes and the membrane. No such layer was observed in the MEA subjected to an accelerated aging process. Review of the accelerated aging protocol may be warranted to ensure that the degradation processes remain the same in both the accelerated test and typical usage conditions.

Publications

D. A. Blom and L. F. Allard, "Microstructural Characterization of Proton Exchange Membrane

Fuel Cells," DOE 2002 Review, OTT Fuel Cells Program, National Renewal Energy Laboratory, May 9–10, 2002.

E. Nano-Particulate Porous Oxide Electrolyte Membranes as Proton Exchange Membranes

M. Isabel Tejedor, Marc A. Anderson, and Walt Zeltner

Environmental Chemistry and Technology Program

University of Wisconsin

Room 109, 660 North Park Street

Madison, WI 53706

(608) 262-2674; fax: (608) 262-0454; e-mail: nanopor@facstaff.wisc.edu

Mark A. Janney and James O. Kiggans

Metals and Ceramics Division

Oak Ridge National Laboratory

P.O. Box 2008, MS 6087

Oak Ridge, TN 37831-6087

(865) 574-8863; fax: (865) 574-8271; e-mail: kiggansjo@ornl.gov

DOE Technology Development Managers: Nancy Garland

(202) 586-5673; fax: (202) 586-9811; e-mail: nancy.garland@ee.doe.gov

JoAnn Milliken

(202) 586-2480; fax: (202) 586-9811; e-mail: joann.milliken@ee.doe.gov

Contractor: University of Wisconsin—Madison

Prime Contract No.: DE-FC02-99EE50583

Objectives

- Develop microporous inorganic oxide-based membranes of TiO₂ with high proton conductivity that can operate at above 100EC with minimal water management problems.
- Develop processes to fabricate porous nickel or graphite paper electrodes that support the membrane.
- Demonstrate fuel cell behavior in porous oxide electrolyte membrane- (POEM-) based membrane electrode assemblies (MEAs).

Approach

- Phase 1: (a) Determine conditions under which nano-particle sols of candidate oxides yield microporous gels; (b) measure proton conductivities of these gels as a function of temperature and relative humidity; (c) chemically adsorb anionic or cationic functional groups onto oxide particles contained in xerogels or membranes in order to enhance proton conductivity.
- Phase 2: (a) Develop methods for depositing platinum on asymmetric mesoporous electrodes; (b) deposit crack-free films of POEMs on mesoporous electrodes; (c) characterize permeabilities of H₂ and O₂ through the resulting supported membranes under desired conditions of relative humidity and temperature; (d) fabricate and test an entire inorganic MEA containing a POEM deposited on mesoporous electrodes.

Accomplishments

- Demonstrated proton conductivity in POEMs at temperatures of up to 130EC at a relative humidity of 81%.
- Better defined the effects of pore size and pH on proton conductivity in POEMs.

- Fabricated a first-generation test apparatus to measure the performance of our POEMS and MEAs containing POEMs in a functional fuel cell configuration.
- Collected initial data concerning open circuit potential and current-voltage relationships for an oxide-based anode/POEM configuration (i.e., 2/3 of an MEA) (platinum loading in anode = 0.003 mg/cm²).

Future Direction

- Develop a better understanding of the relationships and interactions among the various layers in the MEA (particularly the cathode layer) and how they control the performance of the overall fuel cell system.
- Characterize and subsequently optimize the performance of fuel cells that contain POEMs.
- Develop testing techniques for measuring proton conductivity at temperatures approaching 150EC at ≥40% relative humidity.
- Investigate the nickel substrate as the support for the cathode instead of the anode in an inorganic MEA.
- Further develop graphite fiber paper supports as a potential substitute for nickel substrates.

Introduction

Nano-particulate POEMs are being developed as a radical alternative to polymeric proton exchange membranes for fuel cells. These new membranes can operate at temperatures over 100EC, retain water at these elevated temperatures, and provide proton conductivities of the same order of magnitude as the Nafion membranes presently employed. In addition, inorganic MEAs that incorporate POEMs should reduce the cost of fuel cells because they substantially reduce the amount of platinum catalyst required to operate the fuel cell and they minimize CO poisoning of the platinum by operating at elevated temperatures.

One constraint in using POEMs is that they must be supported on a structural substrate because the membranes are thin (≤500 nm), porous (~40 vol % void space), and brittle (an inherent property of ceramic membranes). The porous substrate provides both electrical conductivity and gas distribution. Because the POEM itself is composed of 5–10 nm particles, an intermediary sandwich layer (particle diameter 50–500 nm) is required to provide geometric compatibility.

Approach

The objective of this effort is to develop MEAs for H₂ fuel cells based on POEMs. These membranes are made of nano-particle oxides such as TiO₂, SiO₂, ZrO₂, or Al₂O₃ that are hydrophilic and offer higher-temperature stability and operation than

polymeric proton exchange membranes. These membranes are supported on tape-cast porous nickel.

The POEM MEA is a complex materials system, not just a collection of individual components. This oxide-based MEA [anode/membrane electrolyte (separator)/cathode] is a composite material that simultaneously performs a variety of operations. One cannot consider any particular aspect of this materials system in isolation; all functions must operate in concert with one another. The anode must conduct electrons and at the same time convert hydrogen gas to protons at one interface with the POEM. The POEM itself must conduct protons—but not electrons, which would cause a short—while also preventing crossover of hydrogen and oxygen across the POEM. Finally, the cathode must convert gaseous oxygen to O⁻² ions that then combine, at the other interface with the POEM, with protons that have migrated through the POEM. This cathode reaction is a four-electron-transfer reaction that is quite difficult to perform efficiently. More will be said about the cathode layer and about reasons for improving its performance later in this report.

Results and Discussion

Membrane Development—pH Effects

Proton conductivity in fluid-filled, hydrophilic, mesoporous, inorganic membranes such as these POEMs derives from the movement of H⁺ ions (1) by hopping along surface sites from particle to particle, (2) by migrating through the electrical double layer in the pores near the surface of the

particles, or (3) by migrating through the bulk pore fluid. As shown in Figure 1, proton transport and the

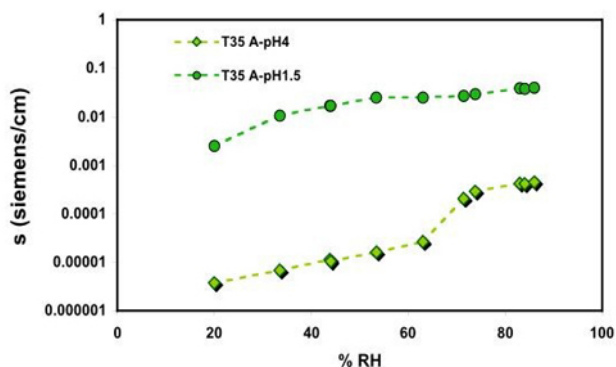


Figure 1. Dependence of proton conductivity on pH at 40EC.

resulting conductivity drastically change with the pH at which the membrane is equilibrated. Note that Nafion-type membranes are often soaked in strong acids to protonate their acid groups. In this regard, our membranes are similar, although full protonation of the surfaces of these inorganic membranes may be reached at higher pH values than are required for Nafion.

Proton transport behavior also greatly depends upon the nature of the oxide, as shown in Figure 2. Note that at lower relative humidities, TiO₂/ZrO₂ and Al₂O₃ membranes have conductivities that are

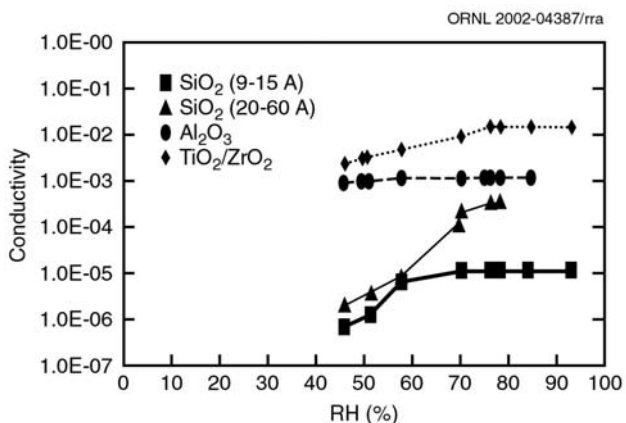


Figure 2. Proton conductivity for various oxides as a function of relative humidity at 80EC.

two to three orders of magnitude higher than those of SiO₂, even though the silica membranes are more acidic. The reason for this behavior is that these

membranes were pre-equilibrated at pH 1.5. This pH is very close to the isoelectric pH (i.e., the pH at which the surface of the oxide is electrically neutral) of SiO₂, which is ≈ 2–3, but 4 to 7 pH units more acidic than the isoelectric pH values of TiO₂/ZrO₂ and Al₂O₃, respectively. As a result, the SiO₂ membranes are **not** highly protonated at pH 1.5, whereas the other two membranes have almost achieved maximum charging and therefore maximum proton conductivity.

Membrane Development—Pore Size Dependence

The conductivity of a particular membrane depends on the conditioning of the surfaces within the pores, as well as the relative humidity. These two factors interact to determine how much water resides inside the pores. In the as-fired condition, the pore surfaces are poorly protonated. Conditioning the membrane material by exposing the membrane to an aqueous solution tends to increase the degree of protonation, depending on the pH of the solution, as noted earlier. However, as can be seen in Figure 3, proton conductivity for TiO₂ at 40EC also depends upon pore size, increasing one order of magnitude at low relative humidity values as pore diameter decreases from 35 to 25 Å. We can reduce the pore size in this membrane even further to about 15 Å, which may further enhance its proton conductivity.

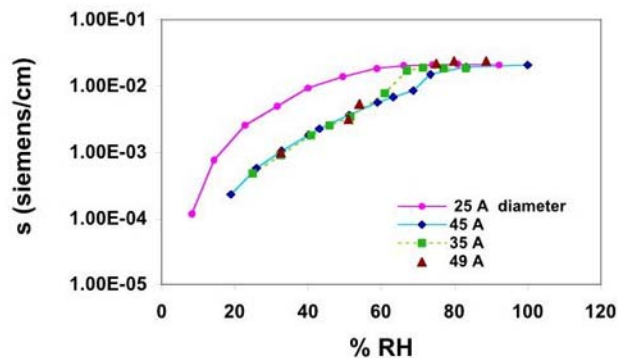


Figure 3. Dependence of proton conductivity on relative humidity for TiO₂ membranes of various pore sizes.

Initial Evaluation of an Inorganic MEA

Because these POEMs are not self-standing materials like organic polymer membranes such as Nafion, we cannot fabricate an MEA unless we cast

our membranes on a rigid but porous support. Furthermore, the support must be electrically conducting and must already be coated with a porous catalyst layer before we cast the membrane. The resulting composite MEA will be activated by imbibing an acid solution into the MEA before it is used.

Enable Fuel Cell Corp. (Middleton, Wis.) fabricated a passive test chamber to evaluate the performance of our materials. For these initial room-temperature tests, we fabricated 2/3 of an inorganic MEA (i.e., porous nickel support/nano-particle TiO_2 membrane loaded with platinum catalyst to serve as one electrode/ TiO_2 POEM). We used a carbon fabric loaded with platinum as the second electrode. We ran the inorganic MEA as either an anode or a cathode depending on the polarity of the test circuit. When hydrogen contacted the inorganic MEA (i.e., our MEA was operated as a working anode), we achieved open-circuit voltages between 0.74 and 1.02 V. When our inorganic MEA was operated as a cathode, we obtained slightly lower voltages (0.76–0.88 V). More will be said about this later.

Unfortunately, it was difficult to seal the cell to prevent hydrogen leaks. In addition, it was difficult to test individual layers of our MEA system because the carbon fabric glued itself to the inorganic MEA and could not be detached without delaminating the MEA. To resolve these issues, we built a new test cell, as shown in Figure 4. As shown, our MEA was now sealed in a metal O ring using ceramic cement. This cell proved to be easily sealed without hydrogen leaks; furthermore, it could be readily disassembled. However, we still need to improve the ohmic contacts to the anode and cathode layers. We used copper wool to provide contacts in this apparatus. However, copper wool easily oxidizes in contact with acids and does not provide a uniform contact with the electrodes.

Test Performance

Shown in Figure 5 are initial current-voltage curves for the 2/3 of an inorganic MEA system described versus a similar Nafion-based system in tests at room temperature. As can be seen, the



Figure 4. Teflon test cell and our membrane electrode assembly system.

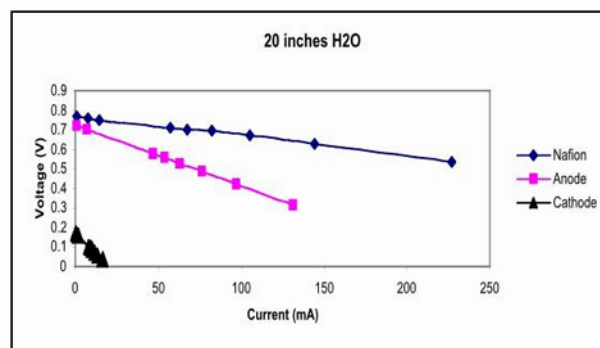


Figure 5. Current-voltage curves for our membrane electrode assembly versus a Nafion system.

Nafion system performs somewhat better than our initial prototype when the inorganic MEA operates as an anode. When we invert the contacts so that the inorganic MEA operates as a cathode, the inorganic MEA system performs much worse. A positive aspect of this performance is that the platinum content of the inorganic MEA is 0.003 mg/cm^2 .

Cathodes and the Total MEA

Shown in Figure 6 is a diagram of a nickel support and a platinum-loaded nano-particulate oxide acting as a porous cathode. Organic-based fuel cell cathodes often add some Nafion to this layer to improve its proton conductivity, but at the cost of decreasing its electrical conductivity. However, we have the reverse problem—we have excellent proton conductivity in our inorganic cathode, but our oxides are electrical insulators. We need to boost the electrical conductivity of our

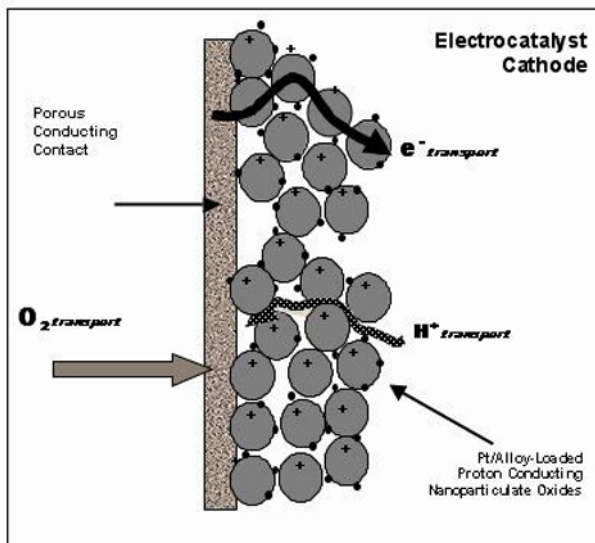


Figure 6. Diagram of an inorganic fuel cell cathode.

cathode in order to fabricate a total inorganic MEA. This is a major objective of our future work.

Conclusions

We have successfully fabricated and tested 2/3 of an inorganic MEA consisting of a porous nickel support, a nano-particle TiO_2 membrane containing platinum catalyst that served as an effective anode, and a nano-porous TiO_2 POEM. A novel test cell

was built to facilitate testing, but additional modifications are needed. Although the performance of this prototype inorganic MEA was not as good as that of a corresponding Nafion-based system at room temperature, the inorganic MEA required only a small amount of platinum to function. In order to prepare this inorganic MEA, a novel method had to be developed for applying a ceramic sandwich layer to the porous, electrically conducting nickel substrate. This method should be useful in other membrane applications.

Efforts will continue to fabricate a full inorganic MEA and to test these systems at high temperatures. It appears that a functional inorganic MEA will require a cathode with higher electrical conductivity than was available in our initial tests. In addition, we are attempting to develop a graphite fiber-based substrate having the requisite chemical compatibility with the proton exchange membrane environment. As part of this development, POEM fuel cell assembly using standard, multilayer manufacturing technologies will be investigated.

Publications/Presentations

Results were presented at the national meeting of the American Institute of Chemical Engineers in New Orleans in March 2002.

F. Bacterial Cellulose Membranes

Hugh O'Neill, Barbara R. Evans, and Jonathan Woodward

Chemical Sciences Division

Oak Ridge National Laboratory

P.O. Box 2008

Oak Ridge, TN 37831-6194

(865) 574 5004; fax: (865) 574 1275; e-mail: oneillhm@ornl.gov

DOE Technology Development Manager: JoAnn Milliken

(202) 586-2480; fax: (202) 566-9811; e-mail: joann.milliken@ee.doe.gov

ORNL Technical Advisor: David Stinton

(865) 574-4556; fax: (865) 241-0411; e-mail: stintondp@ornl.gov

Contractor: Oak Ridge National Laboratory, Oak Ridge, Tennessee

Prime Contract No.: DE-AC05-00OR22725

Objectives

- Synthesize a proton-conductive membrane for a polymer electrolyte membrane (PEM) fuel cell.
- Synthesize a membrane that is stable at temperatures >120EC.
- Synthesize a membrane that maintains the conditions conducive to proton conductance from the anode to the cathode through the polymeric medium while operating at high temperatures.

Approach

- Modify bacterial cellulose so as to preserve its properties that have been identified as useful for PEM fuel cell development, including thermal stability and low hydrogen crossover.
- Modify bacterial cellulose membranes with acid groups to produce a proton-conductive membrane without compromising the structure of the cellulose membrane.

Accomplishments

- Investigated different strategies to confer ion-exchange properties on bacterial cellulose.
- Synthesized a cellulose membrane activated with phosphate groups.
- Evaluated the properties of the cellulose phosphate membrane.

Future Direction

- Complete the characterization of phosphate membranes.
 - Revisit and evaluate other strategies for chemical modification of cellulose.
 - Test performance of ion-exchange membranes in a membrane electrode assembly.
 - Modify cellulose in vivo by using activated glucose monomers.
-

Introduction

Bacterial cellulose is produced by *Gluconoacetobacter* sp. bacteria during growth on carbohydrate sources. Nascent cellulose strands, synthesized by the bacteria, are secreted and form layers at the air-liquid interface (Figure 1A, 1B). This network of cellulose fibrils resembles a sponge and is called a "pellicule." After cleaning to remove cellular debris, the pellicule typically contains more than 99% H₂O; the remainder is cellulose. When the pellicules are dried to remove water, the layers of cellulose collapse on top of each other to produce a very thin membrane (<50 μm thick).

Of particular interest to the DOE fuel cell program is the development of thermostable membranes that will facilitate the transfer of protons from the anode to the cathode during operation of a PEM fuel cell at high temperatures (>120EC). At higher operating temperatures, the electrode kinetics are improved, resistance to poisoning by carbon monoxide is increased, and the catalyst cost is minimized. Bacterial cellulose has several unique properties that potentially make it a valuable material for the development of PEM fuel cells: (1) it is a cheap and nontoxic natural resource, (2) it has good chemical and mechanical stability, (3) it is very hydrophilic, and (4) it does not re-swell after drying.¹ Additionally, its thermal stability and gas crossover characteristics are superior to those of Nafion 117, a material widely used as a proton-conductive membrane in PEM fuel cells.

Approach

There is a wealth of data, in both the scientific and patent literature, on the chemical modification of plant cellulose. All of these methods are equally applicable to bacterial cellulose, given that the two types of cellulose are chemically identical. However, it is the physical structure of bacterial cellulose membranes that makes it a potential material for PEM fuel cells. Therefore, the aim is to modify bacterial cellulose pellicules in such a manner that the structure of the cellulose is retained and the physical properties, such as thermal stability, gas crossover characteristics, and resistance to re-swelling after drying, are not compromised.

Results

Several strategies were employed to modify bacterial cellulose with ion-exchange groups. Of the methods attempted, modification of native bacterial cellulose with phosphate groups was most successful (Figure 2). The properties of the native and modified membrane compared with those of Nafion 117 are presented in Table 1.

Cellulose phosphate had 2.7-fold greater thermal stability and 7.6-fold lower H₂ permeability than Nafion 117. This marked increase in the thermal stability of cellulose phosphate was not unexpected, given that this material was first developed as a flame-retardant material. Unlike Nafion, cellulose phosphate is prone to swelling in H₂O. However, at temperatures of more than 120EC, this characteristic may not pose a problem during operation of the fuel cell. The density of ion-exchange groups available

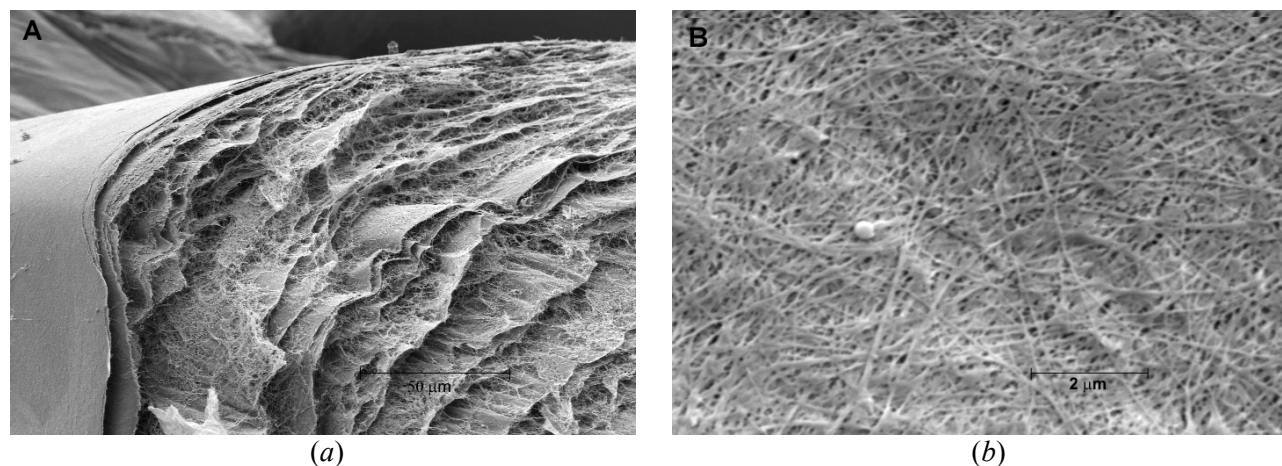


Figure 1. Scanning electron microscope micrographs of freeze-dried bacterial cellulose: (a) transverse section and (b) top view.

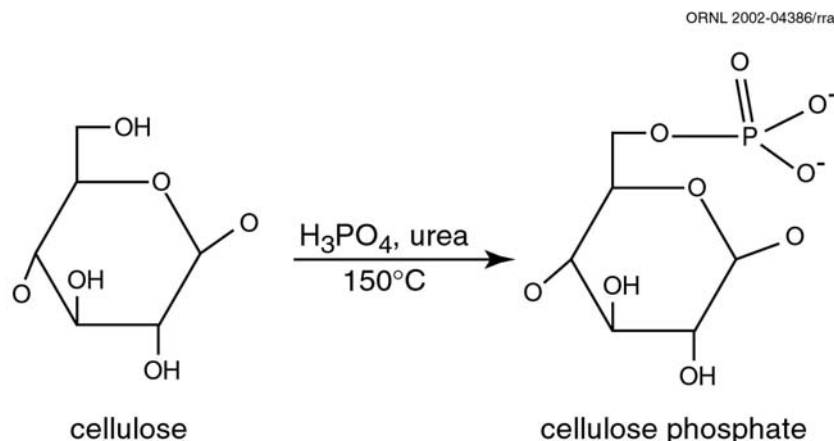


Figure 2. Synthesis of cellulose phosphate.

Table 1. Comparison of the properties of cellulose phosphate with native bacterial cellulose and Nafion 117

Membrane characteristics	Native cellulose	Cellulose phosphate	Nafion 117
Physical properties			
Dry membrane thickness (mm)	0.010	0.023	0.199
Wet membrane thickness (mm) ^a	0.032	0.081	0.225
H ₂ O content / g dry membrane (g/g) ^a	3.47	3.16	0.31
Thermal stability (°C)	130	245	<90
Ion exchange capacity (mequiv/g)	0	1.3	0.9
H ₂ crossover (nmol.mil/h.cm ² .atm) ^b	n.d.	267.2	2039.4
Mechanical stability			
Resistance to crease/crack:			
dry	Yes	No	Yes
hydrated	Yes	Yes	Yes
Resistance to tearing:			
dry	No	No	Yes
hydrated	Yes	Yes	Yes
Resistance to gas pressure (dry)	n.d.	30 psi	>50 psi
Chemical stability			
Acid stability (% weight loss) ^c	12	39	2.5

^aDetermined after heating to 99°C for 2.5 hours in H₂O.

^bMeasured at 20 psi H₂ (100%) and 25°C.

^cDetermined after incubation in 0.5M H₂SO₄ at 95°C for 45 hours.

for proton transport is similar in both materials. The superior mechanical properties of Nafion are probably due to the difference in thickness between the materials.

After incubation of the cellulose phosphate membrane at 95°C for 45 h, the cellulose phosphate lost 39% of its original weight. This increase in sensitivity to acid attack is probably an artifact of the reaction conditions employed in the synthesis.

Modifications of the reaction procedure will be investigated to minimize this unwanted side reaction.

Conclusions

Several properties of cellulose phosphate have been evaluated. The material has good thermal stability and low hydrogen crossover, two

requirements that are important to meet DOE fuel cell program targets. Further characterization of the material is required, especially the determination of proton conductivity. In addition, testing of the material in a membrane electrode assembly will allow the effect of acid stability and swelling properties of cellulose phosphate to be evaluated under typical PEM fuel cell operating conditions.

References

¹H. O'Neill, B. R. Evans, and J. Woodward, "Metallized Bacterial Cellulose Membranes in Fuel Cells," pp. 141–145 in *Fuels Cells for Transportation Annual Progress Report*, 2001.

Publications/Presentations

B. R. Evans, H. O'Neill, V. P. Malyvanh, and J. Woodward, "Palladium-Bacterial Cellulose Membranes for Fuel Cells," submitted to *Biosensors and Bioelectronics*.

B. R. Evans, H. O'Neill, and J. Woodward, "Bacterial Cellulose in Energy Conversion Applications," poster presentation at the 24th Symposium on Biotechnology for Fuels and Chemicals, April 28–May 1, 2002, Gatlinburg, Tenn.

B. R. Evans, H. O'Neill, and J. Woodward, "Micro-Fuel Cell Development Based on Bacterial Cellulose," oral presentation at the 14th World Hydrogen Conference, June 9–13, Montréal, Canada, 2002.

Patents Issued

B. R. Evans, H. O'Neill, V. P. Malyvanh, and J. Woodward, "Metallization of Bacterial Cellulose for Electronic and Electrical Devices," patent pending, invention disclosure 0869, S-96, 631, 2001.

H. O'Neill, B. R. Evans, J. Woodward, "Synthesis of a Novel Ion-Exchange/Proton Conductive Membrane," invention disclosure submitted, ID 1099, S-99, 279, 2002.

G. Carbon Foam for Radiators for Fuel Cells

A. D. McMillan and J. W. Klett

Carbon Materials Technology Group

Oak Ridge National Laboratory

P.O. Box 2008, MS 6087, Bldg. 4508

Oak Ridge, TN 37831-6087

(865) 241-4554; fax: (865) 576-8424; e-mail: mcmillanad@ornl.gov

DOE Technology Development Manager: Nancy Garland

(202) 586-5673; fax: (202) 586-9811; e-mail: nancy.garland@ee.doe.gov

ORNL Technical Advisor: David Stinton

(865) 574-4556; fax: (865) 241-0411; e-mail: stintondp@ornl.gov

Contractor: Oak Ridge National Laboratory, Oak Ridge, Tennessee
Prime Contract No.: DE-AC05-96OR22464

Objectives

- Develop compact, lightweight, more efficient radiators for fuel-cell-powered vehicles using unique high-conductivity carbon foam.
- Evaluate materials issues (e.g., vibration, erosion, corrosion, plugging, thermal shock) for fuel cell cooling systems.
- Work with radiator manufacturer to develop and test fuel cell radiators.

Approach

- Study fundamental mechanisms of heat transfer using the carbon foam.
- Develop a testing method to evaluate the foams and designs using the foams.
- Work with industrial partners to develop a complete understanding of fuel-cell-related issues.

Accomplishments

- Modified the heat transfer test rig to accommodate subscale prototype radiators.
- Implemented new engineering designs, resulting in high heat transfer with an acceptable pressure drop.
- Conducted a collaborative effort with Georgia Tech Research Institute (GTRI) in which the foam integrated into an airfoil showed excellent heat transfer with very low drag.

Future Direction

- Model further engineering designs for even better heat transfer and decreased pressure drop; use them in airfoils.
 - Complete evaluation of materials-related issues such as corrosion, erosion, and vibration.
 - Complete evaluation of alternative precursor materials.
-

Introduction

Dissipation of heat from fuel cells is more difficult than from internal combustion (IC) engines because fuel cells operate at lower temperatures. The smaller driving force to disperse the heat results in a design problem—that is, excess size and weight of the radiator. Unless more efficient and compact thermal management systems can be developed, radiators on fuel-cell-powered vehicles will need to be significantly larger and heavier than those on conventional vehicles.

The development of a high-thermal-conductivity graphite foam¹⁻³ will lead to novel solutions for thermal management problems. The extremely high thermal conductivity of the ligaments combined with the very high surface area (4 m²/g) make carbon foam an ideal material for heat transfer. This material is an enabling technology for thermal management problems ranging from heat sinks to radiators. For example, with the foam used as a heat exchanger and air used for cooling, heat transfer coefficients over two orders of magnitude greater than those of current metallic finned designs have been measured. This result is particularly important with regard to fuel-cell-powered vehicles, as the heat generated by the stack is difficult to dissipate because of the low operating temperatures.

Approach

Material Testing

A primary concern for potential users of the graphite foam is its durability. Previous work has exhibited its superior thermal properties and the material's excellent response to thermal cycling; however, how the material behaves in certain environments is still a concern. This issue is being addressed by tests being conducted under Society of Automotive Engineers (SAE) J1211 as recommended by the Electrical and Electronics Tech Team. A matrix test plan has been developed and implemented to test the foams under thermal cycling of joined unit(s), corrosion, salt spray, erosion, debris fouling, and vibration. The test plan calls for using three different forms of the graphite foam in each test (control, nickel-plated, and polymer-coated), each of which is joined to a variety of substrates (copper, aluminum, stainless steel, and brass). Each sample will be characterized both physically and thermally prior to testing and post-

testing. Compression testing will then be conducted to determine effects on mechanical properties of the foams.

Another area of interest is decreasing the pressure drop in the system while maintaining a high heat transfer coefficient. Studies have been conducted in air and water using various geometries machined into the graphite foam. These samples have been compared with off-the-shelf metal foams.

GTRI Collaboration

GTRI has a patented aerodynamic heat exchanger (AHE), a high-lift airfoil section that incorporates a conventional radiator to provide heat transfer and cooling to an automobile (passenger or heavy vehicle). If flow is allowed through the airfoil, it can seriously degrade the aerodynamics of the system (Figure 1). Thus, a study jointly funded by OAAAT and the Office of Heavy Vehicle Technologies was undertaken to determine the effectiveness of ORNL's graphite foam in this novel airfoil design; the foam has excellent heat transfer characteristics, while engineering designs may allow tailoring of the porosity. Three AHEs—a conventional radiator manufactured by Visteon (like the one installed in the GT MotorSports Formula SAE race car), a solid graphite foam core, and a corrugated graphite foam core—were tested under the same conditions. Each core had cooling tubing passing through internal channels (Figure 2); and for all configurations, the airfoil was mounted on a strain-gage balance below the floor to measure forces and moments. Data were taken first to determine the aerodynamic characteristics of each core by monitoring the slot blowing pressure at a constant angle of attack, as well as the tunnel pressure. Then the thermal performance was measured by having a constant coolant flow rate for variable pressure; further, the tunnel speed was also varied.

Milling Study

While studies regarding areas of interest to fuel cell vehicles are ongoing, several issues continue to arise with regard to industrial use of graphite foam. Two areas of specific concern are being addressed: material isotropy and lower-cost precursor material. A milling study was conducted to address the

isotropy issue, to determine the effectiveness of

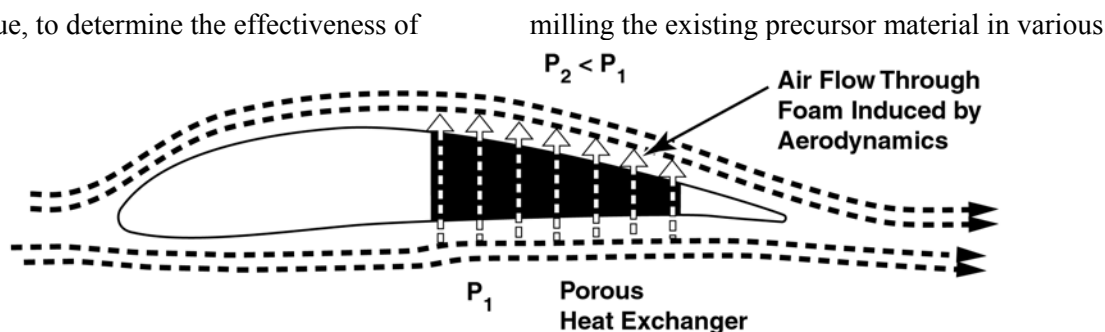


Figure 1. Georgia Tech Research Institute's patented aerodynamic heat exchanger.

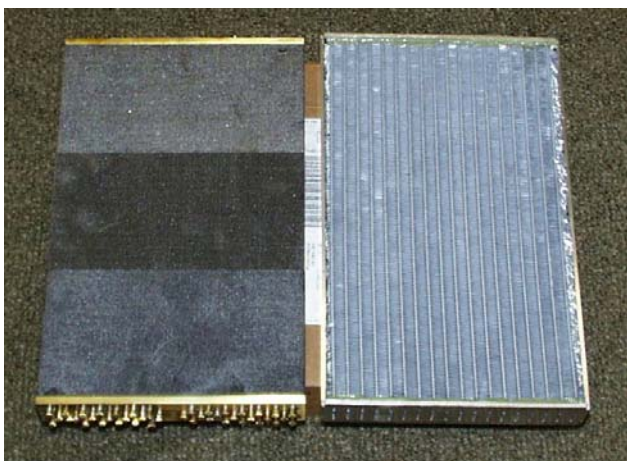


Figure 2. Solid graphite foam (left) and corrugated foam radiator cores.

solvents before foaming. It was thought that in milling, some measure of solvent fractionation might occur and therefore refine the beginning material. In an effort to find a lower-cost starting material, several pitches were included in the milling study. Four pitches were evaluated: Mitsubishi AR (the current precursor), solvated Conoco, Mitsubishi A240, and Koppers. The AR and Conoco were subjected to three different solvents—EtOH, toluene, and xylene; the A240 and Koppers were subjected only to xylene in this study. Additionally, the addition of 5 wt % ground graphitized foam dust (GGFD) to AR milled in EtOH was evaluated under the same conditions.

To avoid cross-contamination, Teflon mill jars were dedicated to a particular pitch. Each mill was loaded with 250 g pitch, 400 g solvent, and 800 g zirconia milling medium. Each mill was subjected to the same amount of milling time at the same speed. After milling, the solution was poured into drying pans and allowed to air-dry. After drying, a 5 × 7 in. pan was loaded with 400 g of pitch and placed in the

furnace to be foamed at 1EC/min; to avoid any temperature variations, only the central loading slots in the furnace were used. Carbonization (0.2EC/min to 1000EC) and graphitization (1EC/min to 2400EC—5EC/min to 2800EC/1 h) were carried out under normal conditions. Characterization of the foams was performed, including scanning electron microscopy, compression tests, electrical resistivity, and thermal conductivity.

Results

Material Testing

The long-term durability tests were initiated in FY 2002 and are ongoing. The corrosion study was conducted in a 50/50 solution of ethylene glycol and water and was 6 weeks in duration. The completed tests were conducted at room temperature, 60EC, and 100EC, and are awaiting final thermal diffusivity measurements to determine any detrimental effects. Only one sample failed—the polymer-coated sample brazed to an aluminum 6061 substrate in the 100EC oven. In this case, the joint failed after approximately 2 weeks, but the sample was subjected to the entire 6 weeks in solution. Until final characterization is complete, it is unknown whether the sample failed because of a galvanic reaction between the graphite and aluminum or because the braze was improperly applied.

The SAE fine and coarse test dusts (NIST traceable) have been received and tests are under way for debris fouling. Although such a test is not part of the test standard, we will examine the possible utilization of the foam's inherent electrical conductivity to discharge any debris buildup. This test should be completed during FY 2003.

Vibration testing has been delayed because of some mechanical difficulties; however, tests are scheduled to be completed during FY 2003.

In an effort to decrease overall pressure drop, we examined several engineering designs, including horizontal blind holes, vertical blind holes, and corrugation. We found that when the foam was machined into a "corrugated" structure (Figure 3), thereby modifying the flow length and web thickness, a pressure drop comparable to that of a copper or aluminum foam was achieved with a heat transfer nearly that of a solid block of graphite foam (Figure 4).

GTRI Collaboration

The heat transferred from the coolant can be expressed as

$$Q = \dot{m}_c C_p (T_{cIN} - T_{cOUT}) \quad .$$

Measurements were made for each configuration at several freestream velocities, coolant flow rates, and blowing rates. Figure 5 shows the comparison of the graphite foam cores to the conventional Visteon core. Interestingly, the solid graphite foam core performed as well as the conventional core but with significantly less drag (Figure 6). Thus, the dense graphite foam core has been shown to be an effective heat transfer medium that does not significantly affect the aerodynamic performance of the AHE.

Milling Study

Samples were cut into 5/8-in., 1-in., or 2-in. cubes. Two different techniques were employed for

measuring density, as density is often the first measure of the isotropy of a graphite foam material. A traditional technique using Euclidean geometry was compared with an immersion density technique to validate the nondestructive technique; an acceptable variation of $\pm 5\%$ or less was measured. Interestingly, it was found that the AR milled in EtOH with the addition of GGFD exhibited the most isotropic density measurements from top to bottom of the blocks of foam (z -direction).

As expected, the compressive strengths varied directly with density. In agreement with previous work, the Conoco pitch exhibited significantly higher strengths, as samples prepared using this pitch have exhibited higher overall densities (Figure 7). Additionally, the Conoco samples exhibited a better isotropy ratio than AR samples, albeit at a lower overall level (Figure 8). Note the AR+GGFD samples retain a high specific thermal conductivity in the z -plane, but more important, the x - and y -planes were increased. This result may be a reflection of the more homogeneous density. Further tests are being conducted with a more refined addition of the dust in an effort to exploit these promising preliminary data. Characterization of the dust particle size, the amount of dust added, and the proportions in which it was added are the variables in this ongoing study.

Microscopy samples were taken from a slice through the thickness of a graphitized block. Micrographs were taken from the bottom of the sample up through the sample to the top, resulting in an evaluation of the entire thickness and any change

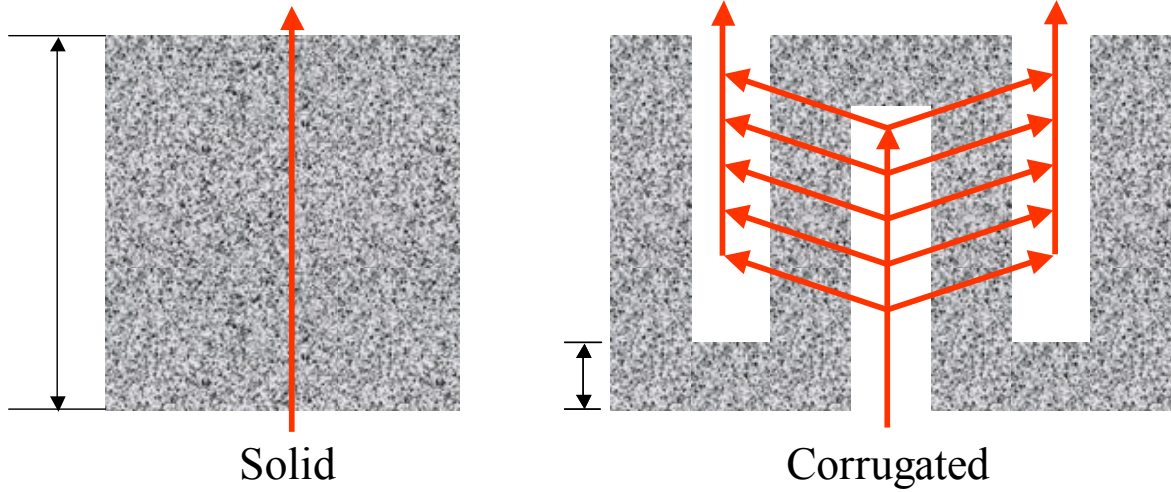


Figure 3. Illustration of the decrease in flow length and web thickness achieved via corrugation.

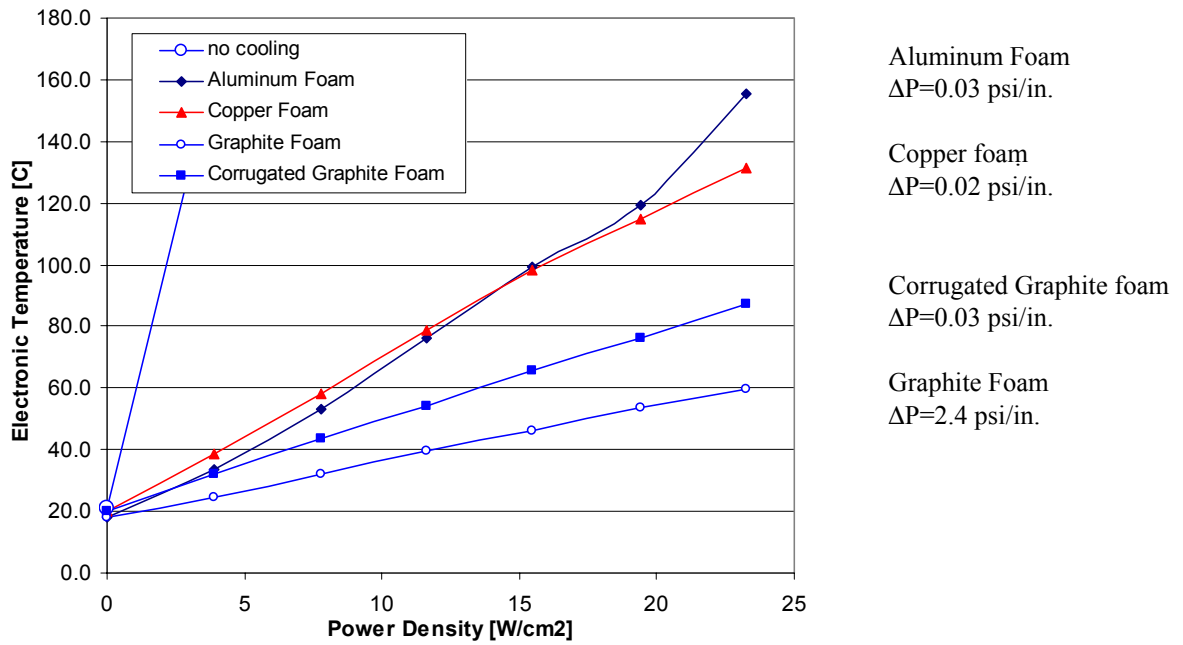


Figure 4. Heat transfer properties of corrugated graphite foam and other foam heat sinks.

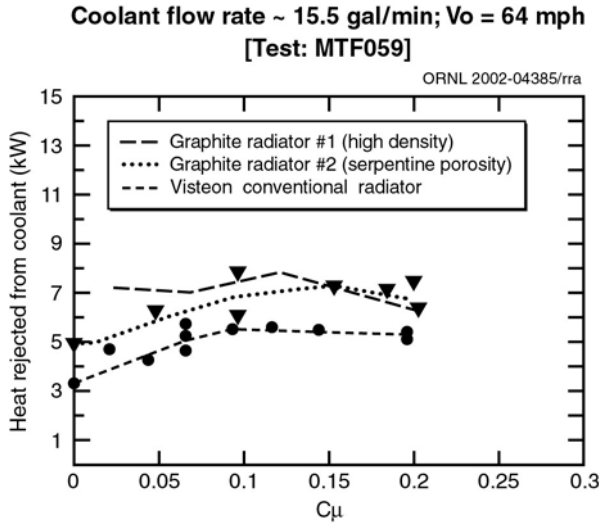


Figure 5. Comparison of different radiator core heat removal rates.

Figure 6. Unblown airfoil lift/drag polars at different angles of attack with and without radiators installed.

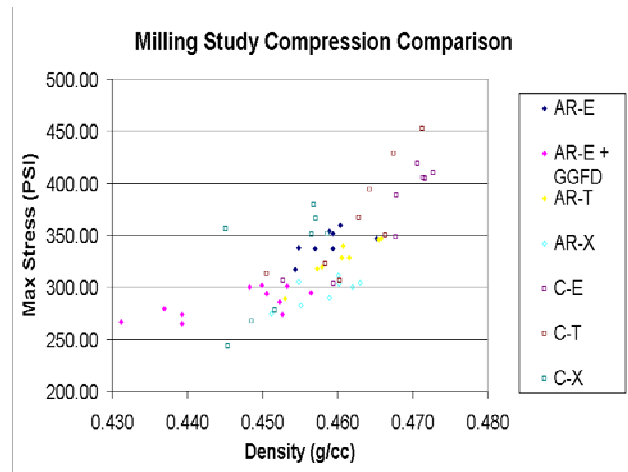
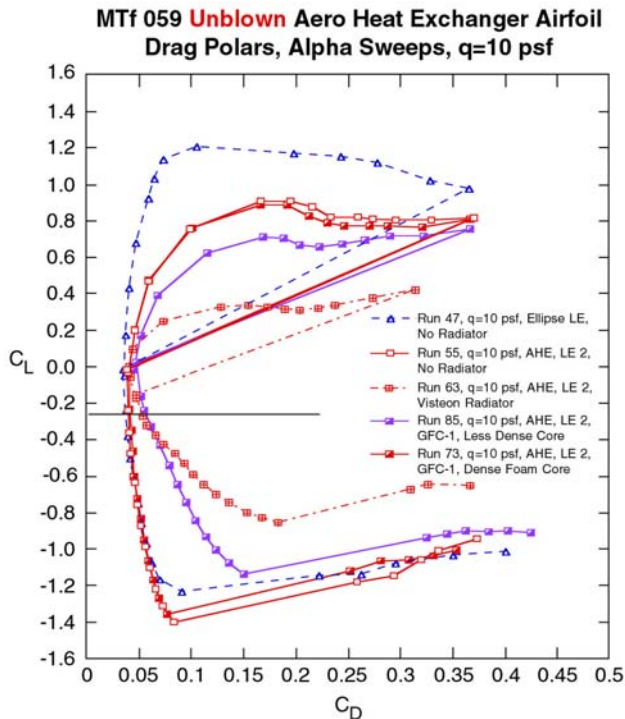


Figure 7. Compression strength of milled graphite foam samples.

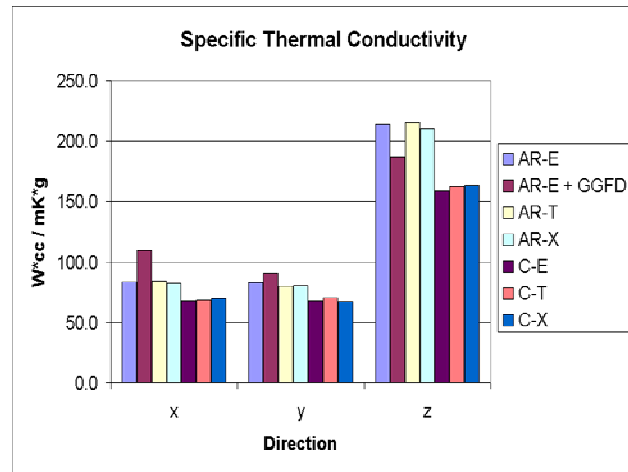


Figure 8. Specific thermal conductivity measurements of milled graphite foams.

in structure (i.e., density gradient). These studies revealed a slight decrease in average bubble size for the Conoco. Also, the decrease in density gradient (as observed by Euclidean measurements) was obvious in the AR+GGFD sample (Figure 9).

Conclusions

Although the data and discussion presented in this paper illustrate the potential of this material to be an

enabling technology, further work is needed. Even though a design for an automobile radiator dramatically smaller than current systems has been developed, ongoing work will determine the effect of the interface at the joint as a function of thermal cycling. Additional studies on vibration, erosion,

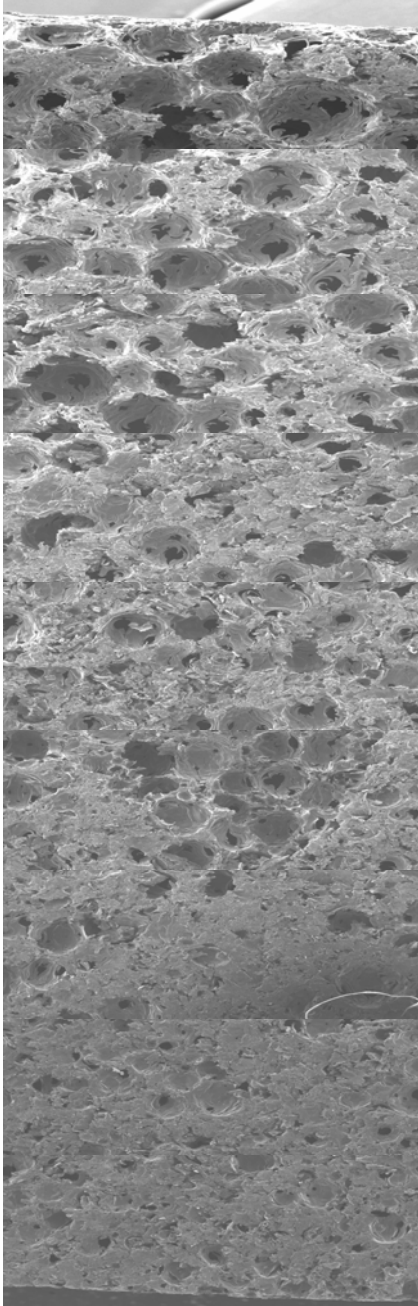


Figure 9. Through-thickness representation scanning electron micrograph of AR milled in EtOH + 5 wt % ground graphitized foam

dust. Mag = 40 \times .

corrosion, and debris fouling are coming to an end. Further, the potential to radically redesign the heat exchanger on a vehicle using the GTRI/ORNL airfoil is very promising. The milling study indicates that the starting material may be treated in such a way as to result in a more homogeneous product. Lower-cost precursor materials, such as Mitsubishi A240 and Koppers, are currently being evaluated. With a more complete understanding of materials properties, the full potential of this material may be realized. A design for a foam core radiator will probably be quite different from the current concept of a radiator. The data presented here illustrate that the foam will be most useful and efficient not when used simply as a replacement for existing thermal management materials, but rather when the full potential of its unique structure is used in out-of-the-box designs.

References

1. J. Klett, R. Hardy, E. Romine, C. Walls, T. Burchell, "High-Thermal-Conductivity, Mesophase-Pitch-Derived Carbon Foams: Effect of Precursor on Structure and Properties," *Carbon* **32**(8), 2000.
2. J. Klett, "High Thermal Conductivity Mesophase Pitch-Derived Graphitic Foams," *Composites in Manufacturing* **14**(4) (1999).
3. J. Klett, C. Walls, and T. Burchell, "High Thermal Conductivity Mesophase Pitch-Derived Carbon Foams: Effect of Precursor on Structure and Properties," p. 132 in *Proceedings of the 24th Biennial Conference on Carbon*, July 11–16, Charleston, S.C., 1999.

FY 2002 Publications

J. Klett, A. D. McMillan, D. Stinton, "Modeling Geometric Effects on Heat Transfer with Graphite Foam," 26th Annual Conference on Ceramic, Metal, and Carbon Composites, Materials, and Structures, Cocoa Beach, Florida, January 2002.

A. D. McMillan, J. Klett, L. B. Klett, "The Effect of Thermal Cycling on Prototype Graphite Foam Heat Exchangers," 26th Annual Conference on Ceramic, Metal, and Carbon Composites, Materials, and Structures, Cocoa Beach, Florida, January 2002.

Patents Issued

J. W. Klett, "Method for Extruding Pitch-based Carbon Foam," U.S. Patent Number 6,344,159, February 5, 2002.

J. W. Klett, "Pitch Based Carbon Foam and Composites," U.S. Patent Number 6,387,343, May 14, 2002.

J. W. Klett, "Method of Casting Pitch-Based Carbon Foam," U.S. Patent Number 6,398,994, June 4, 2002.

J. W. Klett and T. D. Burchell, "Pitch-based Carbon Foam Heat Sink with Phase Change Material," U.S. Patent Number 6,399,149, June 4, 2002.

4. ADVANCED COMBUSTION

A. Materials Improvements and Durability Testing of a Third-Generation Microwave-Regenerated Diesel Particulate Filter

Dick Nixdorf

Industrial Ceramic Solutions, LLC

1010 Commerce Park Drive, Suite I

Oak Ridge, TN 37830

(865) 482-7552; fax: (865) 482-7505; e-mail: nixdorfr@indceramicsolns.com

DOE Technology Development Managers: Nancy Garland

(202) 586-5673; fax: (202) 586-9811; e-mail: nancy.garland@ee.doe.gov

Kathi Epping

(202) 586-7425; fax: (202) 586-9811; e-mail: kathi.epping@ee.doe.gov

ORNL Technical Advisor: David Stinton

(865) 574-4556; fax: (865) 241-0411; e-mail: stintondp@ornl.gov

Contractor: Industrial Ceramic Solutions, Oak Ridge, Tennessee

Prime Contract No.: 4000000723

Subcontractors: Transportation Research Center, East Liberty, Ohio; Lydall Technical Papers, Rochester, N.H.; Northrop Gruman Electron Devices, Williamsport, Pa.; Lubrizol Corporation, Cleveland, Ohio

Objectives

- Design, fabricate, and road-test a pleated ceramic fiber filter system that has reduced engine backpressure compared with conventional particulate filters and will microwave-regenerate at all engine operating conditions.
- Conduct a 7000-mile controlled track test of the filter system, including microwave regeneration at various operating conditions and Federal Test Protocol (FTP) emissions testing to verify filter durability during and after the test sequence.
- Provide filter durability, fuel penalty, and particulate removal efficiency data from the diesel vehicle testing.

Approach

- Conduct papermaking, pleating, and filter cartridge testing to establish an acceptable prototype pleated filter cartridge.
- Use finite element analysis of microwave fields and laboratory air flow/microwave heating tests to design the vehicle-ready test system
- Validate the filter system's particulate removal efficiency on a stationary diesel engine test cell.
- Install and road test the improved microwave filter system on a 7.3-L diesel vehicle.

Accomplishments

- Installed and road-tested a microwave-regenerated filter system on a 1.9-L Volkswagen Jetta vehicle for 200 miles and six filter microwave cleanings. (The testing of the Jetta was abandoned because of engine and exhaust system defects, unrelated to this work, on the vehicle.)
- Developed a pleated ceramic fiber filter cartridge and demonstrated that it achieved 1/20 the exhaust backpressure of a conventional wall-flow particulate filter.
- Tested the Industrial Ceramic Solutions (ICS) ceramic fiber filter cartridge for over 9 months on a Ford 7.3-L truck, under standard highway driving conditions, with no material failures.
- Designed and laboratory-tested a pleated filter cartridge system capable of regenerating at any engine operating condition on a 7.3-L Ford F-250 truck.
- Prepared to test the pleated filter system in a 7000-mile track test in FY 2003.

Future Direction

- Integrate the microwave filter particulate matter (PM) control unit with NO_x, hydrocarbon, and CO emission devices to develop a total system approach to meet Environmental Protection Agency (EPA) Tier II requirements.
- Continue on-road testing on the 7.3-L Ford truck for an additional 20,000 miles, under high-load conditions, to extend the durability performance database.
- Enlist exhaust system, catalyst, engine, and vehicle manufacturers in a joint product development effort to move toward commercialization of the microwave-regenerated particulate filter in 2004.
- Work with microwave suppliers and materials companies to further harden the microwave and filter media components of the pleated filter microwave system against vibration and exhaust forces.

Introduction

Most current diesel engine particulate filter technologies depend on a catalyst to assist in the regeneration of the filter. Catalyst technology requires a minimum exhaust temperature of approximately 300°C to be effective. Small and medium-size diesel engines rarely achieve this exhaust temperature. The microwave-regenerated diesel particulate filter (Mw-DPF) has been developed to provide the required particulate removal efficiencies and regenerate at low exhaust temperatures. A catalyst can be easily applied to the Mw-DPF to allow regeneration at higher exhaust temperatures without microwave assistance. The Mw-DPF is a viable answer to the low-temperature urban driving cycle where catalyst technologies are ineffective (Figure 1).

Engine backpressure created by particulate filters reduces engine performance and fuel economy. The ICS pleated ceramic fiber filter demonstrates 1/20 the backpressure on the engine that is exhibited by the standard wall-flow filter (Figure 2). This device will provide a major

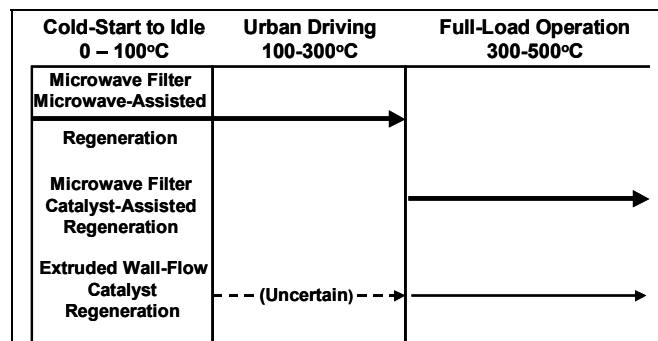


Figure 1. Microwave-regenerated diesel particulate filter regeneration at all engine operating conditions.

breakthrough for customers concerned about optimum engine performance.

Approach

The ceramic fiber wall-flow filter was tested on a Ford F-250 7.3-L compression-ignition, direct-injection (CIDI) truck under routine highway driving conditions for approximately 2000 miles over a period of several months to demonstrate filter durability. The truck filter was removed and

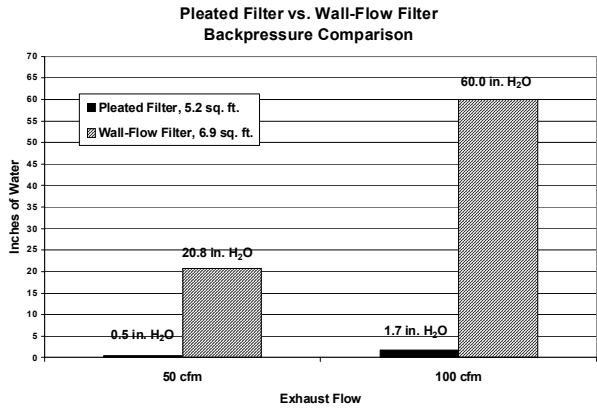


Figure 2. Exhaust backpressure of the ICS pleated filter cartridge vs conventional wall-flow filters.

microwave-regenerated in the laboratory to enable understanding of the effects of microwave heating on the particulate-loaded cartridge.

A second major project for 2002 was installation of a ceramic fiber, wall-flow microwave filter system on a 1.9-L TDI Volkswagen Jetta vehicle for a 7000-mile track test. Microwave regenerations were to be conducted at engine idle conditions. The Volkswagen Jetta, equipped with an onboard microwave regeneration system, was driven for approximately 200 highway miles with six idle condition regenerations conducted. The Jetta vehicle exhibited two preexisting severe mechanical problems. The EGR valve was uncontrollable, opening and closing at random during the engine idle microwave regeneration. This condition resulted in unacceptable exhaust flow variations during microwave regeneration. During stationary engine testing at Oak Ridge National Laboratory (ORNL) on an identical 1.9-L TDI engine, 3 hours were required to load the filter cartridge at normal engine speeds. The same size cartridge on the Volkswagen vehicle was found to load in less than 1 hour. This second problem was high inorganic ash accumulation in the filter, probably due to several years of being parked, as well as previous testing of unusual fuels and lubricants. ICS and DOE agreed that conducting the expensive track testing on such an unreliable test vehicle was counterproductive. Therefore, the 7000-mile track testing was transferred to the Ford F-250 7.3-L truck.

During the test vehicle change, ICS was able to complete the development of a low-backpressure pleated filter cartridge to replace the wall-flow design for the 7000-mile durability track testing. The

pleated filter system for the Ford truck will allow microwave regeneration at conditions other than engine idle, which is a requirement of the diesel engine manufacturers. ICS is currently testing the microwave-heating properties of this system in the laboratory. Particulate emissions testing will be conducted on the pleated filter on a 1.7-L Mercedes engine at ORNL. The 7000-mile track test will be performed at the Transportation Research Center in East Liberty, Ohio. The data from this test will verify system durability using filter efficiency performance in FTP chassis dynamometer testing and will accurately measure the fuel penalty of the Mw-DPF.

Results

Data verifying the durability of the filter cartridge in the Ford truck highway testing are shown in Figure 3. Note how the backpressure of the same cleaned filter increases very gradually over a 9-month period. That testing is still proceeding on the same ceramic fiber filter cartridge with no apparent mechanical damage to the filter cartridge.

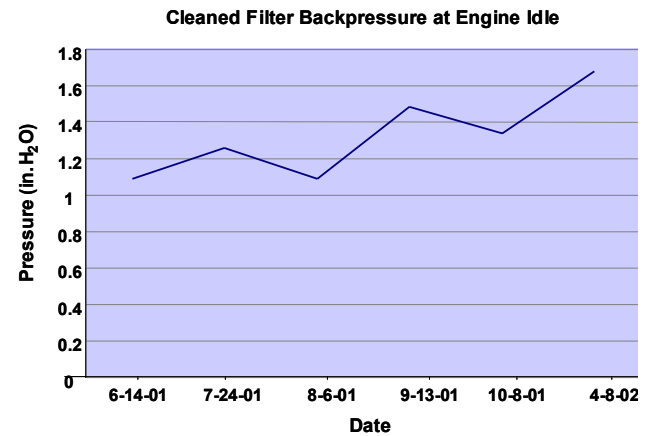


Figure 3. Backpressure increases on a single ICS fiber filter during 9 months of semi-continuous loadings and cleanings on a Ford 7.3-L CIDI vehicle.

The ability of the microwave to clean a particulate-loaded filter to within 95–100% of its clean condition has been demonstrated in engine testing for the last 3 years. Similar results of microwave regeneration on the Volkswagen Jetta vehicle are shown in Figure 4. Again, note how the backpressure of the cleaned filter is approximately constant from regeneration to regeneration. The

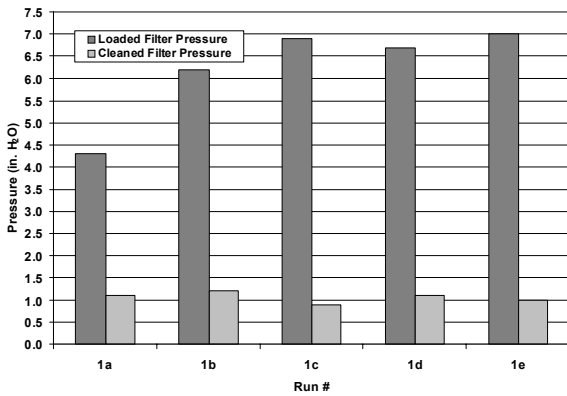


Figure 4. Microwave filter cleaning efficiency using the onboard system of the Volkswagen Jetta vehicle.

design of the new pleated ceramic fiber filter cartridge is displayed in Figure 5. The commercialization plan for the pleated filter is to produce the same size cassette for all vehicles, using multiple cassettes as the engine size increases. The design of the pleated particulate filter system will accomplish microwave regeneration at all engine conditions, as shown in Figure 6. The onboard generator supplying power to the microwave system on the Ford truck is shown in Figure 7. The new uniform-sized pleated cassette concept, using multiple cassettes as engine size increases, will maintain the price of the Mw-DPF below that of current particulate control technologies while providing significant advantages in engine backpressure. Materials improvements in the ceramic fiber filter system have continued in 2002, including filter media burst strength increases from the 6 psi achieved in 2001 to 10 psi in 2002. The application of an inexpensive silicon carbide coating

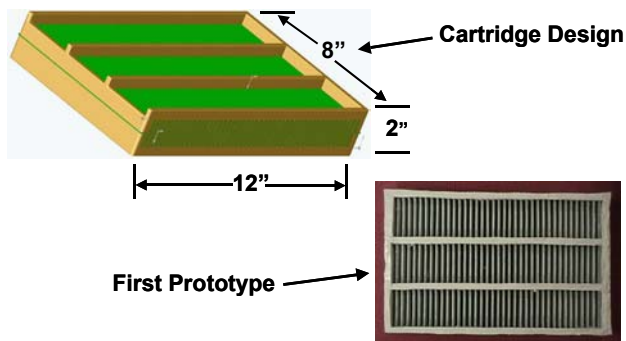


Figure 5. ICS pleated ceramic fiber particulate filter cartridge cassette.

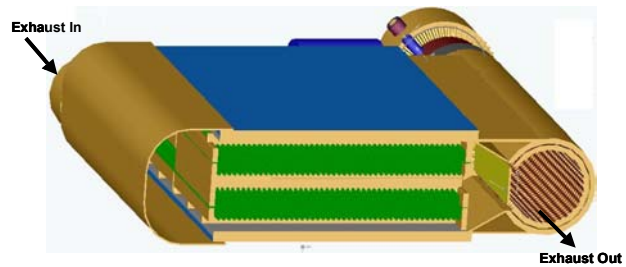


Figure 6. ICS pleated particulate filter system microwave regeneration design.



Figure 7. Onboard generator to supply power to the microwave system for the microwave-regenerated diesel particulate filter on the Ford 7.3-L test truck.

to the filter cartridge has improved the microwave heating ability, as well as the diesel exhaust corrosion resistance. The use of silicon carbide structural members to frame the pleated filter also ensures stability during high temperature excursions.

Conclusions

Filter backpressure and the ability to regenerate a particulate filter at low exhaust temperatures are significant issues with diesel engine manufacturers preparing for the 2007 EPA standards. Laboratory and stationary engine testing of the ceramic fiber microwave-regenerated filter system have shown meaningful progress in those areas. The 7000-mile track test on the Ford 7.3-L vehicle will begin

durability verification. Continuation of the development of the pleated cassette system in 2003 will lead to a commercially viable product for mobile sources by 2004.

FY 2002 Publications/Presentations

R. Nixdorf, "In-Situ Microwave Cleaning of Silicon Carbide Fiber Filtration Media," TechTextile Symposium North America, Atlanta, April 2002.

B. Rapid Surface Modifications of Aluminum Automotive Components for Weight Reduction

C. A. Blue, R. D. Ott, P. J. Blau, P. G. Engleman, and D. C. Harper

Oak Ridge National Laboratory

P. O. Box 2008, Bldg. 4508

Oak Ridge, TN 37831-6083

(865) 574-4351; fax: (865) 574-4357; e-mail: blueca@ornl.gov

DOE Technology Development Managers: Nancy Garland

(202) 586-5673; fax: (202) 586-9811; e-mail: nancy.garland@ee.doe.gov

Kathi Epping

(202) 586-7425; fax (202) 586-9811; e-mail: kathi.epping@ee.doe.gov

ORNL Technical Advisor: David Stinton

(865) 574-4556; fax: (865) 241-0411; e-mail: stintondp@ornl.gov

Contractor: Oak Ridge National Laboratory, Oak Ridge, Tennessee

Prime Contract No.: DE-AC05-00OR22725

Objectives

- Further develop durability-enhancing coatings on steel for environmental protection and wear resistance.
- Develop a method to dramatically reduce the time required to cure an epoxy used to join automotive body panels.
- Develop a procedure for selective heat-treating of aluminum automotive body construction parts in order to soften selected areas to serve as built-in crumple zones.

Approach

- Fuse abrasion-resistant coatings in air to steel using the high-density infrared (HDI) plasma arc lamp.
- Use a focused tungsten halogen lamp line heater to rapidly cure epoxy used for joining body panels.
- Use the HDI plasma arc lamp to soften selected areas of extruded aluminum tubes used as automotive frame rail structures.

Accomplishments

- Successfully fused onto steel abrasion-resistant coatings that show a reduction in porosity, an increase in hardness, and appropriate bonding characteristics.
- Successfully developed the tungsten halogen lamp line heater for the rapid curing of epoxy resin, a process currently being used on the production line at Ford.
- Developed heat flow models to determine the temperature profile during the pulsing of extruded aluminum tubes with the HDI plasma arc lamp, making it possible to predict the degree of hardness reduction achieved.

Future Direction

- Further develop durability-enhancing coatings for the compression-ignition direct-injection (CIDI) exhaust gas environment to improve the corrosion and wear resistance of relevant components and accommodate the more aggressive environment of exhaust gas recirculation (EGR).
 - Resolve accelerated corrosion and wear concerns associated with EGR, especially the use of coatings to prolong the life of critical components such as the intake manifold and EGR valves.
 - Use the HDI plasma arc lamp for rapid surface modification of discrete areas to eliminate fatigue-related problems in cast aluminum engine blocks.
-

Introduction

Three research projects were associated with FY 2002. The first one encompassed the further development of durability-enhancing coatings; this work was performed in conjunction with Caterpillar. Caterpillar was looking for a way to fuse abrasion-resistant coatings to steel with appropriate densities, hardness, and bonding strengths. The HDI plasma arc lamp was used to achieve the required properties. These coatings are potential candidates to enhance the life of exhaust gas components. Because a larger amount of exhaust gas must be combined with the intake mixture to reduce emissions, components such as EGR valves and intake manifolds will see accelerated corrosion and wear. The abrasion-resistant coatings are able to withstand the more severe environment, thus protecting the steel components from premature failure.

The second research project was an effort to reduce the curing time of automotive body filler epoxy. Ford wanted to replace the joining material for body panels with a one-component epoxy, but curing the epoxy took too long for the production line. A focused tungsten halogen lamp line heater was developed at ORNL to help reduce the curing time. Implementing use of the line heater allowed a 2-min reduction in cycle time, eliminated five grinding steps, provided a safer, more environmentally friendly process, reduced energy consumption, and saved \$28 per vehicle.

The third project involved working with Ford on preferential heat treating of extruded aluminum tubes intended for use as automotive frame rail structures. The preferential heating was performed to introduce crash triggers so that the structure would collapse on itself in a controlled manner during impact. Using the HDI plasma arc lamp, it was possible to selectively soften the essential areas,

eliminating the need to introduce the crash triggers mechanically and thus reducing cost. The introduction of aluminum frame rail structures can lead to a significant reduction in the weight of the vehicle, increasing the fuel efficiency.

Results

Abrasion-Resistant Coatings

Caterpillar was interested in evaluating the capability of the HDI plasma arc lamp to fuse abrasion-resistant coatings to steel components. The essential purpose of these coatings is to increase the wear resistance and corrosion resistance of components exposed to exhaust gases, such as EGR valves and intake manifolds. One of the coatings the company was interested in was an Fe-Cr-B-Mn-Si wire arc-sprayed coating. Caterpillar's main concerns were associated with the porosity and the hardness of the coating and the bonding characteristics of the coating to the substrate. Experiments were conducted by varying the arc lamp's reflector geometry, amperage (i.e., power density), and pulse or exposure time. The lamp processing parameters were optimized to obtain the desired coating properties.

It was shown that there was a significant reduction in porosity, increased coating hardness, and adequate metallurgical bonding. The micrographs in Figure 1 reveals a cross-sectional view of a coating, pre- and post-processing. It was also shown that altering the processing parameters could vary the degree of mixing between the substrate and coating. This research demonstrates the plasma arc lamp's capability to rapidly fuse coatings in an air environment. This capability leads to a very robust fusing technique that makes it

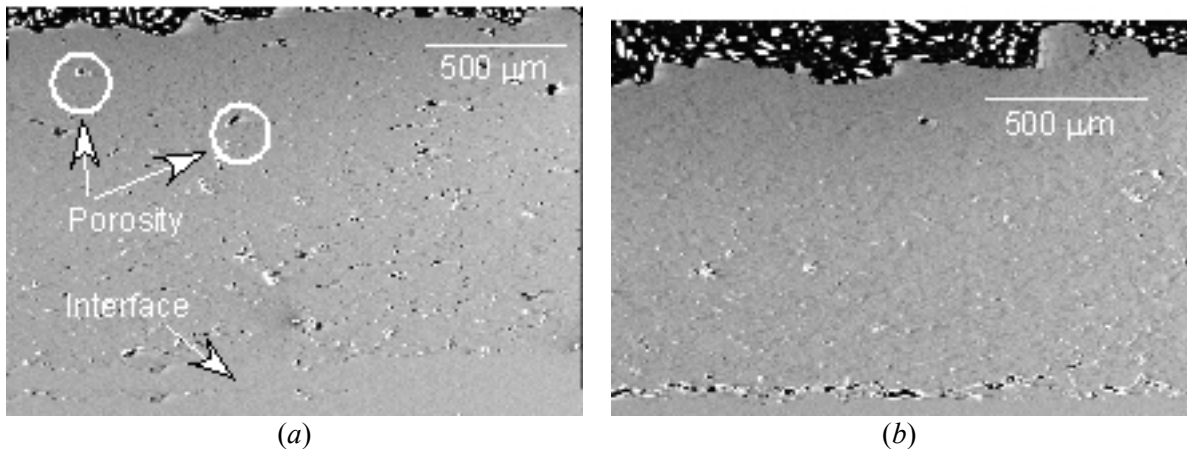


Figure 1. Scanning electron microscope micrographs of a cross section of an abrasion-resistant coating on a steel substrate: (a) pre-processed by the HDI plasma arc lamp (note the porosity) and (b) post-processed by the plasma arc lamp, revealing the densification of the coating.

suitable for high production volumes, ideal for automotive components in the EGR system and combustion chamber.

Rapid Curing of Automotive Body Filler Epoxy

Ford was interested in replacing a welding process for joining body panels with a one-component epoxy. The specific joint to be considered was a welded seam in the C-pillar of the Lincoln LS vehicle. Ford wished to eliminate steps associated with the production of the body to reduce cost. The process being used was operator-dependent and thus susceptible to quality concerns and throughput issues. The major challenge was to develop a process that used a one-component epoxy and a procedure for curing the epoxy in a timely manner.

Ford pursued a collaboration with ORNL to develop a method to rapidly cure the epoxy seam on the C-pillar, since it was not cost-effective to heat the entire component to elevated temperatures to cure the epoxy. After several methods to heat the seam were investigated, the focused tungsten halogen lamp line heater showed the most promise as a robust heating system. It was able to cure the epoxy in approximately 20 s. The line heater is capable of going to full power in less than 1 s and is 90% efficient in converting electrical power to radiant power. Its inherent properties make it ideal for industrial applications. Ford was able to realize a

\$28-per-vehicle savings by using the epoxy filler with the line heater curing method, as well as a 2-min reduction in cycle time. Figure 2 shows the line heater lamp on the production line and the joint after the curing process.

Preferential Heat-Treating of Aluminum Tubes

In an effort to reduce the overall weight of an automobile, Ford has been investigating the use of aluminum for the frame rail structure. One of the main purposes of this assembly, located in the front portion of the body, is to absorb energy during an impact. To do so, its structure must collapse in a certain sequence. This process is accomplished by built-in crash triggers, which are points along the structure that allow the structure to collapse and deform in a controlled manner.

Currently, front frame rail structures are manufactured from steel. Replacing steel with 6063 aluminum alloy would result in considerable weight savings. Extruded square aluminum tubes are more cost-effective than stamped aluminum because of their lower tooling costs. However, it is easy to build crash triggers into stamped aluminum during the manufacturing process; that is not the case for extruded aluminum tubes. Therefore, the HDI plasma arc lamp was used to soften (i.e., reduce the hardness of) selected areas along the aluminum tube to eliminate the need to introduce crash triggers mechanically.

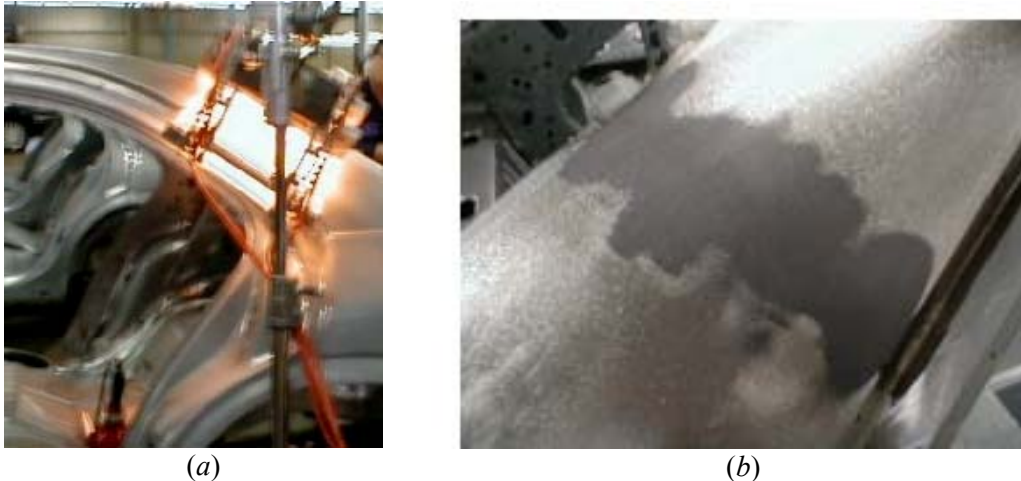


Figure 2. The line heater lamp on the production line curing an epoxy seam (a) and the seam after the curing process (b).

Experiments were performed at ORNL to determine the necessary plasma arc lamp parameters to achieve the required reduction in hardness. It was shown that the required 50% hardness reduction could be reached. From these experiments, a heat flow model was developed to optimize the process, and a microhardness map was developed to determine the required hardness reduction along the profile of the tube. Tubes are currently being pulsed according to the optimized process and will be sent to Ford for crumple test evaluation. Figure 3 shows the crumple test setup.

Microstructural evaluation of the 6063 T-6 aluminum specimens revealed that Mg_2Si precipitates had gone back into solution in regions that had been heat-treated. The microstructure farther away from the heat-treated zone resembled that of the overaged condition, a dense Mg_2Si precipitate matrix with precipitate-free zones at the grain boundaries. The micrographs in Figure 4 show these two regions.

Summary

Work is ongoing in the area of abrasion-resistant coatings for steel and aluminum components. The plasma arc lamp has shown great promise for

processing these coatings for numerous applications. Work also continues on the preferential softening of the aluminum frame rail structure tubes. Aluminum tubes that have been heat-treated by the plasma arc lamp will be crush-tested at Ford to evaluate the optimal heat-treating process. Ford officials believe that this is a viable technology and has a real chance to be implemented into production.

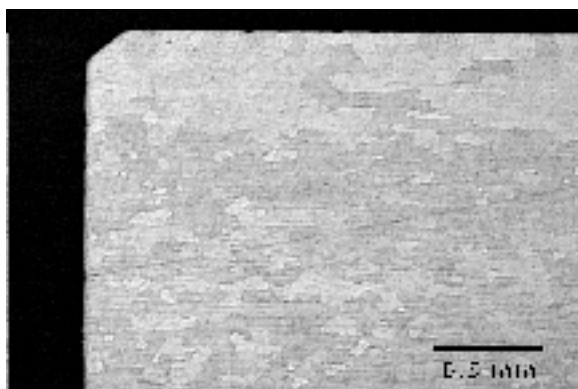
The HDI plasma arc lamp has shown promise in depositing wear- and corrosion-resistant coatings on steel substrates intended for the gaseous oxidant environment of the exhaust gases. The coatings produced by this method have shown promising properties in regard to adherence to the substrate, reduction in porosity, and mechanical strength. They can be deposited quickly in an environment suitable for high production volumes, such as the automotive industry. This process has been shown to be an ideal technology for producing protective coatings to reduce emissions.

Presentations

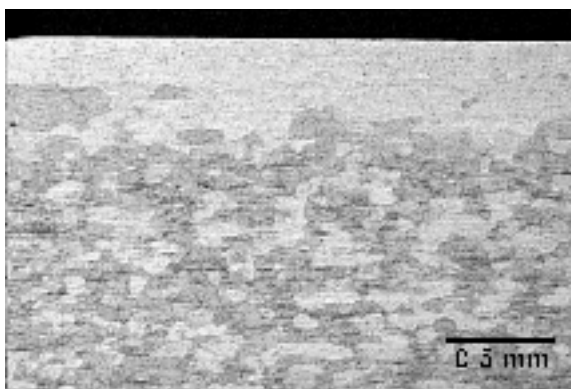
R. D. Ott, C. A. Blue, A. S. Sabau, T. Y. Pan, and A. M. Joaquin, "Preferential Softening of 6063-T6 Aluminum Alloy Utilizing a High Density Infrared (HDI) Plasma Arc Lamp," The Minerals, Metals & Materials Society Fall Meeting, 2002.



Figure 3. An aluminum tube undergoing a crumple test.



(a)



(b)

Figure 4. Micrographs of the (a) heat-treated region and (b) non-heat-treated region of 6063 T-6 aluminum. Notice the lack of grain definition in the heat-treated region compared with the non-heat-treated region. This is due to the dense Mg_2Si precipitate matrix resembling that of the overaged condition.

C. Material Support for Nonthermal Plasma Diesel Engine Exhaust Emission Control

Stephen D. Nunn

Materials Processing Group

Oak Ridge National Laboratory

P.O. Box 2008, MS 6087

Oak Ridge, TN 37831

(865) 576-1668; fax: (865) 574-4357; e-mail: nunnsd@ornl.gov

DOE Technology Development Manager: Nancy Garland

(202) 586-5673; fax: (202) 241-0411; e-mail: nancy.garland@ee.doe.gov

ORNL Technical Advisor: David Stinton

(865) 574-4556; fax: (865) 574-6918; e-mail: stintondp@ornl.gov

Contractor: Oak Ridge National Laboratory, Oak Ridge, Tennessee

Prime Contract No.: DE-AC05-00OR22725

Objectives

- Identify appropriate ceramic materials, develop processing methods, and fabricate complex-shaped ceramic components that will be used in Pacific Northwest National Laboratory (PNNL)-designed nonthermal plasma (NTP) reactors for the treatment of diesel exhaust gases.
- Fabricate and ship components to PNNL for testing and evaluation in prototype NTP reactors.
- Develop a component design and establish a fabrication procedure that can be transitioned to a commercial supplier.
- Assemble and test a prototype NTP reactor on a laboratory diesel engine.

Approach

- Evaluate commercially viable forming methods to fabricate complex-shaped ceramic components that meet PNNL design specifications.
- Modify processing as needed to accommodate material and design changes.
- Evaluate bonding and sealing materials for preparing assemblies of the ceramic components.
- Investigate metallization materials and processes to apply electrodes to the ceramic components.

Accomplishments

- Modified the processing procedure for fabricating the ceramic components to improve reliability and simplify the production.
- Identified a sealing glass composition for joining together the ceramic components that are used in the NTP reactor assembly.
- Selected a preliminary NTP reactor design for conducting functional testing of the device on a 1.7-L diesel engine in an engine test cell.

Future Direction

- Finalize the selection of sealing materials to bond and seal the various ceramic and metal components of the NTP reactor into a complete assembly for functional testing.
- In collaboration with PNNL, select an NTP reactor design for assembly and testing to determine the operational performance of the device.
- Fabricate an NTP reactor assembly and test the device in a diesel engine exhaust gas stream.

Introduction

NTP reactors have shown great potential as an effective means for eliminating unwanted exhaust gas emissions from diesel engines. In particular, the NTP reactor is very effective in reducing NO_x. Researchers at PNNL are developing new, proprietary design configurations for NTP reactors that build on past experimental work. To improve the effectiveness, these designs include ceramic dielectric components having complex configurations. Oak Ridge National Laboratory (ORNL) has extensive experience in the fabrication of complex ceramic shapes, primarily based on prior work related to developing ceramic components for gas turbine engines. The ORNL expertise is being used to support PNNL in its development of the new NTP reactor designs.

Approach

Collaborative discussions between ORNL and PNNL are used to establish new ceramic component designs for improved NTP reactors. The need to meet NTP reactor design objectives is balanced with the limitations of ceramic manufacturability to arrive at a new component configuration. The ceramic processing facilities and expertise at ORNL are then used to establish fabrication capabilities and to produce components for testing at PNNL. This is an iterative process as both parties gain more knowledge about fabricating the components and about their performance in NTP reactor tests. The ultimate goal is to identify a design that performs well and that can be readily produced by a commercially viable process.

Results

In the early stages of this project, complex-shaped ceramic components were fabricated by the gelcasting process. Although these parts performed well in laboratory tests, it was decided that the

fabrication process was too complicated to be feasible for commercial production. A new fabrication process was developed that uses commercially available tape-cast ceramic materials. In the green (unfired) state, the ceramic tape is flexible (Figure 1). The tape can be shaped and laminated to form the ceramic dielectric components for the NTP reactor. Figure 2 illustrates this process, showing where grooves have been formed in the outer layers that will be laminated with flat tape layers to form the final assembly. Using a flat core is a modification of the original process that simplifies fabrication and improves yield. Silver electrodes are applied to the insides of the grooved areas and then extended to the outside of one end of the assembly. A stack of sintered components is shown in Figure 3. The individual dielectric plates are separated by alumina ceramic spacers to produce a precise gap between the plates.

In the NTP reactor assembly, the ceramic components will be fixed in place in a metal housing, with ceramic spacers used to maintain the separation between the individual plates. To form

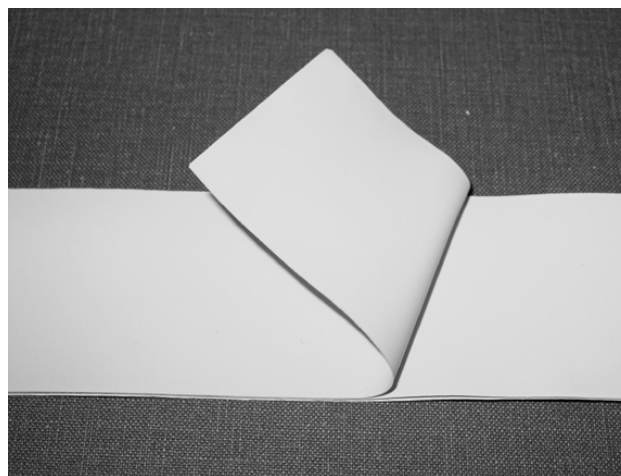


Figure 1. Photograph of pieces of the tape-cast ceramic material showing the flexibility of the unfired tape.

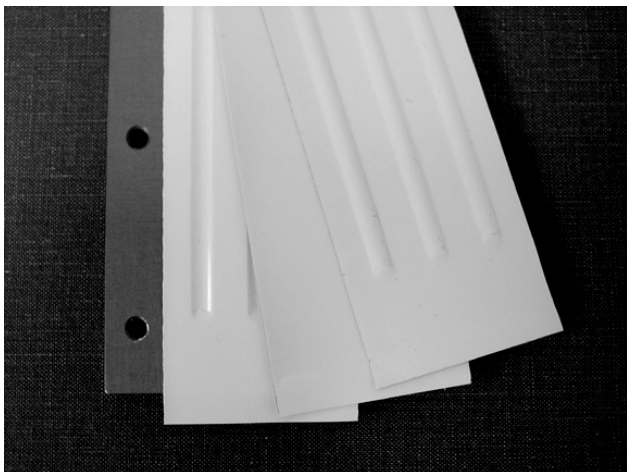


Figure 2. Examples of formed and flat tape segments illustrating how they are assembled to form the ceramic dielectric components.



Figure 3. Sintered dielectric plates assembled in a stack with individual plates separated by alumina ceramic spacers.

the assembly, a bonding and sealing material is needed to fix the ceramic components in position and to form a gas-tight seal to contain the exhaust gases. The bonding/sealing material must be an electrical insulator and must have an appropriate thermal expansion match to maintain a tight bond during thermal cycling. Several glass compositions have been evaluated for use in joining the various components. An example of a test sample is shown in Figure 4, where pieces of the dielectric ceramic and the spacer are bonded in a sandwich. A photomicrograph of the bond is shown in Figure 5. The glass wets and bonds the materials together and forms a fillet of material at the outer surface to make a gas-tight seal. Additional testing will be required to identify an appropriate bonding material to join the ceramic components to the metal housing.

Plans are now being made to make a complete NTP reactor during the coming fiscal year and to conduct tests of the performance of the device on a 1.7-L diesel engine in an engine test cell.

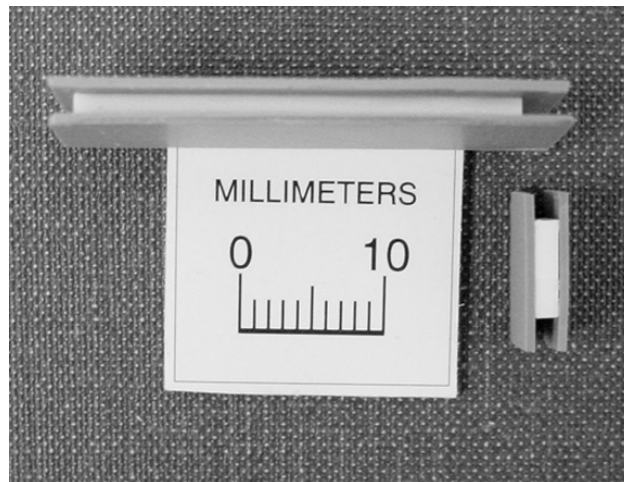


Figure 4. Test assembly for evaluating bonding and sealing of the NTP reactor component materials.

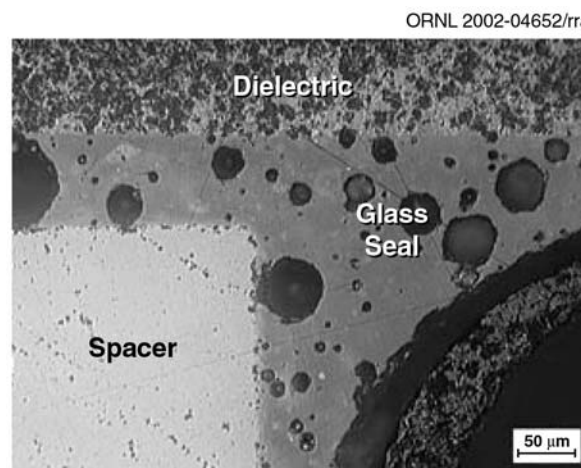


Figure 5. Micrograph showing the adhesive bond between the dielectric material (top) and the spacer (lower left). A smooth fillet has formed where the outer portion of the two materials join (center) forming a gas-tight seal. The bar equals 50 microns.

Conclusions

The fabrication procedure for ceramic dielectric components was modified to simplify the production of parts for the NTP reactors. The new procedure should be lower in cost and should improve the reliability and yield of the components. A sealing glass was identified for joining together the ceramic components of the NTP reactor, but additional testing is needed to find a material that will bond the ceramics to the metal housing of the reactor.

D. Fabrication of Small Fuel-Injector Orifices

John Woodford and George R. Fenske

Argonne National Laboratory

9700 South Cass Avenue

Argonne, IL 60439

(630) 252-0910; fax: (630) 252-4798; e-mail: gfenske@anl.gov

DOE Technology Development Manager: Nancy Garland

(202) 586-5673; fax: (202) 586-9811; e-mail: nancy.garland@ee.doe.gov

ORNL Technical Advisor: David Stinton

(865) 574-4556; fax: (865) 241-0411; e-mail: stintondp@ornl.gov

Contractor: Argonne National Laboratory, Argonne, Illinois

Prime Contract No.: W-31-109-Eng-38

Objectives

- Develop a methodology for reducing the diameter of fuel injector orifices to 50 μm by applying material to the internal diameter (ID) of a conventional 200- μm diameter orifice.
- Characterize the spray and combustion properties of the fuel injector systems so treated.
- Transfer the technology to an industrial partner.

Approach

- Identify and rate potential thin- and thick-film deposition technologies for reducing the diameter of diesel engine fuel injector orifices.
- Perform laboratory-scale evaluations of the most promising technology or technologies.

Accomplishments

- Selected electroless nickel (EN) plating as the primary candidate, with electroplating and/or physical vapor deposition (PVD) as possible secondary candidates.
- Began benchtop evaluation of EN plating for injector tips.
- Reduced orifice diameter from 200 μm to 100 μm with EN plating.
- Began forced-flow EN plating tests.
- Identified the critical role of particulates in EN orifice plating quality.

Future Direction

- Complete construction of forced-circulation multicomponent plating system.
- Analyze spray characteristics of coated injectors.
- Provide coated injector tips to Argonne National Laboratory (ANL) Energy Systems personnel for combustion tests.

- Determine the vulnerability of EN-plated injectors to deposit formation. If necessary, vary plating chemistry to ameliorate vulnerability.

Introduction

Recent work on the control of particulate matter (PM) emissions and improvement of engine combustion efficiency in diesel engines has shown the effectiveness of reduced injector orifice diameter in promoting fuel atomization, leading to more complete combustion and reduction in soot formation.^{1,2} Using electrodischarge machining (EDM), the current method for fabricating injector orifices, the minimum achievable orifice diameter is on the order of 125 μm . To see significant improvement, orifice diameter should be 50 μm or less. Work toward refining EDM techniques to allow economical large-scale fabrication of 100- μm orifices is ongoing. In addition, two other technologies may be used to manufacture small orifices: laser drilling and LIGA. Both technologies have disadvantages precluding their commercial use in the near- to mid-term. Therefore, we propose another method.

There are currently a wide variety of techniques for depositing moderately thick ($>10 \mu\text{m}$) films onto various surfaces. It may be possible to reduce the diameter of an extant orifice by depositing material onto its interior (Figure 1). We propose to select and evaluate an appropriate technique for doing so, and if it appears that this approach is successful, we will develop a method and transfer it to an industrial partner. We are currently working with Siemens, which has provided us with sample injector tips and information.

Approach

As mentioned earlier, there are a large number of coating techniques to be considered. Our first step, therefore, is to perform a survey of deposition methods and determine which may be used to coat orifice IDs. We will then rank those methods offering a reasonable chance of success by ease of overall implementation, taking into account such factors as coating cost, startup cost, and environmental friendliness.

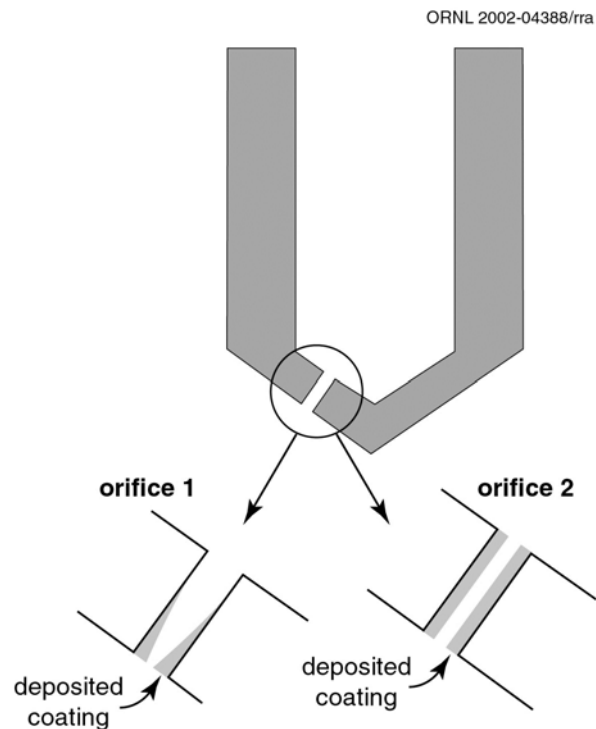


Figure 1. Schematic illustration showing the proposed method of reducing the orifice diameter.

With the ranked list in hand, we will work toward implementing the easiest method on a laboratory scale and examining the feasibility of working on others. Our criteria for success are as follows:

- The technique allows reduction in the orifice diameter to at least 50 μm .
- The coating adheres well to the substrate.
- The coating is at least as damage-resistant as the substrate.

In addition, we will consider the effort a limited success if the surface chemistry of the (adherent, damage-resistant) coating is such that deposit formation is minimized, even if we are unable to achieve the goal of an ID of 50 μm .

As part of the evaluation process, we will examine the flow-through and spray characteristics of coated nozzles and will provide them to industrial partners or other collaborators for combustion studies. Although our focus in this project is on

deposition methods, we understand that the overall goal is to improve fuel combustion in diesel engines.

Following a successful laboratory-scale demonstration of the coating technology, we will work with Siemens or another industrial partner to transfer the technology.

Results

We completed a process comparison in the second quarter (Table 1). The most promising candidate method was EN plating, which offered a combination of rapid deposition rate, ability to coat IDs, ready scalability, overall maturity level, low-expense facilities, and durability of coating. We then set out to evaluate the process according to the criteria described earlier.

EN plating is a method of depositing nickel/phosphorus (or nickel/boron) alloys (usually Ni-P or -B solid solutions, with NiP or NiB precipitates) onto metallic surfaces from an aqueous solution. Samples are placed in a plating bath of the appropriate composition, the bath is heated to approximately 70–95°C, and the nickel/phosphorus coating grows directly from the bath via a surface-catalyzed chemical reaction.

Initial results have been quite promising. We have coated the orifice IDs on sample injector tips provided by Siemens (Figure 2) with reasonable uniformity (Figure 3). We have also established the adherence of the EN plating on the injector tips. Although we have not yet achieved reduction to 50 μm , we have deposited an EN plate that is about 50 μm thick onto the ID of 200- μm diameter orifices, reducing them to 100 μm in diameter.

In order to obtain greater uniformity, better adhesion on the interior of the injector tip, and more rapid deposition, we began to plate injector tips by forcing the plating bath through the injector orifices during the coating process. This approach approximately doubled the deposition rate to around 50 $\mu\text{m}/\text{hour}$. However, we found that the bath needed to be filtered to prevent clogging of the nozzles with small nickel particles. In fact, if the bath is not filtered, the nickel particles nucleate the growth of metallic threads inside the body of the injector tip. In addition, the pump we were using did not develop enough pressure to force the bath through the orifices once they had closed to around 100 μm in diameter. We are in the process of constructing a larger-scale plating bath with a capacity of several gallons, a more powerful pump, a filter on the supply line, and a manifold for coating multiple injector tips at a time.

Conclusions

EN plating has been shown to be an effective method of reducing the ID of fuel injector tip orifices. Further work toward improving the method is ongoing.

References

1. John B. Heywood, *Internal Combustion Engine Fundamentals*, McGraw-Hill, 1988.
2. Lyle M. Pickett and Dennis L. Siebers, "Orifice Diameter Effects on Diesel Fuel Jet Flame Structure," Paper 2001-ICE-399, ICE-Vol. 37-1, 2001 Fall Technical Conference, American Society of Mechanical Engineers, 2001, ed. V. W. Wong.

Table 1. Process comparison

Process	MOCVD (vacuum)	PVD	MOCVD (atmo)	Thermal spray	EP	EN
Inexpensive?	No	No	Variable	Yes	Yes	Yes
Reliable?	Yes	Variable	Yes	Yes	Yes	Yes
Green?	Variable	Yes	Variable	Yes	Variable	Variable
Adherent?	Yes	Variable	Yes	Variable	Yes	Variable
Uniform?	Unknown	Probably not	Unknown	No	Unknown	Yes

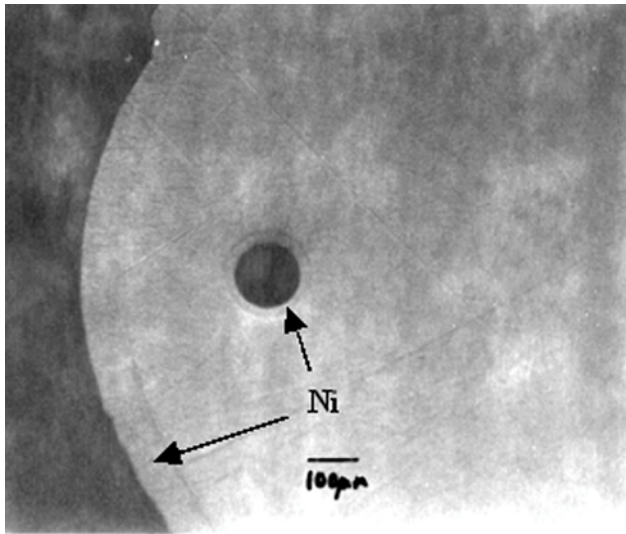


Figure 2. Micrograph of the cross section of the coated fuel injector tip orifice. The nickel plate is the lighter-colored ring around the orifice ID.

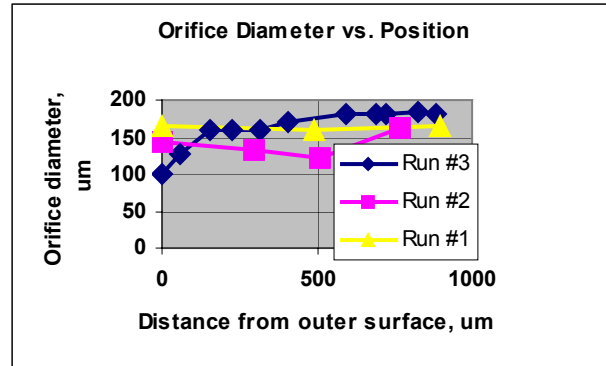


Figure 3. Graph of coating thickness as a function of position along the length of the orifice.

E. Technology for Producing Small Holes in Advanced Materials

Stephen D. Nunn

Materials Processing Group

Oak Ridge National Laboratory

P.O. Box 2008, MS 6087

Oak Ridge, TN 37831

(865) 576-1668; fax: (865) 574-4357; e-mail: nunnsd@ornl.gov

DOE Technology Development Manager: Nancy Garland

(202) 586-5673; fax: (202) 586-9811; e-mail: nancy.garland@ee.doe.gov

ORNL Technical Advisor: David Stinton

(865) 574-4556; fax: (865) 241-0411; e-mail: stintondp@ornl.gov

Contractor: Oak Ridge National Laboratory, Oak Ridge, Tennessee

Prime Contract No.: DE-AC05-00OR22725

Objectives

- Explore methods for producing ultra-small holes (<50 μm) in advanced materials for fuel injector nozzles.
- Evaluate carbide-based cermets and high-temperature ceramics as candidate materials.
- Devise methods to precisely produce a desired pattern of holes having a well-controlled size and shape.

Approach

- Form holes in situ during the sintering process by incorporating various pore formers in the green (unsintered) body while it is being shaped.
- Use nickel alloy wires in nickel aluminide (Ni_3Al)-bonded titanium carbide (TiC) to form holes during sintering.
- Embed combustible organic fibers in gelcast ceramic materials that will vaporize during sintering at high temperatures.
- Gelcast ceramic materials around metal wires that can be removed from the green body prior to sintering, leaving a hole in the part.

Accomplishments

- Formed $\sim 30\text{-}\mu\text{m}$ holes in gelcast alumina by embedding polymer fibers in the green body and sintering the material at 1500EC.
- Formed $\sim 35\text{-}\mu\text{m}$ holes in alumina that was gelcast around fine metal wires, which were removed prior to sintering at 1500EC.

Future Direction

- Demonstrate the ability to form holes in cermets and additional ceramic materials.
 - Evaluate techniques to form arrays of holes in precise locations in the sintered parts.
 - Investigate microfabrication by coextrusion as an additional method for forming ultra-small holes in advanced materials.
-

Introduction

To meet the ever-growing demand for improved efficiency and reduced emissions, future fuel injection systems will require improvements in both design and materials. The objective of this project is to explore new methods of forming ultra-small (<50- μm) holes in advanced materials. Carbide-based cermets (ceramic/metallic composites) and high-temperature ceramics are candidate materials to be used in this study. These materials have the desirable properties of high strength, high modulus, and low density compared with steel. In addition, they are corrosion resistant and, because of their high hardness, also resistant to wear and erosion.

Currently, fuel injector nozzle holes in steel are 150 to 200 μm in diameter. This size is at the limit for machined holes. One of the major challenges to using advanced materials for improved nozzles is the inability to manufacture very fine holes in the densified material by conventional machining processes. To overcome this limitation, this project will explore methods for the in situ fabrication of holes during the sintering step that is a normal part of the advanced material fabrication process. Various techniques for incorporating fugitive pore-formers will be investigated. These pore-formers will be incorporated in the green body during the forming process and will be removed before or consumed during the sintering step to leave precisely controlled pores (holes) in the densified material. If successful, this technique will not only allow the formation of simple holes, but also add the potential to form holes having a variable geometry.

Approach

It has been observed in past studies of the cermet Ni_3Al -bonded TiC that the presence of metal particles in the unsintered powder compact can leave voids in the sintered part as a result of the metal's being drawn into the carbide particle array by capillary action when the metal becomes molten. This tendency will be exploited in the present study to intentionally form holes in predetermined locations. Nickel alloy wires of the appropriate size will be located in the unfired material to form fine holes in the sintered part.

Several ceramic materials will be investigated in this project. Among the ceramics being considered are alumina (Al_2O_3), silicon nitride (Si_3N_4), silicon carbide (SiC), and zirconia (ZrO_2). The approach for

forming holes will be to incorporate fugitive pore formers in gelcast ceramic green (unsintered) bodies. Gelcasting is a method of forming powdered materials into complex shapes. Organic monomers are added to an aqueous slurry of the ceramic powder. Through initiation of a polymerization reaction, the organic molecules and the slurry are transformed into a solid (gelled) body. Casting the slurry in a mold and then gelling can form a complex-shaped part. One approach to forming holes in the gelcast ceramic part would be to place fibers in the mold that would be trapped in desired locations in the gelled part. These fibers would then be burned away during the sintering process, leaving holes in the densified part. The fibers can be synthetic polymers (e.g., nylon, polyethylene), natural fibers (cotton, silk), or even graphite. The second approach to forming holes in gelcast ceramic parts is to locate fine metal wires within the casting mold. As with the fibers, the metal wires would be trapped in the gelled part. But, rather than burning out, the wires can be withdrawn from the green body prior to sintering. Even very fine holes in the green part can be retained in the sintered ceramic.

Another method being considered for later study would involve the use of coextrusion to form complex arrays of holes on a very fine scale.

Results

Funding for this project became available midway through the second quarter of FY 2002. Despite the short time available to conduct research, some interesting results have been obtained. Tests were begun with gelcast Al_2O_3 , and the initial results look very promising. Figure 1 shows micrographs of holes that were formed by embedding metal wires in a gelcast part. The wires, 38 μm (0.0015 in.) in diameter, were removed from the gelled part before sintering. The resulting holes are about 30 μm in diameter. One of the holes is shown lengthwise in the micrograph in Figure 2. The hole was exposed by grinding away the ceramic material. The ground surface is not quite parallel to the axis of the hole, and the hole actually goes below the surface at the location indicated by arrow 1. Some damage due to the grinding operation is seen at arrow 2. Holes more than 15 mm long were produced using this method.

Figure 3 shows holes that were formed in gelcast Al_2O_3 by incorporating polymer fibers in the

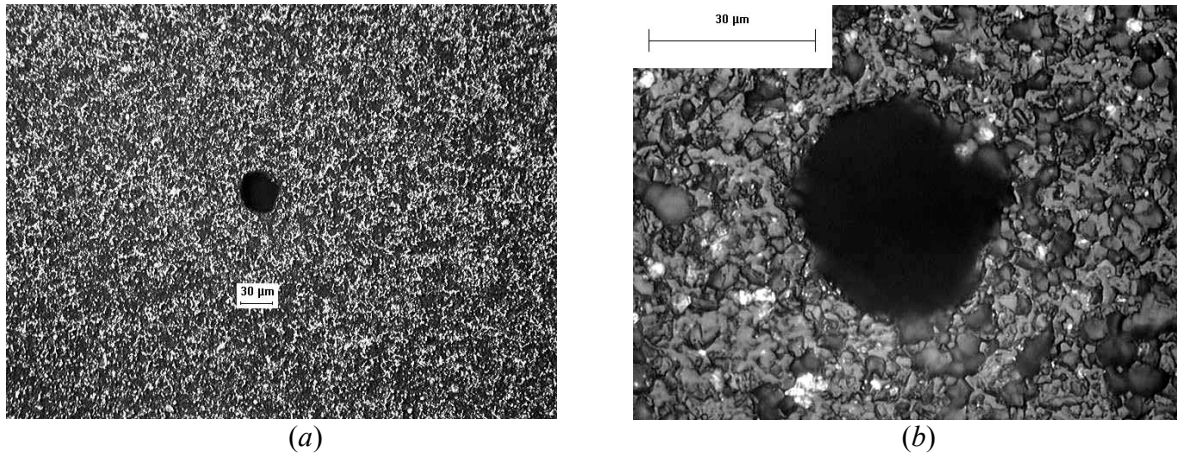


Figure 1. Micrographs showing holes in sintered alumina ceramic that were formed by embedding metal wires in the gelcast ceramic green body. The wires were removed prior to sintering, and the holes were retained in the densified ceramic. The same hole is shown at (a) low and (b) high magnification.

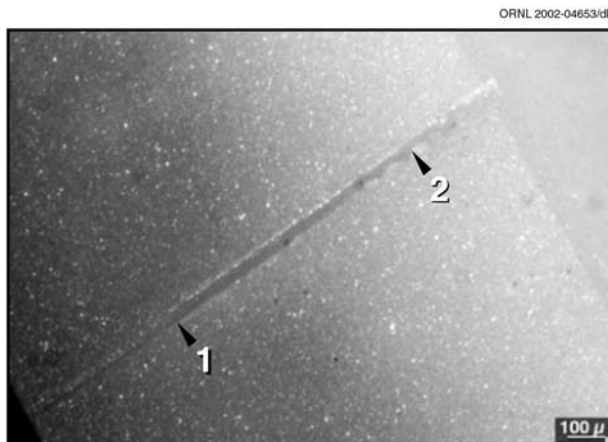


Figure 2. Micrograph of a hole in sintered alumina ceramic shown lengthwise by grinding away the ceramic surface. The ground surface is not quite parallel to the hole axis, and the hole actually goes below the surface at the point indicated by arrow 1. The chipping at the edge of the hole shown at arrow 2 is due to grinding damage.

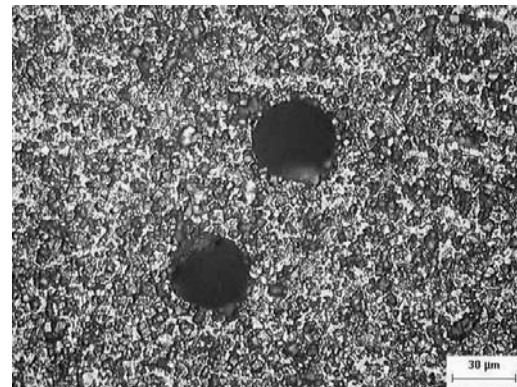


Figure 3. Micrograph showing holes in sintered alumina ceramic that were formed by incorporating polymer fibers in the gelcast ceramic green body. The fibers burned away during sintering, leaving holes in the dense ceramic.

gelcast material. The fibers burned away during sintering and left well-defined holes in the ceramic. These holes are also about 30 μm in diameter and were as long as 20 mm. Both of these methods were effective in producing ultra-fine-diameter holes in ceramics and demonstrate the feasibility of using these techniques to make fuel injector nozzles having holes smaller than 50 μm in diameter.

Conclusions

Preliminary tests to produce ultra-fine holes in Al₂O₃ ceramic have been very successful. Holes that are about 30 μm in diameter and as long as 20 mm have been produced. Additional testing will be done using other advanced ceramic materials and the cermet compound. Future efforts will begin to focus on producing arrays of holes in a predetermined pattern.

F. Electrochemical NO_x Sensor for Monitoring Diesel Emissions

L. Peter Martin and Ai-Quoc Pham

Lawrence Livermore National Laboratory

P.O. Box 808, MS L-353

Livermore, CA 94551-0808

(925) 423-9831; fax: (925) 424-3215; e-mail: martin89@llnl.gov

DOE Technology Development Manager: Nancy Garland

(202) 586-5673; fax: (202) 586-9811; e-mail: nancy.garland@ee.doe.gov

Contractor: Lawrence Livermore National Laboratory, Livermore, California
Prime Contract No.: W-7405-Eng-48

Objectives

- Develop a compact, rapid-response electrochemical NO_x sensor for compression-ignition, direct-injection (CIDI) exhaust gas monitoring.
- Fabricate a first-generation laboratory prototype for sensitivity/selectivity testing at Ford Research Laboratory.
- Continue the investigation of materials and sensing mechanisms to optimize performance.

Approach

- Utilize an ionic (O²⁻) conducting ceramic as an electrolyte and mechanical support (substrate).
- Use colloidal spray deposition to apply metal oxide electrodes to the electrolyte substrate.
- Evaluate electrode materials and processing conditions for sensitivity and response time.
- Test operating modes (potentiometric and amperometric) to optimize performance.
- Demonstrate stability and cross-sensitivity with interfering gases.

Accomplishments

- Developed a potentiometric sensor with high NO₂ response, negligible NO sensitivity, and fast response time at 700°C.
- Identified a current-biased mode of potentiometric operation giving the best NO sensitivity and response speed (~27 mV at 500 ppm NO, 10% O₂, 650°C, 1.5 s response).
- Selected electrode materials for the current-biased NO sensor.

Future Direction

- Investigate sensor stability and oxygen sensitivity.
 - Send the first-generation laboratory prototype sensor to Ford for sensitivity/selectivity testing.
 - Continue to investigate electrode materials/microstructure (FY 2002, FY 2003).
 - Design and build integrated (self-heated) prototype sensor (FY 03)
 - Perform fundamental investigation to identify NO sensing mechanism (FY 03)
-

Introduction

The most promising NO sensors for exhaust gas monitoring are based on ionically conducting solid state electrochemical devices.^{1,2} These devices typically consist of a solid ceramic electrolyte onto which two or more metal or metal-oxide electrodes are deposited, and they can be operated in either potentiometric or amperometric modes. Significant progress has been made toward the development of deployable sensors using yttria-stabilized zirconia (YSZ) as the electrolyte and catalytically active metal oxides as the sensing electrodes.³ However, improvements are still needed in sensitivity, response time, reliability, and cross-sensitivity.

The current work is directed toward the development of a fast, high-sensitivity electrochemical NO_x sensor. Target operating parameters for the proposed sensor (based on discussion with Ford collaborators) are sensitivity to the total NO_x content in the range of 1 to 1000 ppm, operating temperature of >600°C, and response time ≤1 s. The elevated operating temperature is to ensure compatibility with a possible conversion catalyst that will convert the total NO_x to one species, probably NO. In addition, the sensor should be simple and reliable, and cross-sensitivity with other oxidizing/reducing gases should be minimized. Finally, it should be noted that the relative merits of NO₂ versus NO selective sensors are not clear at the present time.

Approach

The proposed approach is to develop a sensor using catalytic metal oxide electrodes on a solid ionic conductor electrolyte. Similar technology has been widely investigated for various gas sensing applications and has been successfully developed for use as exhaust gas oxygen sensors. The current effort approaches the problem by the application of novel materials and fabrication processes designed to optimize electrode microstructures. In addition, a potentially novel mode of operation has been identified that yields enhanced NO response amplitude and speed.

Sensors were prepared by spray deposition of metal oxide electrodes onto YSZ electrolyte substrates, followed by sintering at 1000–1100°C. NO_x sensing experiments were performed in a quartz tube inside a furnace. All tests were performed using 500 ppm NO or NO₂ in 10% O₂, balance N₂, at a

flow rate of 1000 mL/min. The design of a typical sensor and test apparatus are shown schematically in Figure 1. All tests were performed in the temperature range of 600 to 700°C.

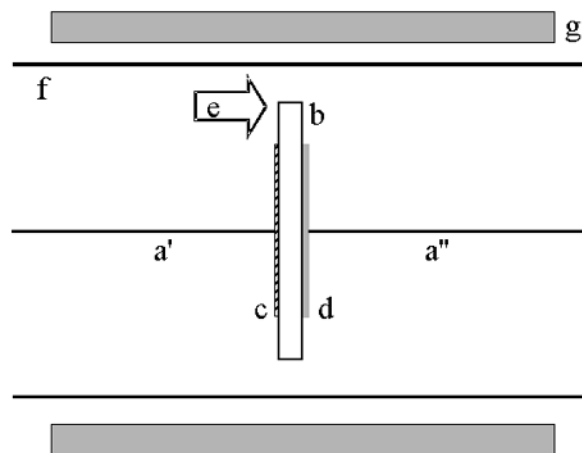


Figure 1. Schematic of the experimental test setup showing: (a', a'') wire leads, (b) YSZ electrolyte, (c) metal oxide electrode, (d) platinum or metal oxide electrode, (e) test gas flow, (f) quartz tube, and (g) furnace hot zone.

Results

Figure 2 shows the mixed potential response from a sensor using a composite YSZ/doped-lanthanum manganate sensing electrode and a platinum metal reference electrode. The data show a baseline near 0 mV when the gas stream is composed of 10% O₂, balance N₂, at 700°C, and a response in excess of 40 mV when 500 ppm NO₂ is introduced. The 90% recovery (turn-off) time for this sensor is 2.5 s, which approaches the target 1 s (the datum points in all figures are spaced 0.5 s apart). The sharp peaks at the beginning of each response result from a transient overpressure when the NO₂ is introduced into the gas stream. The sensor has negligible NO sensitivity, making it highly selective for NO₂. It was observed that potentiometric sensors that provided reasonable sensitivity to NO at temperatures >600°C—for example, sensors with NiCr₂O₄ as the sensing electrode—had recovery times that were much too long (>10 s). Thus alternate modes of operation were investigated.

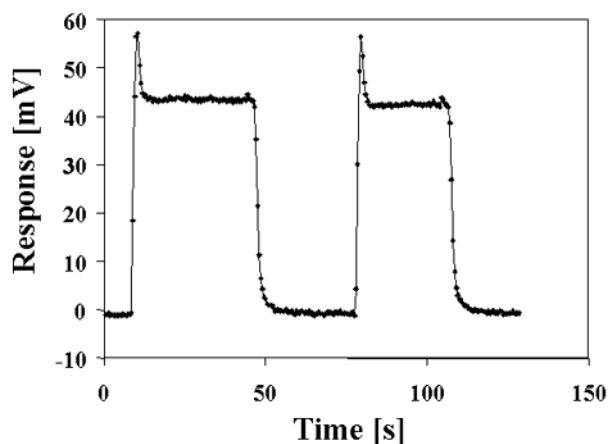


Figure 2. Potentiometric response of a NO_2 sensor, operated at 700°C , with a composite sensing electrode (YSZ and doped-lanthanum manganate). The gas contains 10% O_2 and 500 ppm NO_2 .

Since the electrochemical sensing mechanisms for the NO_x species involve oxidation/reduction reactions, it is logical to think that one could modify the kinetics, and perhaps speed up the response, by appropriately biasing the sensor electrodes. Other investigators have attempted to correlate the gas composition with the current resulting from a fixed potential-bias across the electrodes. In the 10% O_2 environment, however, this biasing causes a high O_2 pumping current that overwhelms the NO_x sensing response. To correct for this high O_2 current, it is generally necessary to pump out the oxygen from the sample gas stream using, for example, a YSZ pump. This requirement contributes to the complexity of the sensor and to concerns relating to the possible decomposition of the NO_x during the pumping operation. We have developed a related technique in which a fixed current, rather than a fixed potential, is applied between the sensing and reference electrodes. The potential required to maintain this current is then measured and correlated to the gas composition. Figure 3 shows data from a sensor using an NiCr_2O_4 sensing electrode and a YSZ/doped-lanthanum manganate reference electrode at 650°C . The response is +27 mV when 500 ppm NO is introduced into the gas stream, and the 90% recovery time is 1.5 s. It is interesting to note the positive sign of the response, which is indicative of the reduction of NO and is consistent with the direction of bias of the electrodes. Under

the current-biasing conditions shown in Figure 3, the sensor has high NO_2 sensitivity ($\sim 3\times$ the NO sensitivity).

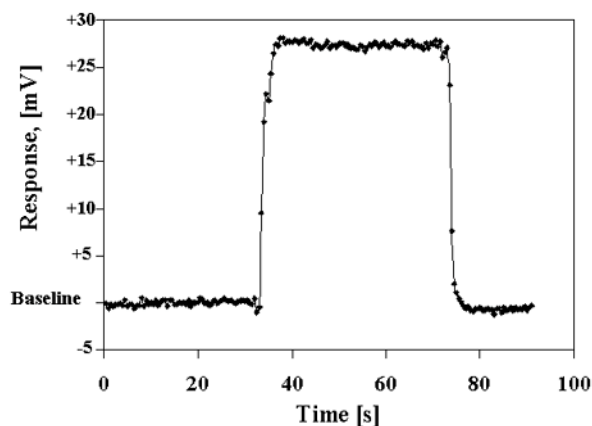


Figure 3. Response of the current-biased sensor to 500 ppm NO in 10% O_2 at 650°C . The sensor uses an NiCr_2O_4 sensing electrode and a composite reference electrode.

It is possible, by operating under different biasing conditions, to make the sensor shown in Figure 3 insensitive to NO_2 . Under those conditions, the sign of the response becomes negative, indicating that the sensor response comes from the oxidation of NO to NO_2 . Thus, changing the biasing can actually change the operating mechanism of the sensor. In addition, the sensitivity nearly doubles (to 45 mV for 500 ppm NO), but the response time becomes slower (90% recovery increases to 7 s).

Conclusions

We have developed a potentiometric NO_2 sensor with high sensitivity, selectivity, and speed at 700°C . We have developed an alternative mode of operation for NO detection that uses a current-bias across the electrodes. This mode of operation gives good NO sensitivity (~ 27 mV at 500 ppm NO) and response speed (1.5 s) when operated at 650°C in 10% O_2 . When operated under different biasing conditions, this mode of operation gives enhanced NO response and negligible NO_2 sensitivity at the expense of response time. To the best of our knowledge, this mode of operation has not been reported in the literature pertaining to electrochemical NO_x sensors. Continued investigation is necessary to optimize the

performance, quantify the cross-sensitivity, and establish the stability of the sensor.

References

1. F. Menil, V. Coillard, and C. Lucat, "Critical Review of Nitrogen Monoxide Sensors for Exhaust Gases of Lean-Burn Engines," *Sensors and Actuators B*, **67**, pp. 1–23 (2000).

2. N. Miura, G. Lu, and N. Yamazoe, "Progress in Mixed-Potential Type Devices Based on Solid Electrolyte for Sensing Redox Gases," *Solid State Ionics*, **136–137**, pp. 533–542 (2000).

3. T. Ono, M. Hasei, A. Kunimoto, T. Yamamoto, and A. Noda, "Performance of the NO_x

Sensor Based on Mixed Potential for Automobiles in Exhaust Gases," *JSAE Rev.*, **22**, pp. 49–55 (2001).

Publications/Presentations

L. P. Martin, Q. Pham, and R. S. Glass, "Electrochemical NO_x Sensor for Monitoring CIDI Vehicle Emissions," presented at National Laboratory CIDI and Fuels R&D Merit Review and Peer Evaluation, Argonne, Illinois, May 14, 2002.

L. P. Martin, Q. Pham, and R. S. Glass, "Effect of Cr₂O₃ Electrode Morphology on the NO Response of a Stabilized Zirconia Sensor," submitted to *Sensors and Actuators B* (June 2002).

APPENDIX A: ACRONYMS AND ABBREVIATIONS

AHE	aerodynamic heat exchanger
ANL	Argonne National Laboratory
ASTM	American Society for Testing and Materials
CIDI	compression-ignition direct-injection
CO	carbon monoxide
CVI	chemical vapor infiltration
DF	dissipation factor
DOE	U.S. Department of Energy
EDM	electrodischarge machining
EDX	energy-dispersive X-ray spectroscopy
E/E	Electrical and Electronics
EGR	exhaust gas recirculation
EN	electroless nickel
EPA	Environmental Protection Agency
F	fluorine
FTP	Federal Test Protocol
GGFD	ground graphitized foam dust
GM	General Motors
GTRI	Georgia Tech Research Institute
HA-ADF	high-angle annular dark-field
H ⁺	hydrogen ion
H ₂	hydrogen gas
HDI	high-density infrared
HEPA	high-efficiency particulate air (filter)
IC	internal combustion
ICS	Industrial Ceramic Solutions
ID	internal diameter
LANL	Los Alamos National Laboratory
L/D	length-to-diameter
MEA	membrane electrode assembly
MLCC	multi-layer ceramic composite
MDM	mechanical properties microprobe
MW-DPF	microwave-regenerated diesel particulate filter
NEP	National Energy Policy
NFC	near-frictionless carbon
NIST	National Institute for Standards and Testing
nm	nanometer, 10 ⁻⁹ meters
NO _x	oxides of nitrogen

NSA	National Security Agency
NTP	nonthermal plasma
OAAT	Office of Advanced Automotive Technologies
OEM	original equipment manufacturer
OHVT	Office of Heavy Vehicle Technologies
OM	optical microscope
ORNL	Oak Ridge National Laboratory
OTT	Office of Transportation Technologies
PEM	polymer electrolyte membrane
PEMFC	polymer electrolyte membrane fuel cell
Pd	palladium
PM	permanent magnet
PNGV	Partnership for a New Generation of Vehicles
PNNL	Pacific Northwest National Laboratory
POEM	porous oxide electrolyte membrane
PPS	polyphenylene sulfide
Pt	platinum
PVD	physical vapor deposition
PVP	hydroxylated polystyrene
R&D	research and development
S	sulfur
SAE	Society of Automotive Engineers
SEM	scanning electron microscope
SHE	standard hydrogen electrode
SNL	Sandia National Laboratories
SO ₃ ²⁻	sulfonate group
STEM	scanning transmission electron microscope
T	Tesla
TEM	transmission electron microscope
TiN	titanium nitride
TIVM	toroidal intersecting vane machine
WC	tungsten carbide
YSZ	yttria-stabilized zirconium
Z	characterized by a high atomic number